EMERGENCE OF COOPERATION AND HOMEODYNAMICS AS A RESULT OF SELF ORGANIZED TEMPORAL CRITICALITY: FROM BIOLOGY TO PHYSICS

Korosh Mahmoodi

Dissertation Prepared for the Degree of

DOCTOR OF PHILOSOPHY

UNIVERSITY OF NORTH TEXAS

August 2018

APPROVED:

Paolo Grigolini, Major Professor
Arkadii Krokhin, Committee Member
Yuri Rostovtsev, Committee Member
James Roberts, Committee Member
Michael Monticino, Interim Chair of the Department of Physics
Su Gao, Dean of the College of Science
Victor Prybutok, Dean of the Toulouse Graduate School

Mahmoodi, Korosh. *Emergence of Cooperation and Homeodynamics as a Result of Self Organized Temporal Criticality: From Biology to Physics*. Doctor of Philosophy (Physics), August 2018, 171 pp., 47 figures, 184 numbered references.

This dissertation is an attempt at establishing a bridge between biology and physics leading naturally from the field of phase transitions in physics to the cooperative nature of living systems. We show that this aim can be realized by supplementing the current field of evolutionary game theory with a new form of self-organized temporal criticality. In the case of ordinary criticality, the units of a system choosing either cooperation or defection under the influence of the choices done by their nearest neighbors, undergo a significant change of behavior when the intensity of social influence has a critical value. At criticality, the behavior of the individual units is correlated with that of all other units, in addition to the behavior of the nearest neighbors. The spontaneous transition to criticality of this work is realized as follows: the units change their behavior (defection or cooperation) under the social influence of their nearest neighbors and update the intensity of their social influence spontaneously by the feedback they get from the payoffs of the game (environment). If units, which are selfish, get higher benefit with respect to their previous play, they increase their interest to interact with other units and vice versa. Doing this, the behavior of single units and the whole system spontaneously evolve towards criticality, thereby realizing a global behavior favoring cooperation. In the case when the interacting units are oscillators with their own periodicity, homeodynamics concerns, the individual payoff is the synchronization with the nearest neighbors (i.e.,

lowering the energy of the system), the spontaneous transition to criticality generates fluctuations characterized by the joint action of periodicity and crucial events of the same kind as those revealed by the current analysis of the dynamics of the brain. This result is expected to explain the efficiency of enzyme catalyzers, on the basis of a new non-equilibrium statistical physics. We argue that the results obtained apply to sociological and psychological systems as well as to elementary biological systems.

ACKNOWLEDGMENTS

I would like to express my sincere thanks to my advisor, professor Paolo Grigolini. Also, I would like to thank professor Bruce J. West for his fruitful collaboration.

I gratefully acknowledge the Army Research Office and Welch Foundation for financial support through grants No. W911NF-15-1-0245 and No. B-1577, respectively.

TABLE OF CONTENTS

LIST OF FIGURES

CHAPTER 1

INTRODUCTION AND MOTIVATION

1.1. Introduction to Evolutionarty Game Therory

The main problem of the field of Evolutionary Game Theory is to explain the evolutionary emergence of cooperation in spite of the selfish nature of the single individuals. Nowak and May in their 1992 pioneer work on Nature [1] adopted the concept of network reciprocity to settle this paradox. Their idea rests on the assumption that the individuals of the complex systems are the nodes of a regular network where the clusters of cooperators are richer than the clusters of defectors. As a consequence, if the players of the game are allowed to change their strategy, selecting the choice done by their most successful nearest neighbors, it may happen that they select cooperation. This approach to settling the altruism paradox is not quite convincing for two main reasons. One of these reasons, concerning the sociological application of their network reciprocity principle, is the fact that the individuals of a social network, in addition to the interaction, described by the prisoners dilemma game, have also a social activity that has been proved to disrupt the benefits of network reciprocity. Another reason is the use of a network structure. Many researchers are assigning to the network topology a scale-free structure, leaving unanswered the question of what the dynamical origin of the scale-free structure may be. In this work, we prove that the social activity may not disrupt the benefit of network reciprocity if the social activity of the individual rests on the Ising-like interaction structure of the DMM, based on the realistic assumption that each individual makes choices based on the influence of the nearest neighbors.

This property is realistic but the assumption that the social imitation strength of the DMM has a critical value for the onset of phase transition is not in turn satisfactory, because the evolutionary process is spontaneous and the crucial value of the imitation strength must be reached as an effect of the interaction between the individuals by itself. Our attempt at bypassing this problems led us to a way of settling the altruism paradox with a theoretical

proposal that is equivalent to a new approach to criticality, the Self-Organized Temporal Criticality (SOTC). This theoretical proposal settles the altruism paradox by assuming that each individual decides to increase or decrease the degree of her social attention to the nearest neighbors according to whether her payoff, done on the basis of the choices made by her nearest neighbors, increases or decreases.

1.2. Introduction to Complexity Matching and Homeodynamics

Complexity matching is an attractive way of emphasizing the caution we have to adopt in order to transport information from one complex system to another and the mechanism can be traced back to the 1957 Introduction to Cybernetics by Ross Ashby. Unlike this earlier work we argue that complexity can be expressed in terms of crucial events, which are generated by the processes of spontaneous self-organization. The Complex processes, ranging from biological to sociological, must fit the homeodynamic condition and should host the crucial events that in the recent past have been shown to drive the information transport between complex systems. We adopt a phenomenological approach, based on the subordination to periodicity that makes it possible to combine homeodynamics and self-organization induced crucial events. The complexity of crucial events is defined by the waiting time probability density function (PDF) of the intervals between consecutive crucial events, which have an inverse power law (IPL) PDF $\psi(\tau) \propto 1/(\tau)^{\mu}$ with $1 < \mu < 3$. We establish the coupling between two temporally complex systems using a phenomenological approach inspired by models of swarm intelligence and prove that complexity matching, namely sharing the same IPL index μ facilitates the transport of information, generating perfect synchronization, reminiscent of, but distinct from, those obtained in the field of chaos synchronization. We use this phenomenological approach to recover the recently derived main results on social cognition, as well as, on the EEG dynamics of subject addressing the solution of difficult tasks.

It is slightly over a half century since Ross Ashby, in his masterful book [2] warned scientists, aware of the difficulty of regulating biological systems, that "the main cause of

difficulty is the variety in the disturbances that must be regulated against". This insightful observation need not lead to the conclusion that complex systems cannot be regulated: It is possible to regulate them if the regulators share the high intelligence of the systems being regulated. Herein we refer to the Ashby's principle as *complexity matching*. The term complexity matching was widely used in the recent past [3, 4, 5, 6, 7, 8] to denote the synchronization between the finger tapping and a complex metronome interpreted to be a system as complex as the human brain. These synchronizations are certainly a realization of the regulation of the brain fitting the remarks of Ashby.

It is important to stress that there exists further research work aiming at the foundation of social learning [9, 10, 11, 12] that is even more closely connected to the ambitious challenge by Ashby. In fact, this research work aims at evaluating the transfer of information from the brain of one player to the brain of another player through the interaction that the two players establish the one with the other through their avatars. The results are exciting: the trajectories of the two players turn out to be significantly synchronized.

Even more important than synchronization is the fact that the trajectories of the two avatars have universal structure shared EEGs of the human brain. This work affords a proper theory to understand this universal structure, representing either the brain of two interacting individuals or the communication between the heart and the brain [13]

The transfer of information has been addressed using different theoretical tools, such uas *chaos syncronization* [14], *self-organization* [15], *resonance* [16]. On the other hand, in a system as complex as the brain [17] there is experimental evidence of the existence for crucial events. These crucial events can be interpreted as organization rearrangement or renewal failures. The interval between consecutive crucial events is described by a waiting-time IPL PDF $\psi(t) \propto 1/t^{\mu}$, with $\mu < 3$. The crucial events are generators of ergodicity breaking and are widely studied to reveal fundamental biological statistical properties [18].

Another important property of biological processes is homeodynamics [19], which seems to be in conflict with homeostasis advocated by Ashby. Lloyd *et al* [19] invoke the existence of bifurcation points to explain the transition from homeostasis to homeodynamics.

The transition from homeostasis to homeodynamics, moving from Ashby's emphasis on the fundamental role of homeostasis, has been studied by Ikegami and Suzuki [20] and by Oka et al. [21] who coined the term *dynamic homeostasis* using Ashby's cybernetics to deepen the concept of self and to establish if the behavior of Internet is similar to that of the human brain.

Experimental results exist for the correlation between the dynamics of two distinct physiological systems [22], but they are not explained with any of the earlier mentioned theoretical approaches [14, 15, 16, 17, 18]. Here we relate this correlation to the occurrence of crucial events. The crucial events are responsible for the generation of $1/f$ noise, $S(f) \propto 1/f^{3-\mu}$ [23] and the results of the psychological experiment of Correll [24] imply that activating cognition has the effect of making $\mu < 3$ cross the barrier between the Lévy and Gauss basins of attraction, namely making $\mu > 3$. This has the devastating effect of violating the linear response condition, according to which a perturbation should be sufficiently weak as to not affect the dynamical complexity [25]. As a result of this experimental observation we have to go beyond the linear response theory adopted in earlier works to explain the transfer of information from one complex system to another, through the matching of the power index μ of the crucial events of the regulator with the IPL index μ of the crucial events of the system being regulated [26, 27]. The earlier work of Ref. [28] shows that a system at criticality can force another system at criticality to synchronize. A system either in the subcritical or supercritical condition cannot force a system at criticality to synchronize. These numerical results, which can be interpreted as a genuine form of complexity matching, are observed at the level of single realizations with no need of making averages on a large number of responses to the same perturbation as done in [26, 27], in spite of the fact that the intensity of the forcing is modest but large enough as to violate the linear response theory. These results were obtained by assuming that a small fraction of the units of the driven system can perceive the mean field of the driving system. This small fraction, at criticality is large enough as to make the driven system synchronize with the driving system. This important property of criticality is interpreted as *swarm intelligence* [29].

CHAPTER 2

IMITATON-INDUCED CRITICALITY: NETWORK RECIPROCITY AND PSYCHOLOGICAL REWARD

In this chapter we study the case where the nodes of a regular two-dimensional lattice play a game based on the joint action of two distinct levels. At the beginning of the game, using a random prescription half players are assigned the cooperation and half the defection state. At the bottom level the strategy choice is done on the mere basis of imitation according to the *homo imitans* principle, generating a form of collective intelligence that makes the system sensitive to the criteria determining the strategy choice adopted at the top level. The units of the top level, in fact, play the prisoner's dilemma game and are allowed to update their strategy either by selecting the strategy of the most successful nearest neighbor, *success model*, or merely on the basis of the criterion of the best financial benefit, *selfishness model*. The intelligence emerging from imitation-induced criticality leads in the former case to the extinction of defection and in the latter case to the extinction of cooperation. The former case is interpreted as a form of network reciprocity enhanced by the imitation-induced criticality and contributing to the evolution towards cooperation. Then the selfishness model gets perturbed with a form of morality pressure, exerted by a psychological reward λ for cooperation, to establish the sensitivity of collective intelligence to morality. We find that when λ gets a crucial value λ_c, exceeding the temptation to cheat, the system makes a transition from the supercritical defection state to the critical regime, with the warning that an excess of morality and religion pressure may annihilate the criticality-induced resilience of the system.

2.1. Introduction

The unification of behavioral sciences is an attractive and challenging enterprise that would be impossible without using game theory [30]. The recent book by Gintis [30] aims at the unification of Behavioral Sciences, namely, at the ambitious purpose of unifying biology,

psychology, economics, anthropology and political science, stressing however that game theory alone is not enough to realize this important goal. Game theory is a theoretical attempt at explaining why the selfish action of single individuals is compatible with the emergence of altruism and cooperation. Nowak and May [1] have attracted the attention of an increasing number of researchers on the network reciprocity, a special condition where spatial structure favors the emergence of altruism, see also [31], in spite of its nodes playing the prisoner's dilemma game [32], which is expected to favor defection. Actually, since the patch owner, either a cooperator C or a defector D is replaced by the neighbor with the largest payoff [1], this is equivalent to updating the strategy of each player adopting that of the most successful neighbor, and a cluster of cooperators has the effect of protecting the units of the cluster from the exploitation of the defectors.

As illustrated in the recent review paper of Wang *et al* [33], the research work in this field is now focusing on the topology of networks and especially on the emerging field of multilayers networks to explain the pattern formation with production of clusters protecting cooperators from the exploitation of the defectors so as to favor their survival of cooperators. This work adopts a multilayers perspective, by using however *dynamical* rather than merely topological arguments, in such a way as to be as close as possible to the project of unification of behavioral sciences recently proposed by Grigolini *et al* [34, 35], as an attempt at addressing the challenge of Gintis [30]. Furthermore the multiple layers do not necessarily correspond to different nodes, but here refer to different levels of human behavior, the social, the financial and the spiritual. The bottom layer of this work is based on the observation that the individuals of a network playing the prisoner's dilemma game are the units of a human society and are expected to be strongly influenced by imitation [36, 37]. The individuals of this network make a choice between the cooperation state C and the defection state D, without any form of cognition. This choice is not determined by the wish of maximizing the personal benefit through imitation of the most successful neighbor [31] or by the greedy choice of an immediate payoff, but imitation is as blind as the bird tendency to select their flying direction on the basis of the flying directions of the neighbor birds [38], with

no consideration of the personal benefit, either direct or indirect. The imitation strength is a control parameter hereby denoted by the symbol K_1. A critical value of K_1, called K_{1c}, exists making it possible for the swarm to fly as a whole. Although the action of the single individuals of the network does not require any form of cognition, as stressed by the authors of Ref. [29, 39], criticality generates a form of collective intelligence. This collective intelligence is characterized not only by the criticality-induced long-range correlation but also, and especially, by temporal complexity [40, 29, 41], a condition making the complex network flexible and resilient. It is important to stress that the supercritical condition is characterized by fluctuations around a non vanishing mean field as random as the fluctuations around the vanishing mean field of the subcritical regime, thereby lacking the flexibility and resilience of criticality.

At the top layer the units play the prisoner's dilemma game [32] and exert an influence on the bottom level choosing their strategy according to either the success or selfishness criterion.

The *success model* is realized as follows. For most of time steps the choice of strategy is determined by the bottom level, and from time to time the units are allowed to select their strategy adopting that of their most successful nearest neighbor, as suggested by the pioneer work of Ref. [1]. The success model yields the impressive effect of annihilating the emergence of the branch with the majority of defectors when the system adopting this choice is made intelligent by imitation-induced criticality. This effect affords a solid explanation of the evolution towards cooperation.

We compare the *success model* to the *selfishness model*, where the player does not adopt the strategy of the most successful nearest neighbor, but she makes her choice only on the basis of her personal benefit. She evaluates the financial benefit derived from the defection choice and the financial benefit that she would get from the cooperation choice, giving larger weight to the maximal profit. The benefit of a given choice is done assuming that the unit in action can play with equal probability with all her neighbors. The selection of the convenient strategy is weighted with a second control parameter K_2, with the ratio

$\rho_K = K_2/K_1$ establishing if the link with the top layer is stronger, $\rho_K > 1$, or weaker, $\rho_K < 1$, than the link with the bottom layer. Switching on the interaction with the top layer has the effect of leading to the extinction of cooperation with a big loss for society, even if, as we shall see hereby, $K_1 > 0$ yields imitation-induced clusters of cooperators with financial benefit for society, this being the reason why the *success model*, for $K \gg K_{1c}$ leads to the extinction of defectors. The strategy choice determined by the criterion of maximal personal benefit, rather than by the choice of the strategy of the most successful nearest neighbor [1], on the contrary, yields the extinction of cooperation, with an even very small value of ρ_K, as an effect of imitation-induced intelligence.

To complete the illustration of the role of criticality-induced intelligence we study the influence of morality on the dynamics of the *selfishness model* showing that as an effect of imitation-induced intelligence the system becomes so sensitive to morality as to make a psychological reward moderately exceeding the temptation to cheat, robust enough as to prevent the collapse of the social system into the sub-criticality disorder. In principle the influence of morality on the system should be established by the interaction of the network with an additional layer. For simplicity's sake, we modify the conventional prisoner's dilemma game [30, 42] through the introduction of the psychological reward for the choice of cooperation. The strength of psychological, called λ, affords a simplified way to describe the influence that an additional layer, concerning morality and religion, may have on the selfishness model. We find that, when the bottom layer operates at criticality, a crucial value λ_c exists with the effect of preventing the extinction of cooperators and of recovering the criticality-induced temporal complexity that is essential for the healthy behavior of the social system. We call this *Asbiyyah* effect [43], this arabic world meaning *group feeling*, namely the natural tendency of human beings to cooperate. This natural disposition is enhanced by religion and it has the eventual effect of increasing the social prosperity, but, in accordance with the observation of Ahmed [44], we find that $\lambda > \lambda_c$, the super-asbiyyan condition, may be as bad as the lack of social cohesion.

well known Prisoner's Dilemma game [32] rests on the crucial inequality

$$T > R > P > S, \tag{2.1}$$

where R denotes the reward that a cooperator gets when playing with another cooperator. The parameter $T > R$ is the payoff of a defector: it is larger than R thereby $t = T - R$ is a measure of the temptation to cheat. S is the payoff of a cooperator playing with a defector, and $P < R$ is the payoff of a defector playing with another defector. The condition

$$2R > T + S \tag{2.2}$$

indicates that the community gets a larger benefit from the play between two cooperators than from the play between a cooperator and a defector. Of course, also the play between two defectors with $2R > 2P$ is less beneficial to the community than the play between two cooperators. We adopt the choice made by Gintis [30, 42] and we set $R = 1$, $P = 0$, $T = 1+t$ and $S = -s$. To study the influence of morality on the selfishness model we introduce the psychological reward λ, setting

$$R = 1 + \lambda, \tag{2.3}$$

$$T = 1 + t, \tag{2.4}$$

$$P = -\lambda \tag{2.5}$$

and

$$S = -s. \tag{2.6}$$

In this work we adopt always but in Fig. 2.3 the choice

$$s = 3 \tag{2.7}$$

and

$$t = 2. \tag{2.8}$$

Note that we denote by N the total number of players. They are the nodes of a two-dimensional regular network of size 32. We adopt $N = 32X32$. We use the symbol L to denote the number of time steps, ranging from $L = 10^4$ to $L = 10^6$.

2.3. Decision-Making, Success, Selfishness and Influence of Morality Model

To establish an interaction between the bottom and the top level we adopt a natural extension of the *Decision Making Model* (DMM) of Ref. [36]. The transition rate from the cooperator to the defector state, g_{12}, is given by

$$g_{12} = g_0 exp\left[-K_1\left(\frac{M_1 - M_2}{M}\right) - K_2\left(\frac{\Pi_C - \Pi_D}{|\Pi_C| + |\Pi_D|}\right)\right] \tag{2.9}$$

and the transition rate from the defector to the cooperator state, g_{21}, is given by

$$g_{21} = g_0 exp\left[K_1\left(\frac{M_1 - M_2}{M}\right) + K_2\left(\frac{\Pi_C - \Pi_D}{|\Pi_C| + |\Pi_D|}\right)\right]. \tag{2.10}$$

The meaning of this prescription is as follows. The parameter $1/g_0$ defines the time scale and we set $g_0 = 0.1$ throughout. We consider N units. Each unit has M neighbors (four in the case of the regular two-dimensional lattice used in this work). The cooperation state corresponds to the state $|1>$ and the defector state to the state $|2>$. In the case $K_2 = 0$, this is the ordinary DMM of Ref. [36]. If the unit is in the cooperator state, $|1>$, and the majority of its neighbors are in the same state, then the transition rate becomes smaller and the units sojourns in the cooperation state for a longer time. If the majority of its neighbors is in the defector state, then the unit that has to make a decision sojourns in the cooperator state for a shorter time. Analog prescription is used if the unit is in the defector state. Note that at $K = K_{1c}$ the units move from a dynamical condition where they are virtually independent the ones from the others to a condition where global order emerges. In the case of two-dimensional regular lattice of this article, $K_{1c} \approx 1.65$.

Fig. 2.1 illustrates the second-order phase transition generated by the DMM, namely, the model of this work when $K_2 = 0$. This corresponds to the condition where no bias exists for the choice of either cooperation or defection. In the initial condition the N units of the

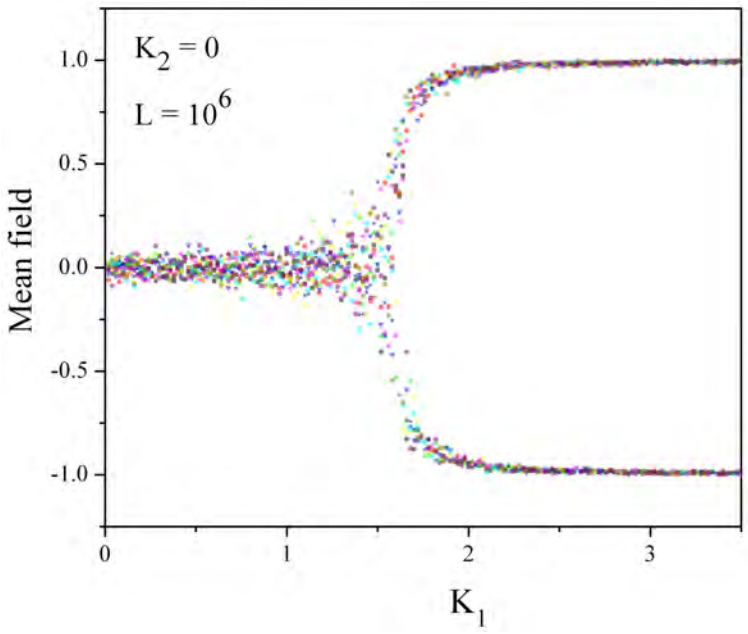

FIGURE 2.1. Mean field of the bottom level when $K_2 = 0.10$ realizations had done.

network are randomly assigned to either the cooperation or the defection state with the same probability, making zero the mean field of the network

$$\langle \xi \rangle \equiv \frac{\sum_i^N \xi_i}{N}, \tag{2.11}$$

where either $\xi_{=}1$ or $\xi = -1$, according to whether the $i-th$ unit is in the cooperation or in the defection state. Of course, due to the fact that, as earlier stated, we are using a finite number of units, $N = 1024$, the mean field fluctuates around the vanishing mean value. As we increase K_1 the intensity of fluctuations tends to increase. This is a finite-size effect discussed in detail in the applications of the DMM model [40]. In the case where each node is coupled to all the other nodes, the DMM yields analytical results for the mean field that can be interpreted as the space coordinate of a particle in a non-linear over-damped potential under the action of a random fluctuation generated by the finite size effect. At criticality, the potential is quartic, exerts a weaker containment on diffusion and makes larger the width of its equilibrium distribution. The mean field fluctuation around the origin has an inverse power law with index $\mu = 1.5$: a form of temporal complexity ensuring the maximal efficiency in the transport of information from one network to another with the same complexity[29].

This important effect has been proved also in the case of a neural network model [41], thereby suggesting that criticality-induced temporal complexity may be a condition of great importance for the sensitivity of a complex system to its environment. Temporal complexity must not be confused with critical slowing down [40]. Both properties are manifestations of criticality and both properties are characterized by the emergence of an inverse power law, which makes the survival probability not integrable. However, critical slowing down is a property of the thermodynamic limit, implying that the number of units N is virtually infinite, whereas temporal criticality is a finite size effect [45]. Temporal complexity, in the ideal case where the inverse power law is not truncated has to be thought of as a form of perennial out of equilibrium condition, which should force physicists to extend the linear response theories to the non-ergodic condition [35].

Note that the cooperator and the defector payoffs are determined by the states of the nearest neighbors. Thus, we have

$$\Pi_C = (1+\lambda)\frac{M_C}{M} - s\frac{M_D}{M} \tag{2.12}$$

and

$$\Pi_D = (1+t)\frac{M_C}{M} - \lambda\frac{M_D}{M}, \tag{2.13}$$

where M_C is the numbers of neighbors in the cooperative state and M_D is the number of neighbors in the defector state. We remind the readers that in this work $M = 4$. It is important to state that we evaluate also the financial benefit for the community by making an average over all possible pairs of interacting units, according to the prescription:

$$B_{ij} = 2, \tag{2.14}$$

if both units of the pair (i, j) are cooperators,

$$B_{i,j} = 1 + t - s, \tag{2.15}$$

if one unit of the pair (i, j) is a cooperator and the other is a defector,

$$B_{i,j} = 0, \tag{2.16}$$

if both units of the pair (i, j) are defectors.

Notice that the choice between the cooperation and defection state is done with $\lambda \geq 0$, while the financial benefits for the society are evaluated, as shown by Eqs. (2.14), (7.3) and (2.16), by setting $\lambda = 0$. This is so because λ, the psychological reward, is an incentive to cooperate that does not directly increase the social payoff, even if it has the eventual effect of increasing the society wealth by stimulating cooperation. In conclusion, the societal benefit Π is given by

$$\Pi = \sum_{(i,j)} B_{ij}, \tag{2.17}$$

denoting the sum over all possible pairs (i, j).

To define the *selfishness model* we set $\lambda = 0$ and we establish the interaction between the bottom and the top level by assigning a positive value to the coupling coefficient K_2. In this case, a cooperator is encouraged to adopt the cooperator state for a longer time if the financial benefit associated the choice of the cooperator condition, Π_C, is larger than the financial benefit Π_D, corresponding to selecting the defector state. The *success model* is established by setting both $\lambda = 0$ and $K_2 = 0$. The influence of the top on the bottom level is established by randomly selecting a fraction r of the total number L to allow each unit to adopt the strategy of the most successful nearest neighbor. Note that small values of r play the same role as small values of ρ_K in the selfishness model. The influence of morality on the selfishness model is studied by setting $\lambda > 0$, while keeping $\lambda = 0$ for the evaluation of the social benefit, as earlier stated.

2.4. Criticality-Induced Network Reciprocity

In Fig. 3.1 we show the social benefit as a function of K_1 when $K_2 = 0$, namely, the strategy choice is only determined by imitation. The social benefit in the supercritical regime is obviously maximal when all the units select the cooperation strategy and it vanishes when all the units select defection. Much more interesting is the social benefit for $K < K_{1c}$. We see that there is an increase of social benefit with increasing K_1. This is a consequence of

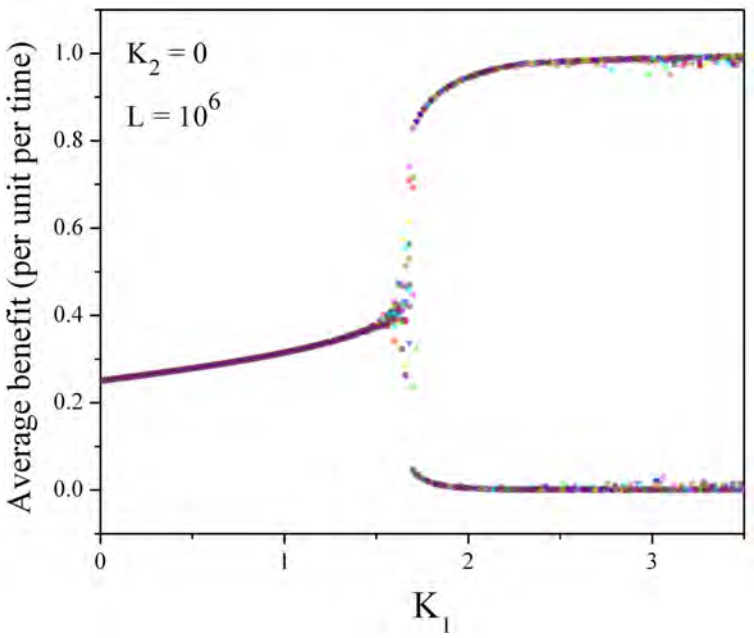

FIGURE 2.2. Social benefit as a function of K_1 when $K_2 = 0.10$ realizations had done. Notice that the social benefit increases upon increase of K_1 in the whole subcritical region.

the fact that imitation generates clusters of cooperators and clusters of defectors and the increasing social benefit is due to the increasing size of the clusters of cooperators.

The results of Fig. 3.2 support our claim. In fact, we see that the social benefit increases in a way that is qualitatively very similar to the increase of the number of units that have four neighbors in the same state, either cooperation or defection state. A cluster of units belonging to the same state increases as a function of K_1 with a prescription qualitatively similar to the increase of the number of units with four neighbors in the same state.

We now adopt the *success model*, namely, we perturb the imitation-induced strategy choice making the units pay some attention to the success of their nearest neighbors. We run the model for L time steps, and we randomly select 1% of them to update their strategy adopting the one of their most successful nearest neighbor. As earlier stated, we use a two-dimensional regular network, where each unit has 4 neighbors. The results illustrated by Fig. 2.3 are impressive. The adoption of the strategy of the most successful nearest neighbor has a very modest effect in the subcritical region. At criticality, on the contrary, the effects

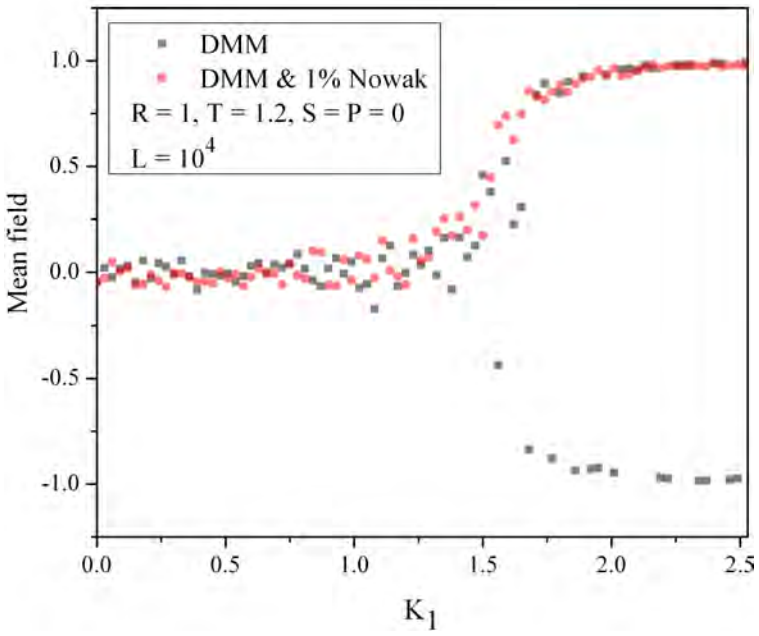

FIGURE 2.3. The mean field of the imitation model as a function of K_1 randomly selecting 0.1% of L steps to update the strategy of each unit by adopting the strategy of the most successful nearest neighbor.

of this choice become macroscopic and the imitation-induced phase transition, when the two branches, one with a majority of cooperator and one with a majority of defectors, are generated with equal probability, the success model selects the branch with a majority of cooperators. At very large values of K_1 this leads to the extinction of defectors. On the basis of the results done by our group on the DMM dynamics we make the very plausible conjecture that this effect is independent of the topology of the adopted network. In fact, moving from one topology to another has only the effect of reducing the intensity of the effort necessary to get consensus, the condition $K_1 = 1$ representing the ideal topology requiring the weakest effort to get consensus [36].

2.5. Morality Stimulus on the Selfishness Model at Criticality

As earlier mentioned the parameter λ is only a psychological benefit implying no direct financial benefit for society. We interpret λ as the strength of the influence that the

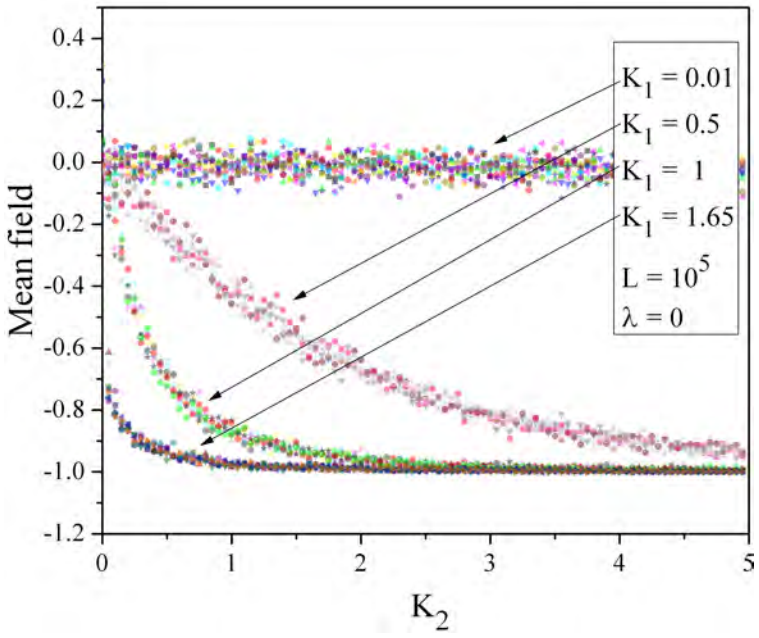

FIGURE 2.4. The mean field of the selfishness model as a function of K_2 for different values of K_1. We make ten realizations.

morality network has on the selfishness model.

Here we find the imitation-induced intelligence has a twofold effect. The collective intelligence is proved to lead to the abrupt extinction of cooperators, if $\lambda = 0$, and to the abrupt extinction of defectors when $\lambda = \lambda_c$. With the values of the parameters adopted here, $\lambda_c = 2.5$. Fig. 3.4, illustrating the effect of a strategy choice when $\lambda = 0$, shows that in the sub-critical regime a very large value of ρ_K is required for the extinction of cooperation. As we approach criticality, namely as the system becomes more and more intelligent, an even very weak interest for the personal financial benefit leads to the extinction of cooperators, which, in fact, is shown to occur for $\rho_K \approx 0.06$ when $K_1 = 1.6$.

The swarm intelligence of the system makes the model very sensitive to the influence of morality, as it is clearly shown by Fig. 2.5. We see, in fact, that as consequence of the imitation-induced criticality, the average social benefit undergoes a kind of first-order transition at $\lambda_c = 2.5$, with a jump from the lack of benefit to a very large value, when $K_1 = 1.65$ and $\rho_K \approx 0.12$. This indicates that the criticality-induced intelligence wisely turns the psychological reward for the choice of cooperation into a significant social benefit.

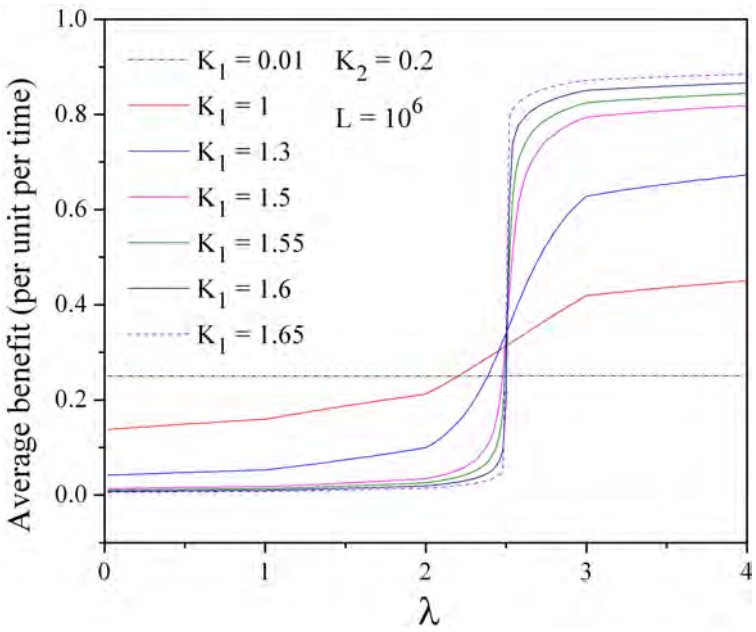

FIGURE 2.5. The personal benefit of the selfishness model as a function of λ. We make an average on ten realizations.

However, a value of λ too large may have the same bad effects as a value of λ too small. The corresponding cumulative probability is illustrated by Fig. 2.6, which shows that the distribution density of the time distances between two consecutive renewal events is an inverse power law with the power index $\mu = 1.5$ when $\lambda = \lambda_c = 2.5$ and it is an exponential function for both $\lambda < \lambda_c$ and $\lambda > \lambda_c$. This is a clear sign that the collective intelligence generated by criticality [40, 29, 41] is lost if the moral incentive to altruism λ is either weak or excessive.

2.6. Concluding Remarks

In conclusion we have proved that imitation-induced criticality has the effect of enhancing the phenomenon of network reciprocity. The adoption of the strategy of the most successful nearest neighbor not only protects the cooperator from extinction, as in the pioneer work of Nowak and May [1], but, at criticality, it annihilates the branch with the majority of defectors. If we adopt the selfishness model for the choice of strategy, the imitation-induced

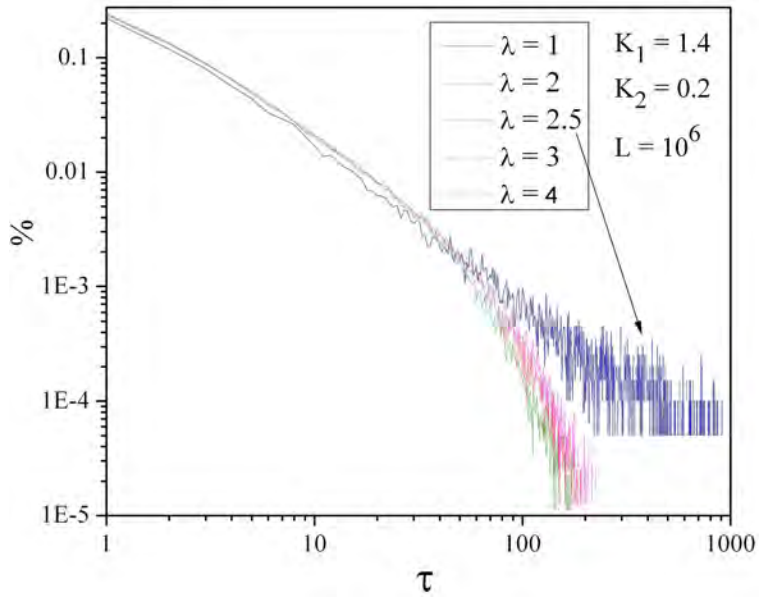

FIGURE 2.6. The cumulative probability of the time distances between two consecutive regressions to the origin.

criticality has the effect of favoring the extinction of cooperators. Under the influence of morality stimulus, however, imitation-induced criticality has the opposite effect of leading to the extinction of defectors. However, the temporal complexity of the system is lost for both $\lambda < \lambda_c$ and $\lambda > \lambda_c$, indicating, in accordance with Ahmed [44], that a condition of super-asabiyya is detrimental for human society as the lack of asabiyya.

CHAPTER 3

EVOLUTIONARY GAME THEORY AND CRITICALITY

Here we study a regular two-dimensional network of individuals playing the Prisoner's Dilemma game with their neighbors, assigning to each individual the adoption of two different criteria to make a choice between cooperation and defection. For a fraction $q < 1$ of her time the individual makes her choice by imitating those done by the nearest neighbors, with no payoff consideration. For a fraction $\epsilon = 1 - q$ the choice between cooperation and defection of an individual depends on the payoff difference between the most successful neighbor and her payoff. When $q = 1$ for a special value of the imitation strength K, denoted as K_c, the model of social pressure generates criticality. When $q = 0$ a large incentive to cheat yields the extinction of cooperation and a modest one leads to the survival of cooperation. We show that for $K = K_c$ the adoption of a very small value of ϵ exerts a bias in favor of either cooperation or defection, as a form of criticality-induced intelligence, which leads the system to select either the cooperation or the defection branch, when $K > K_c$. Intermediate values of ϵ annihilated criticality-induced cognition and, as consequence, may favor defection choice even in the case when a wise payoff consideration is expected to yield the emergence of cooperation.

3.1. Introduction

The unification of behavioral sciences is an attractive and challenging enterprise that would be impossible without using game theory [30]. The recent book by Gintis [30] aims at the unification of Behavioral Sciences, namely, at the ambitious purpose of unifying biology, psychology, economics, anthropology and political science, stressing however that game theory alone is not enough to realize this important goal. Nowak and May [1] have attracted the

This chapter was adapted from Mahmoodi, Korosh and Grigolini, Paolo, "Evolutionary game theory and criticality ", published on 30 November 2016 in Journal of Physics A: Mathematical and Theoretical, Vol. 50, 015101, with permission from IOP.

attention of an increasing number of researchers on *network reciprocity*, a special condition where spatial structure favors the emergence of cooperation, see also [31], in spite of its nodes playing the Prisoner's Dilemma game [32], with an incentive to defect. Actually, the players update their strategy with the criterion denoted in the literature [46, 47] as Unconditional Imitation (UI), which forces the individuals to select the strategy of the player with the maximal payoff in their neighborhood, including themselves. The adjective *unconditional* suggests that the choice of the largest payoff is not influenced by any inclination to either cooperate or to defect, thereby implying that the emergence of cooperation only depends on network reciprocity.

The assumption that the use of the UI alone thanks to network reciprocity may be a universal property for the survival of cooperation has been questioned by many authors [48, 49, 50, 51]. How to supplement the evolutionary game theory with dynamical properties that may overcome the limits of the Nowak and May UI? We find very promising the approach by Vilone *et al.* [47]. The players are the members of a society and as consequence they make the choice between cooperation and defection not only on the basis of UI, but, as wisely pointed out by the authors of Refs. [47], under a social pressure *without a rational background*. Thus, the single individuals make the choice between cooperation and defection strategy adopting the UI prescription with probability $1 - q$ and with probability q under the influence of their nearest neighbors, as prescribed the Voter Model (VM) [52].

This article is based on realizing the social pressure by means of the Decision Making Model (DMM) of [36], rather than through the VM. We note that both DMM and UI are decision making models with the main difference though, that UI focuses on payoff whereas DMM is merely based on imitation. To stress this difference we refer to DMM as Local Conformism Model (LCM).

To a first sight one may have the misleading impression that our proposal is essentially equivalent to that of Vilone *et al.* [47], since both LCM and VM belongs to universality class of Ising models. The authors of Vilone *et al.* [47] adopt a condition equivalent to the Ising model at zero temperature [52, 53] with the complex network moving towards the all

spin up condition with the average interface density $\rho(t)$ changing in time either as $t^{-1/2}$ (one-dimensional condition) or as $1/lnt$ (two-dimensional condition). We note that this is a form of critical slowing down and that the authors of Ref. [40] devoted some attention to make a clear distinction between *critical slowing down* and *temporal complexity*. The LCM model is characterized by a control parameter K, changing from $K = 0$, corresponding to the single individuals undergoing Poisson dynamics with no correlation the ones from the others, to a critical value K_c, at which a phase transition from disorder to order occurs, and beyond it. At criticality, when the total number of individuals N is very large, the mean field of the system, $x = (N_C - N_D)/N$, namely, the difference between the individuals selecting cooperation and those selecting defection divided by N, makes a regression to equilibrium from an initial out of equilibrium condition with the decay $t^{-1/2}$, which is critical slowing down. The important property of LCM, responsible for interesting social effects, is *temporal complexity* [54], which is a *small size* effect. Temporal complexity refers to the time distance between two consecutive regressions of the mean field x to the vanishing value. In a time scale smaller than $T_{eq} \propto \sqrt{N}$, corresponding to the time it takes the mean field to perceive the repulsive quartic potential generated by criticality [40], the time distance between two consecutive regressions to $x = 0$ is given by the waiting time distribution density $\psi(\tau) \propto \tau^{-0.5}$, which must not be confused with critical slowing down [40]. Temporal complexity is closely related to the criticality-induced long-range correlation establishing a form of interaction between individuals acting at large distance the ones from the others [55]. These individuals are the nodes of a network, and the distance between two nodes is evaluated counting the minimal number of links to go through to move from one to the other nodes. The network topology influences the critical value K_c, namely the strength of the social pressure necessary to get consensus, but temporal complexity, long-range correlation and the double-well potential created by criticality are conjectured to be independent of the network topology. Furthermore, although the intensity of the correlated fluctuations generated by temporal complexity tends to vanish for $N \to \infty$, there exists a crucial value N_{min}, below which no phase transition occurs and no form of dynamical complexity emerges

[56, 57].

In this article each individual uses UI for a randomly selected fraction $\epsilon < 1$ of her time. We show that criticality may produce big effects even if the condition $\epsilon \ll 1$ is adopted. Note that the parameter ϵ is related to the parameter q of Vilone [47] by the relation $\epsilon = 1-q$ so as to emphasize the originality of this article compared to the model of Vilone *et al.* [47], where the small parameter producing big effects is q rather than ϵ. We show that, thanks to the criticality of LCM social pressure, the individuals of this model playing UI for even a small fraction of their time, $\epsilon \ll 1$, make all the social network sensitive to the choices that the system would do with $\epsilon = 1$, with the impressive effect of suppressing either the branch of cooperators or the branch of defectors, while with $\epsilon = 0$ both branches occur with equal probability [40]. This is a form of intelligence that we refer to as criticality-induced intelligence. A solid foundation of this form of intelligence is given by the results of numerical experiments Refs. [40, 54, 55, 56, 57, 40, 58], but hereby we use the figures of Section 4 and Section 5 to explain these properties with intuitive and qualitative arguments.

To make the role of criticality more evident we do not limit our discussion to the condition of very small ϵ but we move from $\epsilon = 0$, where only the imitation-induced social pressure is active, to $\epsilon = 1$, where the systems evolves only under the influence of UI. Note that we denote by N, as earlier mentioned, the total number of players and by T the number of time steps we run the dynamical model. Throughout the whole article we adopt $N = 1024$ (namely, we use a two-dimensional regular network of size 32) and $T = 10^6$.

3.2. Local Conformism Model (LCM)

With probability q we adopt the *Decision Making Model* of Ref. [36], here referred to as Local Conformism Model (LCM). The transition rate from cooperation to the defection, g_{CD}, is given by

$$g_{CD} = g_0 exp\left[-K\left(\frac{M_C - M_D}{M}\right)\right] \tag{3.1}$$

and the transition rate from defection to the cooperation, g_{DC}, is given by

$$g_{DC} = g_0 exp\left[K\left(\frac{M_C - M_D}{M}\right)\right]. \tag{3.2}$$

The meaning of this prescription is as follows. The parameter $1/g_0$ defines the time scale and we set $g_0 = 0.1$ throughout. We consider N individuals. Each individual has M neighbors (four in the case of the regular two-dimensional lattice used in this article). If the individual is in C, and the majority of its neighbors are in the same state, then the transition rate becomes smaller and the individual sojourns in the cooperation state for a longer time. If the majority of its neighbors are in D, then the individual sojourns in the cooperator state for a shorter time. Analog prescription is used if the individual is in the defection state. We evaluate

Fig. 2.1 illustrates the second-order phase transition generated by the LCM, when $q = 1$. This corresponds to the condition where no bias exists for the choice of either cooperation or defection. In the initial condition the N individuals of the network are randomly assigned to either the cooperation or the defection state with the same probability, making zero the average over many realizations. Fig. 2.1 shows the mean field of ten single realizations. We run the LCM for the time T and at time T we evaluate

$$x(T) \equiv \frac{\sum_i^N \xi_i}{N}, \tag{3.3}$$

where $\xi = 1$ or $\xi = -1$, according to whether the $i - th$ individual is in the cooperation or in the defection state, respectively. Of course, due to the fact that, as earlier stated, we are using a finite number of individuals, $N = 1024$, the mean field fluctuates around the vanishing mean value.

Note that at $K = K_c$ the individuals move from a dynamical condition where they are virtually independent the ones from the others to a condition where global order emerges. In the two-dimensional regular lattice of this article $K_c \approx 1.5$.

It is important to stress that the single realizations for $K < K_c$ fluctuate around $x = 0$ and for $K > K_c$ they fluctuate around non-vanishing equilibrium values [40]. As discussed in Ref. [40], the time evolution of $x(t)$ is equivalent to the motion of a particle in

an over-damped potential and at $K > K_c$ this potential turns into a double-well potential, with the two wells, one corresponding to the C state, and one corresponding to the D state, separated by a bell-shaped barrier. The choice of the initial condition $x = 0$ locates the system at the top of the barrier and a very weak erratic fluctuation makes the system fall with equal probability either into the state C or into the state D, the top and the bottom branch of Fig. 2.1, respectively. An external field of intensity larger than this fluctuation can make the system select either the state C or the state D and with enough large intensity it can lead to the complete extinction of the other state. The main result of this article is that a very small probability ϵ of adopting UI makes the system select either the state C or the state D as effect of criticality-induced intelligence. This is a dynamical process that is impressively different from the action of an external field on a Ising-like phase transition process.

We notice that in the region $K \sim K_c$ the fluctuation intensity is larger, in accordance with the results of Refs. [40, 54, 55, 56, 57, 40, 58]. This is the region characterized by long-range correlation [55] generating criticality-induced intelligence, termed as swarm intelligence in Refs. [29, 30]. This is a form of Turing intelligence [39] allowing the lookout birds of a flock to communicate to all the other individuals the arrival of a predator [29, 30]. In this article the LCM-induced swarm intelligence makes it possible for the small number of individuals adopting at a given time the UI directions to transmit their choice to all the other individuals, with the effect of generating a bias that can be mistaken as being equivalent to an external field. In fact, increasing the parameter ϵ makes the dynamics of this system depart from the swarm intelligence condition with the consequence of conflicting with the UI direction.

3.3. Unconditional Imitation Model (UI)

As well known [32], Prisoner's Dilemma game rests on the crucial inequality $T > R > P > S$, where R denotes the reward that a cooperator gets when playing with another cooperator. The parameter $T > R$ is the payoff of a defector: it is larger than R thereby $t = T - R$ is a measure of the temptation to cheat. S is the payoff of a cooperator playing

with a defector, and $P < R$ is the payoff of a defector playing with another defector. The condition $2R > T + S$ indicates that the community gets a higher benefit from the play between two cooperators than from the play between a cooperator and a defector. The play between two defectors yields the societal benefit 2P that, due to the condition $P < R$ is less beneficial to society than the play between two cooperators, in spite of the incentive to defect. We adopt the choice made by Gintis [30] and we set $R = 1$, $P = 0$, $T = 1 + t$ and $S = -s$. Let us assume now that the individuals of our network play this game with their 8 nearest neighbors and that they select their strategy according to an updated version of the Nowak and May UI [59] that from now on we shall refer to as probabilistic UI. Notice that this version of UI is less favorable to cooperation than the deterministic version of Ref. [31]. In this version the players adopt the strategy of the most successful neighbor with a probability equal to the ratio of the difference between the payoff of the most successful player and their own payoff to the sum of the absolute values of these two payoffs, if the payoff of the successful player is larger that their own payoff. If it is smaller, they keep their strategy. In the model of Ref. [31], termed by us as deterministic UI, the payers adopt with no uncertainty the strategy of the most successful neighbor and keep their strategy if they are the most successful players of their environment. The main result, illustrated in Section 4, rests on the use of probabilistic UI, but, as stressed in Section 5, the use of deterministic UI yields identical results.

Fig. 3.1 compares the probabilistic to the deterministic model, showing the mean field as a function of (t, s) at time $T = 10^6$. It is evident that the (t, s) region generating a large majority of cooperators, and so a large mean field close to 1, intense yellow squares, is much broader in the case of deterministic UI. The sea dominated by defectors, intense blue squares, is less extended and hosts many cooperation islands. Furthermore we notice that the patterns of cooperators are unpredictable, this being a consequence of the spatial chaos pointed out by the authors of Ref. [31]. In other words, the deterministic UI favors cooperation much more than the probabilistic UI.

The individuals of our model use the portion ϵ of their time to perceive the influence

of UI. In Fig. 2 we select three indicator points, a, b and c, for the purpose of defining a moderate influence in favor of cooperation, a, a strong influence in favor defection, b, and a strong influence in favor of cooperation, c. Notice that the mean field corresponding to a is: $x(T) = 0.5$, probabilistic UI, $x(T) = 0.9$, deterministic UI. The mean field corresponding to b is: $x(T) = -1$ for both probabilistic and deterministic UI. The mean field of c is: $x(T) = 1$, probabilistic UI; $x(T) = 0.9$, deterministic UI. Notice that the moderate influence in favor of cooperation of the probabilistic UI is selected to be smaller than the moderate influence in favor of cooperation of the deterministic UI. In the deterministic case the mean field moves from 1 and it will remain close to 1 before dropping to values close to -1. This is the reason why the moderate field in favor of cooperation of the deterministic UI is significantly larger than moderate field of the probabilistic UI. The strong influence in favor of cooperation of the probabilistic UI has intensity larger than the strong influence in favor of cooperation of the deterministic case. The readers have to keep in mind these choices to fully appreciate the results of Section 5.

The annihilation, illustrated in Section 4, of either the D or the C branch of Fig. 1, as an effect of a bias in favor of cooperation or defection, is discussed using the probabilistic UI (no change occurs using the deterministic UI). For this reason here we limit ourselves to make comments on the points a, b and c of the left panel of Fig. 2. The points $a = (0.2, 0.2)$ and $b = (0.3, 0.3)$ correspond to two crucial conditions illustrated in Fig.2, the first being compatible with the survival of cooperators, while the second, already imbedded in the defection (blue) region, due to the large incentive to cheat and the large punishment to the sucker, yields extinction of cooperators and the mean field close to $x(T) = -1$. In Section 3.4 we show that the joint action of LCM and UI makes condition b produce effects symmetric to those of condition a, in spite of the fact that the modulus on the negative field b is smaller than the positive field of a. We consider also the condition $c = (0.1, 0.1)$ which strongly favors cooperation. The numerical calculations of this article show that the response to the bias of a is virtually indistinguishable from the response to the bias of c, thereby suggesting that the swarm intelligence is sensitive only to the sign of the bias. The

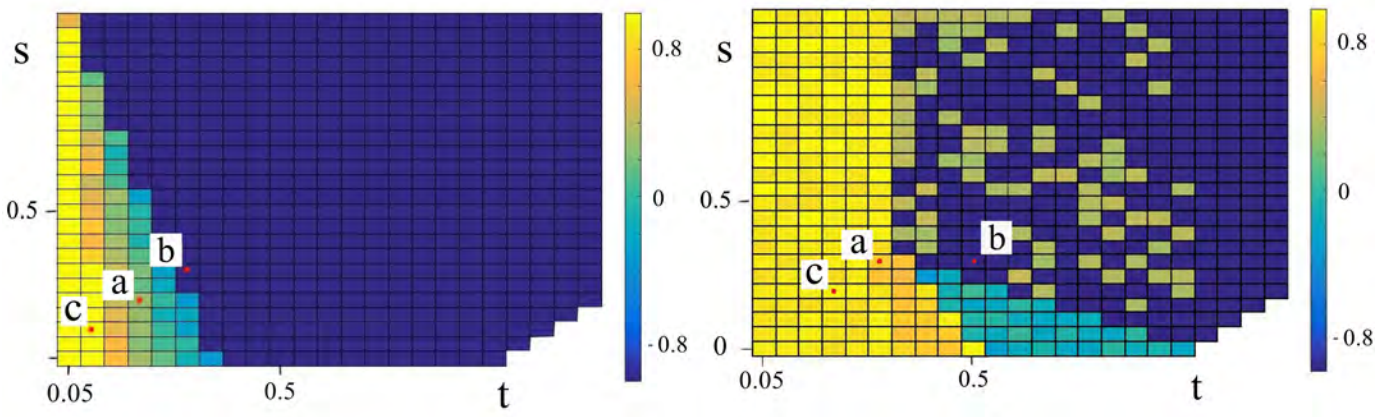

FIGURE 3.1. Mean field of individuals playing only UI at time $T = 10^6$, probabilistic UI, left panel; deterministic UI, right panel. One realization for each (t,s). The points a, b and c are the indicators of three different kind of influences exerted by UI on the individuals playing it. Probabilistic UI, $a = (0.2, 0.2)$, $b = (0.3, 0.3)$ and $c = (0.1, 0.1)$; Deterministic UI, $a = (0.3, 0.3)$, $b = (0.5, 0.3)$, $c = (0.2, 0.2)$.

swarm intelligence makes the system select either the cooperation branch or the defection branch as an effect of criticality-induced cognition, if ϵ if very small. Section 3.5 shows that the effect of increasing ϵ is impressively different from that of an external field on an Ising-like model. This is a consequence of the fact that LCM disrupts the action of UI, in the absence of criticality-induced cognition.

Notice that the main purpose of UI is to explain why society makes the choice of social benefit with individuals paying attention to their payoff, and the purpose of this work is to prove that, thanks to criticality, the social pressure exerted by LCM may confirm this choice. We evaluate the social benefit for the community, independently of either UI or LCM, or of their joint use, by making an average over the payoff B_{ij} of all possible pairs of interacting neighbors, according to the prescription $B_{ij} = 2$, if both individuals of the pair (i, j) are cooperators, $B_{ij} = 1 + t - s$, if one individual of the pair (i, j) is a cooperator and the other is a defector, and finally $B_{ij} = 0$, if both individuals of the pair (i, j) are defectors.

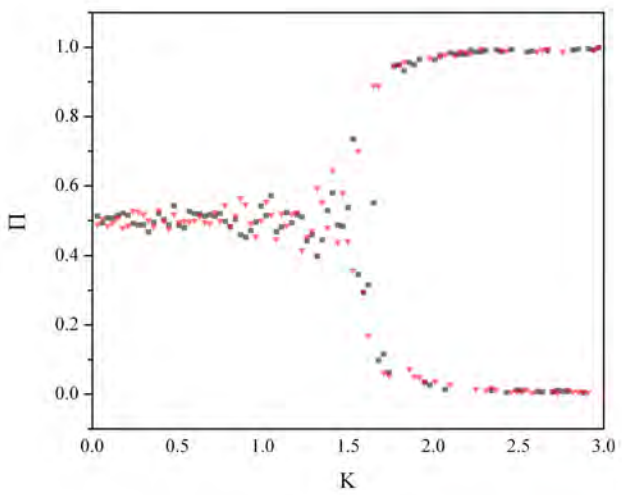

FIGURE 3.2. The social benefit generated by the use of the LCM social pressure alone. It is evaluated using Eq.(4.6). The red triangles correspond to $a = (0.1, 0.1)$ and the black squares correspond to $b = (0.3, 0.3)$ of the left panel of Fig. 2.

In conclusion, the societal benefit Π is given by

$$\Pi = \frac{\sum_{(i,j)} B_{ij}}{4N^2}, \tag{3.4}$$

with the sum being done, as earlier mentioned, over all possible pairs (i, j).

This allows us to turn the bifurcation structure of Fig. 1 into to social benefit bifurcation of Fig. 3, obtained playing only LCM and evaluating the corresponding social benefit with Eq. (4.6). We see that the selection of the cooperation branch yields the maximal social benefit as possible for $K \gg K_c$ and the selection of the defection branch leads to no social benefit in the same limit, as a consequence of the fact that according to Prisoner's Dilemma model defectors benefit from cooperators and the extinction of cooperators yields no payoff for defectors.

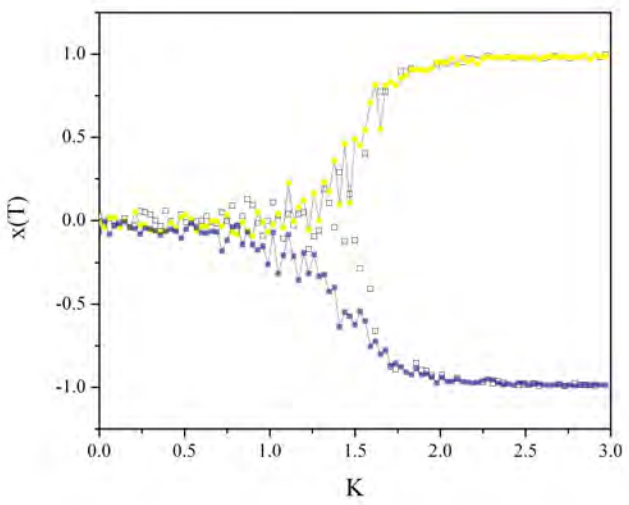

FIGURE 3.3. The mean field as a function of K. The empty squares correspond to $\epsilon = 0$. The yellow squares correspond to $\epsilon = 0.01$ with the condition $a = (0.2, 0.2)$ of Fig. 3.1. The blue squares correspond to $\epsilon = 0.01$ with the condition $b = (0.3, 0.3)$ of Fig. 3.1.

3.4. Joint Action of LCM and UI

This Section shows the main result of this article. Hereby we study the joint action of social pressure and probabilistic UI. Each individual of the network adopts LCM for most of time and probabilistic UI for a randomly selected fraction $\epsilon = 0.01$ of it. Note that UI in the absence of the social pressure would generate the mean field of the top-left panel of Fig. 3.1.

Fig. 3.3 shows that the condition $a = (0.2, 0.2)$, favoring in Fig. 3.1 the survival of cooperators, annihilates the branch of defectors, whereas the condition $b = (0.3, 0.3)$, which in the absence of social pressure, as shown by Fig. 3.1, would fill the whole network with defectors, annihilates the branch of cooperators. The adoption of the condition $c = (0.1, 0.1)$ generates effects virtually indistinguishable from those of condition $a = (0.2, 0.2)$. Plotting these results would have made Fig. 4 blurring and for this reason we plot only the results produced by condition $a = (0.2, 0.2)$.

It is impressive that such a modest use of probabilistic UI, namely the individuals using this UI for only 1% of their times, generates the visible departure illustrated by Fig. 3.3, from the unbiased phase transition. However, these macroscopic effects are a natural consequence of the LCM properties discussed in the earlier work of Refs. [40, 54, 55, 56, 57, 40, 58].

Let us use intuitive and qualitative arguments to explain these results, examining first the supercritical condition. For $K > K_c$ the system selects either the state C or the state D as an effect of a very weak fluctuation, with no bias. The small fraction $\epsilon = 0.01$ of time spent by the individuals under the influence of the UI with a bias favoring cooperation, condition $a = (0.2, 0.2)$, is large enough as to overcome the fluctuations that may make the system fall in the D state. On the same token, the small fraction $\epsilon = 0.01$ of time spent by the individuals under the influence of the UI prescription with a bias favoring defection, condition b, is large enough as to overcome the fluctuations that may make the system fall in the C state.

At $K = K_c$ there is no barrier, and it is apparently more difficult to explain why a small bias may lead the system to select the upper or bottom branch. This is where we must invoke the criticality-induced swarm intelligence discussed in [29, 30]. The authors of Refs. [29, 30] showed that at criticality a small number of lookout birds can make the system adopt their choice. The lookout birds are a small fraction of individuals who perceive, for instance, the arrival of a predator, and select the flying direction permitting them to avoid a danger. The criticality-induced long-range correlation allows them to transmit this information to all the other individuals, thereby making it possible for the whole swarm to avoid the danger. In this article the individuals adopting the probabilistic UI perceive the benefit of the cooperation choice, condition $a = (0.2, 0.2)$, and transmit the convenience of selecting cooperation to all the other individuals, thereby making the whole system select the cooperation branch. On the same token, if the probabilistic UI yields condition $b = (0.3, 0.3)$ favoring the extinction of cooperators, social pressure-induced criticality makes all the individuals aware of the personal convenience of adopting defection, thereby generating

the extinction of the cooperation branch.

We do not illustrate the effect of using the deterministic UI, which generates the same extinction process of the branch of defector, if the condition a is used, and of the branch of cooperator if the condition b applies. However, in Section 5 we show also the deterministic UI in action for the main purpose of making our arguments on the role of criticality much more compelling.

3.5. Illustration of Criticality Effects

The main aim of this Section is to prove with additional numerical results that changing the intensity of the parameter ϵ is not equivalent to changing the intensity of an external field acting on a Ising-like phase transition process. For extremely small values of ϵ the probabilistic UI exerts a small bias on the system, in favor of either the C or the D state, and the intensity of this bias does depend on the intensity of the mean field generated by the probabilistic UI. As earlier mentioned, the adoption of condition $c = (0.1, 0.1)$ for very small values of ϵ makes the extinction of the defection branch indistinguishable from that generated by the adoption of condition $a = (0.2, 0.2)$.

Fig. 5 allows us to establish that the phenomenon of criticality-induced cognition requires that $\epsilon < 0.1$. We notice, first of all, that, in a qualitative accordance with Vilone, [47], the social pressure on the UI choice has the effect of disrupting the effects of UI dynamics. The mean field generated by UI alone is either positive, condition a and c , or negative, condition b. The use of a very small value of q has the effect of decreasing the intensity of the mean field, in the first two cases, and of increasing it in the last case. Moving from $\epsilon = 1$ to $\epsilon = 0$ corresponds to move from the action of UI alone to the action of LCM alone. This has the effect of producing a behavior quite different from that earlier found from Vilone *et al.* [47].

Let us consider the condition a, top panel of Fig. 5, and the adoption of probabilistic UI first, namely, more precisely, the top-left panel of the same figure. We notice that the blue curve, illustrating the mean field at criticality, moves from the value 0.5, determined by

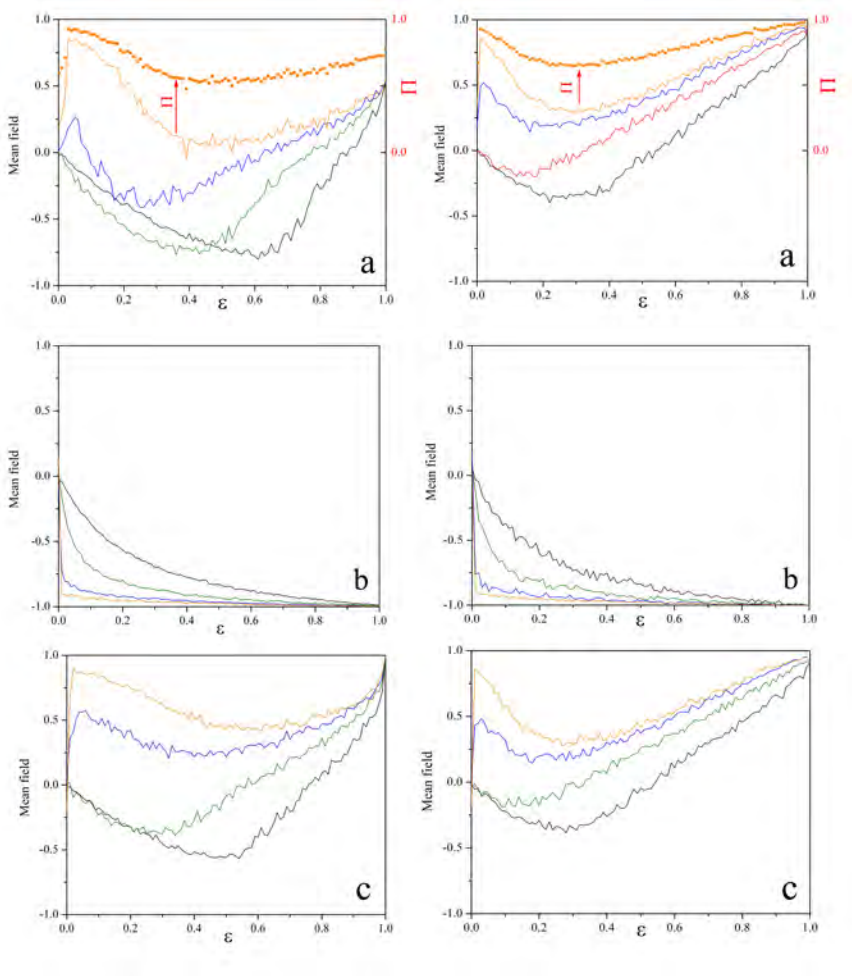

FIGURE 3.4. The mean field as a function of ϵ for different values of K. In the top panel, in addition to the mean field we illustrate also, using orange squares, the social benefit Π of Eq. (4.6) corresponding to $K = 1.8$, the intensity of which is defined in the right ordinate . In all the panels the colors orange, blue, green and black refer to $K = 1.8$, $K = 1.5$, $K = 1$ and $K = 0.1$, respectively. The top, middle and bottom panel lllustrate the mean field as a function of ϵ for the conditions a, b and c, of Fig. 2, respectively.

the probabilistic UI to smaller values upon decrease of ϵ. The disruption effect, in qualitative accordance with the numerical results of Vilone *et al.* [47], yields a fast decrease of the mean field that makes it become negative. However, at criticality, when $\epsilon = 0$ is adopted, the mean field must vanish. As a consequence of that the dependence of the mean field on ϵ

is not monotonic. At about $\epsilon = 0.2$ a minimal value is reached and a further decease of ϵ is expected to yield an increase of the mean field. This is, in fact, what we can see in the top-left panel of Fig. 5. However, the mean field at about $\epsilon = 0.08$ is positive. This peak is not a statistical fluctuation, but it is the manifestation of swarm intelligence. About 8% of individuals perceive the indication that the system should move to the positive mean field of about 0.5, to get the largest payoff. The number of the other 92% individuals is large enough as to properly maintain the phase-transition structure of LCM, and especially the condition of temporal complexity occurring at $K \approx 1.5$. This is the real reason why the mean field gets a value that is approximately equal to 0.25. Smaller values of ϵ generate smaller positive mean field, this being the main reason why at bifurcation the system selects the cooperation branch.

Let us move to consider the orange curve, corresponding to the supercritical value $K = 1.8$. In this case when $\epsilon = 0$, the mean field generated by the LCM is about 0.75, significantly larger than the equilibrium mean value of 0.5 established by the probabilistic UI. Yet, also in this case the disrupting action of LCM makes the mean field decrease with the decrease of ϵ from the maximal value of 1. At about $\epsilon = 0.4$ an inversion occurs, and for values of ϵ of the order of 0.01, the system adopts the value of the mean field of about 0.6 of the cooperation branch, corresponding to $K = 1.8$, as shown in Fig. 4.

It is interesting to notice that the same non-monotonic behavior is generated in the subcritical region. In this case, however, the disruptive action of LCM combined with the lack of cognition of the subcritical condition makes the mean field remain negative for the whole range from $\epsilon = 0$ to $\epsilon \approx 0.8$. This is a clear consequence of the lack of cognition: preventing the emergence of cognition favors defection.

It is interesting to notice that the adoption of the condition $b = (0.3, 0.3)$ at criticality yields a monotonic behavior. This is a consequence of the fact that in this case the disruption action of LCM generates an increase of the mean field. The equilibrium value of the probabilistic UI is negative and, at criticality, the LCM mean value vanishes. Thus, in this case the disruptive nature of LCM makes the system move in a monotonic way towards

the vanishing mean field generated by the action of LCM alone. Yet, also in this case the adoption of the supercritical condition $K = 1.8$ makes the system move from probabilistic UI mean field to the LCM mean field of the defection branch that is very close to -1.

Finally, let us discuss condition $c = (0.1, 0.1)$, the left panel of Fig. 2. The illustration of the effect of social pressure on this condition, shown in the bottom-left panel of Fig. 5, explains why the numerical calculation done to get Fig. 4 makes condition $c = (0.1, 0.1)$ virtually identical to condition $a = (0.2, 0.2)$. In fact, we see that this condition yields a dependence on social pressure qualitatively identical to that of the top-left panel of the same figure, corresponding to a weaker UI field. The consequence of this condition is that when the value $\epsilon = 0.1$, where swarm intelligence becomes active, the mean field is larger than 0.5, whereas in the top panel is about 0.25. The swarm intelligence makes the system aware of the financial benefit of cooperation. However, with $\epsilon = 0.01$ the mean field is significantly smaller and this is the reason why in Fig. 4 it would be impossible to see the difference between the two conditions.

The adoption of the deterministic UI (top-right, middle-right and bottom-right of Fig. 5) yields results confirming the crucial role of criticality as a generator of intelligence. In fact, also in this case we have a non monotonic dependence of the mean field $x(T)$ on the parameter ϵ for both top and bottom panel and a monotonic behavior with the middle panel. It is impressive that the criticality-induced intelligence yields effects that are very sensitive to the intensity of the UI influence. In fact, as mentioned in Section 3, for condition a the deterministic mean field $x(T)$ is 0.9, to be compared to the value 0.5 of the probabilistic UI. As a consequence, the bump emerging after inversion of the mean field upon decrease of ϵ, corresponds to the mean field getting the value of about 0.5, to be compared to the corresponding value of about 0.25 of the left panel. This maximum is reached with $\epsilon \approx 0.06$ versus the corresponding value of the left panel, which is $\epsilon \approx 0.04$. In this case the criticality-induced intelligence is generated by about 96% of the individuals playing LCM, to be compared to about the 94% of the individuals of the corresponding case of the top-left panel. In the bottom panel the reverse condition applies. As pointed out in Section 3,

for condition c the deterministic UI influence is exerted through a mean field $x(T) = 0.8$, which is smaller than the corresponding value of $x(T) = 1$ of the bottom-left panel, and, as a consequence, the intensity of the criticality-induced peak is slightly smaller than 0.5, whereas the corresponding value of the bottom-left panel is significantly larger than 0.5.

3.6. Concluding Remarks

In this article we benefit from the adoption of the proposal of Vilone *et al.* [47], but the adoption of LCM to establish the social pressure has the effect of creating a form of cognition that makes all the individuals realize the social benefit of cooperation or the personal convenience of selecting defection. This is a consequence of the fact that we rest on the criticality of LCM, whereas Vilone *et l.* [47] adopt the VM in the condition corresponding to the Ising model at vanishing temperature, with no temporal complexity.

Increasing the value of ϵ has the effect of perturbing the dynamics of LCM. As a consequence the criticality-induced swarm intelligence is reduced or even completely annihilated with the effect of favoring defection also in the case where the probabilistic UI dynamics would favor cooperation. The main result of this article, Fig. 4, is obtained using the probabilistic UI, but the adoption of the deterministic UI [1], which is more favorable to cooperation, yields a virtually identical result.

On the basis of the earlier work of Ref. [58] changing network topology has the effect of increasing or reducing the imitation effort K to reach criticality. However, the criticality-induced effects illustrated in this article are expected to be independent of the network topology.

It is important to stress that criticality-induced temporal complexity has also the effect of making the complex network flexible [40, 40, 30, 41]. This is the reason why a complex network at criticality is sensitive to the influence of other networks at criticality. However, this important aspect of criticality is beyond the purpose of this article, even if we believe that future research work will prove it to be very important for the field of evolutionary game theory.

The content of this work can be summarized as follows. The individuals of a society make decision on the basis of two processes, the blind imitation of the choices made by the neighbors and the imitation of most successful neighbor. This second kind of choice, called UI, may lead to the cooperation choice, if the incentive to cheat is not too large. However, the big problem to address in this case is as to the cooperation decision is made also when the choices of the single individuals are mainly determined by a fully blind social pressure. One may expect that the social pressure may annihilate the benefits of social reciprocity. This work shows that it is not so if the social pressure is established through the LCM at criticality. The conclusion is therefore that criticality is an important property that the rapidly evolving field of evolutionary game theory should take into account.

CHAPTER 4

SELF-ORGANIZING COMPLEX NETWORKS: INDIVIDUAL VERSUS GLOBAL RULES

We introduce a form of Self-Organized Criticality (SOC) inspired by the new generation of *evolutionary game theory*, which ranges from physiology to sociology. The single individuals are the nodes of a composite network, equivalent to two interacting subnetworks, one leading to strategy choices made by the individuals under the influence of the choices of their nearest neighbors and the other measuring the Prisoner's Dilemma Game payoffs of these choices. The interaction between the two networks is established by making the imitation strength K increase or decrease according to whether the last two payoffs increase or decrease upon increasing or decreasing K. Although each of these imitation strengths is selected selfishly, and independently of the others as well, the social system spontaneously evolves towards the state of cooperation. Criticality is signaled by temporal complexity, namely the occurrence of non-Poisson renewal events, the time intervals between two consecutive crucial events being given by an inverse power law index $\mu = 1.3$ rather than by avalanches with an inverse power law distribution as in the original form of SOC. This new phenomenon is herein labeled self-organized temporal criticality (SOTC). We compare this bottom-up self-organization process to the adoption of a global choice rule based on assigning to all the units the same value K, with the time evolution of common K being determined by consciousness of the social benefit, a top-down process implying the action of a leader. In this case self-organization is impeded by large intensity fluctuations and the global social benefit turns out to be much weaker. We conclude that the SOC model of this work fits the requests of a manifesto recently proposed by a number of European social scientists.

This chapter was adapted from Mahmoodi, Korosh and West, Bruce J and Grigolini, Paolo, "Self-organizing Complex Networks: individual versus global rules", published on 07 July 2017 in Frontiers in physiology, Vol. 8, 478, Open access.

4.1. Introduction

One of the main goals of computational social models is to quantify the mechanisms generating the emergence of collective behavior of social groups. A particularly useful modeling tool in this regard has been evolutionary game theory. This tool was used to explain the emergence and survival of cooperation in society, in contrast to the widely recognized selfish character of single individuals. Axelrod and Hamilton [32] have addressed the apparent contradiction and their work has drawn the attention of an increasing number of researchers to the surprising condition that altruism may have originated much earlier than the dawn of human civilization. Altruism may, in fact, correspond to the birth of life itself, although the concepts of kinship and reciprocity, widely adopted in game theory, seem to refer to complex social networks and not to individuals. In fact, Axelrod and Hamilton based their life evolution study on the use of the Prisoner's Dilemma game, with its crucial conflict between the individual's temptation to cheat and to act in the community's benefit, a model that seems to apply only to human society.

More recently, evolutionary game theory concepts, which were apparently introduced to discuss the social effect of public good, are used to gain insight into enzyme chemistry processes [60]. Another sociological concept, currently adopted to illustrate the conflict between the use of limited shared resources and individual self-interest [61], "the tragedy of the commons", has been used [62] to discuss the evolution of cooperation in ecological networks.

The argument of network reciprocity, in the form illustrated by Nowak and May [1], rests on the observation that in a network of cooperators and defectors, the richer environment of cooperators prevents the spreading of defectors. This argument has been questioned by some, noting the social activities in which the individuals are engaged, who are also involved in playing the Prisoner's Dilemma game. The additional social interaction of the individuals within this social group was found to disrupt network reciprocity [47]. However, when this additional activity is based on individuals imitating the choices made by their nearest neighbors, it may favor the survival of cooperation [63]. This survivability

is a consequence of the imitation strength being sufficiently strong to generate criticality as in the Decision Making Model (DMM) [36].

The criticality condition exploited by Mahmoodi and Grigolini [63] is obtained by tuning the imitation strength to the theoretical value that in the limiting case of an infinitely large network is expected to be determined by an Ising-like prescription, since the DMM used is in the Ising universality class [36]. Criticality entails long-range correlation among the members of the society, even those communicating solely by means of nearest-neighbor interactions. Such criticality has been interpreted as a form of global intelligence, identified as *swarm intelligence* [29], a phenomenon that may be shared by microbial communities and mechanisms of carcinogenesis as well as, by neural systems [64]. In the specific case of individuals playing the Prisoner's Dilemma game, the criticality-induced swarm intelligence enables the members of society to become aware of the benefits of network reciprocity, and thereby biases their interactions to favor, rather than disrupt, this network property [63].

The manifesto of computational social science [65] relies on the assumption that criticality is a consequence of self-organization, and thereby implies that social criticality is a form of self-organized criticality (SOC). A word of caution is appropriate here, now that the term SOC has been used. A 25-year review of the concepts and controversies surrounding SOC [66], emphasize that SOC occurs in open, extended, dissipative dynamical systems that automatically go to the critical state. This is distinct from a continuous phase transition where *at a critical point* correlations become long-range and are characterized by an inverse power-law (IPL) probability density function (PDF). In order to arrive at the critical point an external control parameter, such as temperature, must be fine-tuned to its critical value. We refer to that control parameter with the symbol K. On the other hand, SOC occurs universally where any fine-tuning is accomplished by means of its internal dynamics [67]. This independence from an external tuning is the defining property of a SOC phenomenon.

The emergence of SOC is usually signaled by the births of anomalous avalanches, see [68] and [69] for more recent work. Here we illustrate a form of SOC based on the spontaneous search for the critical value of the parameter K, which is selected by the network

through a *bottom up* process, that is, through the dynamic behavior of the individuals and is not externally imposed. The main signature of self-organized criticality is the time interval between two crucial events, with a non-exponential waiting time probability distribution density (PDF), a property referred to as *temporal complexity* in earlier work [54]. *We therefore refer to the form of SOC developed as self-organized temporal criticality (SOTC).* The crucial events are defined by comparing the variable $K(t)$ to its time average $\overline{K}$ and are identified with the variable $\zeta = K(t) - \overline{K}$ changing sign.

We emphasize that the form of SOTC is realized in full accordance with the spirit of the Axelrod and Hamilton [32] theoretical perspective. In fact the payoff of the choices made by the individuals of the composite network is established using the Prisoner's Dilemma game, without neglecting the incentive to defection. The choice of the strategy to adopt is determined by the individual's imitation of the choices made by their nearest neighbors. The single units only decide to increase or decrease their tendency to imitate these choices according to whether on the basis of the last two payoffs this imitation increased or decreased the benefit to them as an individual. This indirect and apparently blind strategy choice does not disrupt the beneficial effects of network reciprocity [1], but it is a way of efficiently establishing the reciprocity condition hypothesized by Axelrod and Hamilton [32].

Returning to the SOTC issue, we stress that the imitation strength K is not a conventional fine tuned control parameter, that is artificially fixed to make the network achieve criticality. The parameter K is freely selected by the dynamics of the network itself.

The numerical calculations presented herein show that increasing the dependence of the individuals on the strategic choices of their neighbors has the effect of increasing their payoff. Imitation of the choices of their neighbors is a form of social interaction that is made at the level of the individuals and is not forced upon them in a top-down process. There exists a parameter, call it χ, which determines the rate of change of K, as a function of the last two payoffs. However, no recourse is made to the fine tuning of this parameter, insofar as changing χ has only the effect of influencing the time scale of the process of transition to altruism. This is, as we show, a bottom-up process that generates self-organization,

and along with self-organization generates swarm intelligence, with the ultimate effect of increasing the wealth of society, thereby affording strong support to the increasing conviction that real social improvements do not require the action of benevolent dictators [70, 71].

4.2. The Prisoner's Dilemma Game

This section is devoted to illustrating the criteria adopted in the subnetwork of logical choices to evaluate the payoff associated to the cooperation or the defection choice. This is done using the Prisonner's Dilemma game. This game was originally introduced as a metaphor for the problems affecting the emergence of cooperation [32]. Two players interact and receive a payoff from their interaction adopting either the defection or the cooperation strategy. If both players select the cooperation strategies, each of them gets the payoff R and their society receives the payoff $2R$. The player choosing the defection strategy receives the payoff T. The temptation to cheat is established by setting the condition

$$T > R. \tag{4.1}$$

However, this larger payoff is assigned to the defector only if the other player selects cooperation. The player selecting cooperation receives the payoff S, which is smaller than R. If the other player also selects defection, the payoff for both players is P, which is smaller than R. The game is based on the crucial inequalities

$$T > R > P > S. \tag{4.2}$$

It is evident that for a player, let us call her #1, the choice of defection condition is always the most convenient, regardless of the choice made by the other player, let us call her #2. In fact, if the player #2 selects cooperation, player #1 receives R, but the better payoff T if she selects defection. If player #2 selects defection, player #1 receives the payoff S if she selects cooperation and the larger payoff P if she selects defection. However, the whole society receives the largest payoff, $2R$, if both players select cooperation, a smaller payoff,

$T+S$, if one selects defection and the other cooperation, and the smallest payoff, $2P$, if both players select defection.

Axelrod and Hamilton [32] noted that if the Prisoner's Dilemma game is played only once no strategy can defeat the strategy of pure defection. If the game is played more than once, reciprocity may make the choice of cooperation become the winning strategy. Nowak and May [1] substantiated this concept with their model of network reciprocity. The players are the nodes of a regular two-dimensional lattice and each players can interact with her nearest neighbors. The players are initially randomly assigned either the cooperation or the defection strategy. After each play, before the next play, they are left free to update their strategy selecting the strategy of their most successful nearest neighbor. Since the environment of the cooperators, as above noted, is wealthier than the environment of defector, it is possible that the most successful nearest neighbor is a cooperator, rather than a defector. This is a rational form of imitation that may lead to the survival of cooperators. Here we use only the Prisoner's Dilemma game to evaluate the payoff and we realize the network reciprocity with the interaction between the two subnetworks that will be described in Section 7.1.3.

4.3. Decision Making Model

In this Section we illustrate the dynamics of the subnetwork where decisions are made by the individuals under the influence of their nearest neighbors. These dynamics are realized by using *Decision Making Model* (DMM) [36]. In the earlier work [63], this model was denoted as Local Conformism Model (LCM), to emphasize that according to the work of Vilone [47] social influence may disrupt the benefits of the Nowak and May network reciprocity [1], if the social influence does not establish a correlation between the dynamics of different individuals. As shall see in Section 7.1.3, the interaction between the DMM subnetwork and the Prisoner's dilemma subnetwork generates criticality. The individuals of the composite networks in this and in the following sections of this work are the nodes of a regular two dimensional network, denoted by the symbol r equivalent to the double index

(i, j).

Here we describe the DMM behavior in the absence of this interaction. The transition rate from cooperation to defection, $g_{CD}^{(r)}$, is given by

$$g_{CD}^{(r)} = g_0 exp\left[-K\left(\frac{J_C^{(r)} - J_D^{(r)}}{J}\right)\right] \tag{4.3}$$

and the transition rate from defection to cooperation, g_{DC}, is given by

$$g_{DC}^{(r)} = g_0 exp\left[K\left(\frac{J_C^{(r)} - J_D^{(r)}}{J}\right)\right]. \tag{4.4}$$

The meaning of this prescription is as follows. The parameter $1/g_0$ defines the time scale of interest and we set $g_0 = 0.01$. Time is discrete, starting from 1 and the distance between two consecutive time events is Δt, which is also selected to be 1. We consider $M = N \times N$ individuals of a regular two-dimensional network with periodic boundary condition. Each individual has J neighbors (four in the case of the regular two-dimensional lattice used herein). $J_C^{(r)}$ neighbors are in the cooperation state and $J_D^{(r)}$ of them are in the defection state. If the individual r is in the cooperation state C, and the majority of its neighbors are in the same state, then the transition rate becomes smaller and the individual sojourns in the cooperation state for a longer time. If the majority of its neighbors are in the defection state D, then the individual r sojourns in the cooperator state for a shorter time. An analogous prescription is used if the individual r is in the defection state.

To denote the effect of imitation we assign to the units selecting the cooperation state the value $\xi_r = 1$ and to the units in the defection state the value $\xi_r = -1$. To establish whether cooperation or defection is selected by the social system we use the mean field $x(t)$ defined by

$$x(t) = \frac{1}{M}\sum_{r}^{M} \xi_r. \tag{4.5}$$

For $K < K_C$ the mean field vanishes, but at criticality, when $K = K_C$, the social system can select either the cooperation or the defection branch yielding for $K \gg K_C$ either the value $x = 1$ or $x = -1$. The critical value of the control parameter K is $K_C = 1$ in the

all-to-all coupling case and $K_C = 1.5$ (M = 100) in the case of a regular two-dimensional lattice [63].

4.4. Self-Organization

The earlier work [63] was based on the assumption that the players are the nodes of a regular two-dimensional network. The players adopt for most of their time the blind imitation of LCM and for a small portion of their time the rational imitation of Nowak and May. Quite surprisingly the exceedingly large use of the blind imitation, rather than disrupting the benefits of network reciprocity, has the effect of forcing the system to select the cooperation branch, leading to the extinction of defectors. This is an interesting effect that is due however to the fine tuning of LCM imitation strength to the critical value generating criticality.

The main purpose of this work is to overcome this limitation with a natural SOC process. This significant step ahead is realized without using the Nowak and May network reciprocity. The earlier work [63] was based on the single units adopting of the Nowak and May network reciprocity for a limited amount of their time and on the criticality-induced swarm intelligence making the network realize the benefits of Nowak and May network reciprocity. Herein the swarm intelligence condition emerges from self organization, which makes it possible for the collective mind to realize that the choice of cooperation makes society wealthier.

We adopt the choice of parameters made by Gintis [30] and set $R = 1$, $P = 0$, $T - R = 0.5$ and $S = 0$. We evaluate the social benefit for the single individual and for the community as a whole as follows. We define first the payoff P_r of the single unit r. Each unit gets a total payoff from the play with its four nearest neighbors. Namely we have to consider four pairs of players. If both players of a pair are cooperators the contribution to the payoff of the unit r is $B_r = 2$. If one the two playing units is a cooperator and the other is a defector, the contribution to the payoff of the unit r is $B_r = T$. If both players are defectors the contribution to the payoff of the unit r is $B_r = 0$. The payoff P_r of the unit r

is the sum over the four B_r. The mean benefit for the units of this society is

$$\Pi = \frac{1}{M}\sum_{r}^{M} P_r. \tag{4.6}$$

Self-induced criticality is realized in two distinct ways: *individual* and *global*:

4.4.1. Individual

It is important to notice that K_r, the value of imitation strength adopted by the generic unit r to pay attention to the choices made by its four nearest neighbors about selecting either the cooperation or the defection strategy, is not necessarily adopted by its four nearest neighbors. In other words, the imitation strength $K_r(t)$ is unidirectional and it goes from r to all its nearest neighbors. The imitation strength $K_r(t)$ changes from individual to individual, as well as in time, and it is consequently very different from the control parameter K of the conventional DMM phase transition processes, where K has a single value throughout the whole network.

Each member is assigned a vanishing initial imitation strength, corresponding to a total independence of the choices made by its nearest neighbors. At each time step the units play the game and they independently change their imitation strength doing the implicit assumption that the increase (decrease) of their individual payoff in the last two trades makes convenient for them to increase (decrease) the imitation strength. More precisely, they adopt the following rule. As stated earlier, time is discrete and the interval between two consecutive time events is $\Delta t = 1$. The imitation strength of the unit (i, j) changes in time according the individual choice rule:

$$K_r(t) = K_r(t - \Delta t) + \chi \frac{(P_r(t - \Delta t) - P_r(t - 2\Delta t))}{(P_r(t - \Delta t) + P_r(t - 2\Delta t))}, \tag{4.7}$$

where the parameter χ determines the intensity of the interest of the units for their payoff. $P_r(t)$ is the payoff of the unit r at time t. The intensity of the imitation strength increases or decreases according to whether in the two last trades the individual payoff increases or decreases. If the payoff does not change, the imitation strength remains unchanged. To

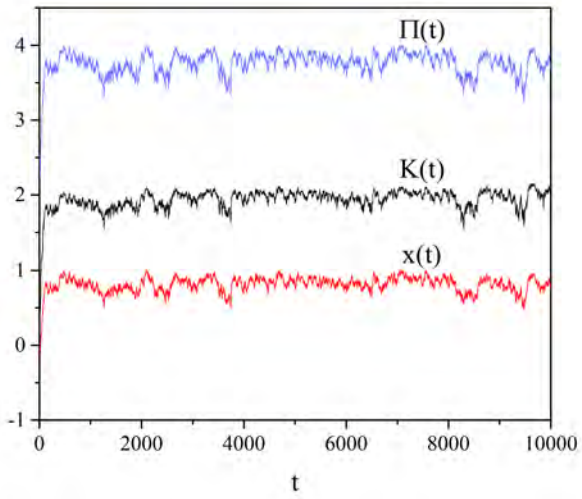

FIGURE 4.1. Individual case: Time evolution of, from the top to the bottom, the benefit $\Pi(t)$ of Eq. (4.6), the variable $K(t)$ of Eq. (4.8) and the mean field $x(t)$ of Eq. (8.8). We adopted the values: $T = 1.5$, $\chi = 4$, $M = 100$.

make a comparison with the global condition we evaluate also the mean imitation strength

$$K(t) = \frac{1}{M}\sum_{r}^{M} K_r(t). \tag{4.8}$$

Fig. 4.1 shows the self-organization of the social system as a result of individual choices of the interacting units. The average imitation strength moves very quickly from the vanishing initial value, corresponding to no social interaction, towards a maximal value which is $K \approx 1.8$. Notice that in the absence of interaction with the Prisoner's Dilemma process, the Ising-like DMM for the case of a regular two-dimensional lattice [36] would require the critical value $K_C \approx 1.65$ for $M = \infty$ and, as earlier mentioned, $K_C \approx 1.5$ for $M = 100$.

It is important to notice that in the case of criticality generated by a fine tuning parameter the fluctuations of the mean field around the equilibrium value have an increasing intensity upon decrease of the number of units [40]. We show that this property is shared by the SOTC. Let us define

$$\zeta(t) = K(t) - \overline{K}, \tag{4.9}$$

$$\zeta(t) = x(t) - \overline{x} \tag{4.10}$$

and

$$\zeta(t) = \Pi(t) - \overline{\Pi}. \tag{4.11}$$

The symbols $\overline{K}$, $\overline{x}$ and t $\overline{\Pi}$ denote the time mean values of the corresponding fluctuations evaluated on the time series of length L. The intensity of these fluctuations is defined by

$$\Delta\zeta = \sqrt{V(\zeta)}, \tag{4.12}$$

where

$$V(\zeta) \equiv \frac{\int_0^L dt\zeta(t)^2}{L}, \tag{4.13}$$

with L denoting the length of time series.

We expect that

$$\Delta\zeta \propto \frac{1}{M^\nu}. \tag{4.14}$$

In the case of the criticality with a fine tuning parameter of Ref. [40], $\nu = 0.25$. Presently we do not have a theory to determine ν for SOTC, but it is interesting to notice that the numerical calculations illustrated in Fig. 4.2 show that $\nu = 0.5$, making fluctuation intensity of $\zeta(t)$ more significant than in the case of the ordinary criticality of [40]. The fluctuations of ζ are determined by the crucial events and their complexity constitutes the information transferred from one to another self-organizing network. Increasing the intensity of these fluctuation favors this transport process, but, as we see in Section 4.5, there exists a crucial value of M, below which no signs of the IPL properties of temporal complexity remain.

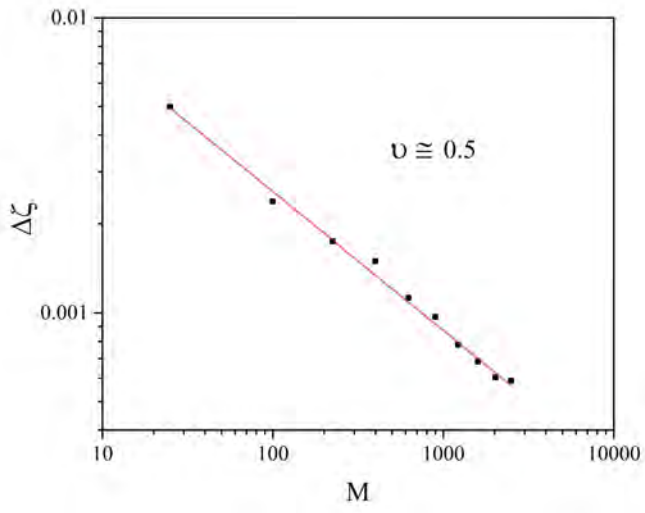

FIGURE 4.2. Individual case: The square root of the fluctuation variance, $\Delta\zeta$ of Eq. (4.12), as a function of M. In this case $\zeta \equiv K(t) - \overline{K}$. We adopted the values: $T = 1.5$, $\chi = 4$.

4.4.2. Global

In the global case we assume that all the units share the same K, which changes in time according global choice rule:

$$K(t) = K(t - \Delta t) + \chi \frac{(\Pi(t - \Delta t) - \Pi(t - 2\Delta t))}{(\Pi(t - \Delta t) + \Pi(t - 2\Delta t))}. \tag{4.15}$$

The global payoff $\Pi(t)$ is evaluated by making a sum over all possible pairs (i, j), as defined by Eq. (4.6). In the global case we select as initial condition $K(0) = 0.5$. The implicit rationale for Eq. (4.15) is that the social community makes the same assumption as the individuals of Eq. (4.7), namely that a payoff increase (decrease) in the last two trades before setting the imitation strength to adopt at time t suggests its increase (decrease) to be convenient. This condition requires a top down process, a decision made by a leader on the appropriate imitation strength that the single units are forced to adopt for the benefit of society.

Fig. (4.3) shows the self-organization of the social system as a result of the global choices with all units sharing the same value of imitation strength. The qualitative behavior

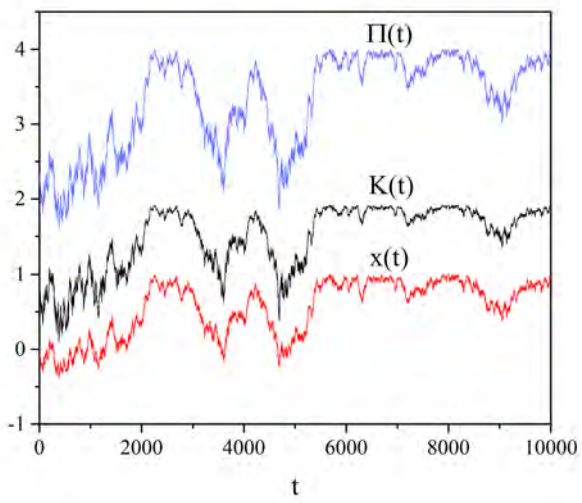

FIGURE 4.3. Global case: Time evolution of, from the top to the bottom, the benefit $\Pi(t)$ of Eq. (4.6), the variable $K(t)$ of Eq. (4.15) and the mean field $x(t)$ of Eq. (8.8). We adopted the values: $T = 1.5$, $\chi = 4$, $M = 100$.

is similar to that of the individual choice, thereby suggesting that the individual choices of the interacting units are characterized by the same intelligence as that of the leader driving the global choice. In fact, the global case is tacitly based on the assumption that the collective payoff is communicated to the individuals who are forced to share the same imitation strength, while the individual choice is based on the realistic assumption that each unit is aware of its individual payoff, without requiring any information transmission from a leader to the individuals. Thus, we are led to the conclusion that the SOC of the model proposed in this work should be interpreted as a spontaneous emergence of the swarm intelligence that in the earlier work is based on tuning a control parameter K to a critical value [29].

The comparison between Fig. 4.3 and Fig. 4.1 leads us to an even more interesting observation. We notice that the global choice yields an intermittent behavior that has the effect of significantly reducing the social benefit, even if, in qualitative accordance with the individual choice rule, the system moves towards cooperation. The individual choice rule

is more efficient than the global choice rule and is not affected by the strong fluctuations that intermittently reduce the social wealth. For this reason we are inclined to identify the society leader of the global choice with the benevolent dictator discussed by Helbing and Pournaras [70]. According to these authors, in fact, the centralized top-down organization has various flaws reducing their efficiency and they propose instead a bottom up pluralistic model inspired by neural processes. We believe that the numerical results of this work lend support to the conclusion that the bottom up process of the individual choice is more efficient than the top down process of the global choice. Therefore it seems that our model of a self-organizing network supports the concluding remarks of Helbing: "I am convinced that co-creation, co-evolution, collective intelligence, self-organization and self-governance, considering externalities (i.e. external effects of our actions), will be the success principles of the future"[71]. In fact, the spontaneous transition to criticality proposed in this work is associated with the emergence of significant resilience and adaptivity. This will be made clear in the next two sections devoted to designate temporal complexity rather than spatial avalanches as a signature of criticality (Section 4.5) and to illustrate the related property of complexity matching (Section 4.6). We think that the individual choice is an example of SOTC more interesting than the global choice and for this reason we restrict our attention to study the individual dependence on M.

4.5. Temporal Complexity

How is criticality defined in a social model? This is a difficult question, because even in the well known condition of the Ising Universality class [36] we have to take into account the observation of systems with a number of units much smaller than the virtually infinite Avogadro number of units in a physical network, which has the effect of breaking the singularity condition of ordinary thermodynamic systems. The authors of Ref. [54, 72] defined the occurrence of criticality through the observation of *temporal complexity*. In the case of a phase transition falling in the range of the Ising Universality class, the occurrence of phase transition in a system with a finite number of interacting units, at criticality the

mean field $x(t)$ fluctuates around the vanishing value and the time interval between two consecutive origin crossings is described by a markedly non-exponential waiting time PDF $\psi(\tau)$ [54]. In the subcritical regime the interval between two consecutive crossings of the origin is exponential and in the supercritical regime the interval between two consecutive crossings of the non-vanishing mean field is again exponential. Temporal complexity emerges at criticality and for the proper function of the network it requires that the IPL PDF of the distances between two consecutive crucial events is exponentially truncated [29, 40, 23].

The adoption of temporal complexity as the signal of criticality occurrence led the authors of Ref. [72] to notice that this may be a more convenient indicator than the observation of avalanches with a PDF becoming IPL. This assumption was confirmed by the authors of Ref. [41], who found that two networks in critical states signaled by temporal complexity exchange information with an efficiency larger than in the correspondence with the state of criticality signaled by IPL avalanches. The reason for the close connection between maximal efficiency of information transport and temporal complexity is based on the theory illustrated in [29, 54] and [30]. Criticality generates non-Poisson renewal events characterized by the IPL indexes and the exchange of information is based on the occurrence of the non-Poisson renewal events of network influencing the occurrence of the non-Poisson renewal events of the other network, this being the Principle of Complexity Management [36].

We conjecture that the SOTC model spontaneously generates temporal complexity. The present section is devoted to establishing that this conjecture is correct and to prove it we use a numerical approach treatment, applied to the individual choice rule.

We monitor the times at which the fluctuations $\zeta(t)$ cross the origin and find that the three waiting time PDF coincide. For simplicity, in Fig. (4.4) we illustrate only the waiting time PDF of $\zeta(t)$ of Eq. (4.10). The fact that fluctuations of $K(t)$, $x(t)$ and $\Pi(t)$ around their average values yield indistinguishable results is an incontrovertible consequence of the fact that all three properties are driven by the non-Poisson renewal events with the same statistical properties.

It is known that in systems of finite size the IPL are exponentially truncated [40].

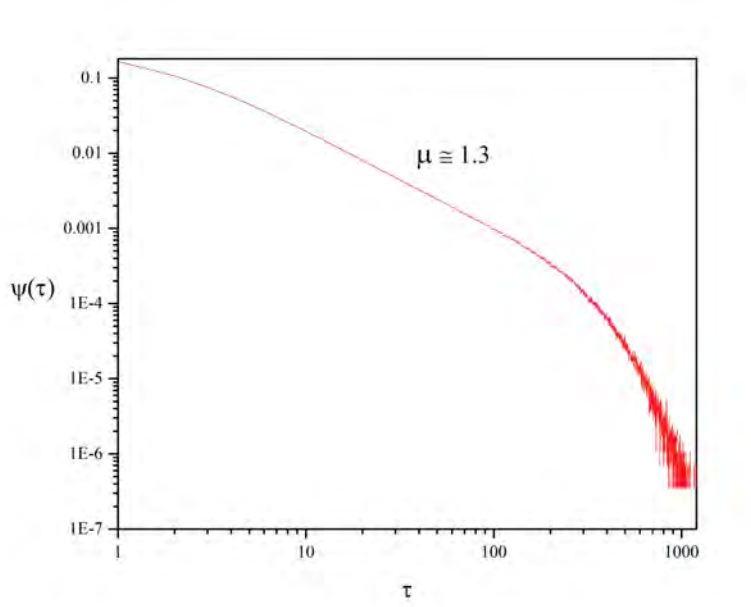

FIGURE 4.4. Waiting time distribution density of the time distance between two consecutive origin crossings of the function $\zeta(t)$ defined by Eq.(4.10) corresponding the function $x(t)$ of Fig. (4.1). We adopted the values: $T = 1.5$, $\chi = 4$, $M = 100$.

As a consequence, the non-Poisson nature of the crucial events is established analyzing the intermediate time region. Therefore, to estimate with accuracy the IPL index generated by the SOTC of Section 4.3 we focus on the time region between $t \approx 2$ and $t \approx 200$, as illustrated by Fig. (4.4). We find that the waiting time PDF is IPL:

$$\psi(\tau) \propto \frac{1}{\tau^{\mu}} \tag{4.16}$$

with

$$\mu = 1.3. \tag{4.17}$$

rather than the traditional $\mu = 1.5$ generated by DMM at criticality [40].

It is interesting to notice the length of the time region characterized by $\mu = 1.3$ depends on M. Fig. (4.5) shows that for $M = 400$ the IPL region is more extended. We also see, Fig. 4.5, that for $M = 25$ the short time region is characterize by a very large value of

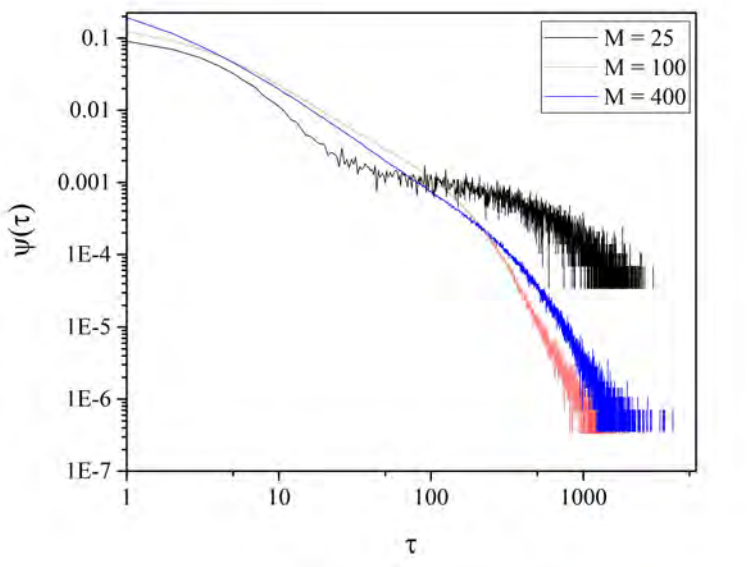

FIGURE 4.5. Waiting time PDF of the time distance between two consecutive origin crossings of the function $\zeta(t)$ defined by Eq.(4.10). We adopted the values: $T = 1.5$, $\chi = 4$.

μ and by a pronounced exponential shoulder, both conditions generating non-crucial events. Although the fluctuation intensity is very large, much larger than for $M = 100$ and $M = 225$ (see Fig. 4.2), the extended IPL region is lost and with it the efficiency of the process of information transport, as we see in Section 4.6.

To help the reader to appreciate the importance of SOTC model we mention that the research work done some years ago [73] on the random growth of surfaces, which can be interpreted as a form of SOC [74], suggests that the Laplace transform of the survival probability

$$\Psi(t) \equiv \int_t^\infty dt' \psi(t') \tag{4.18}$$

has the following form, using the notation $\hat{\Psi}(u) \equiv \int_0^\infty dt exp(-ut)\Psi(t)$,

$$\hat{\Psi}(u) = \frac{1}{u + \lambda^\alpha (u + \Delta)^{1-\alpha}}, \tag{4.19}$$

where $\alpha = \mu - 1 < 1$ and λ is a parameter measuring the interaction between the unit and $\Delta \propto \lambda$ determines the exponential truncation of $\psi(t)$. In the case where $\lambda \gg \Delta$ an extended

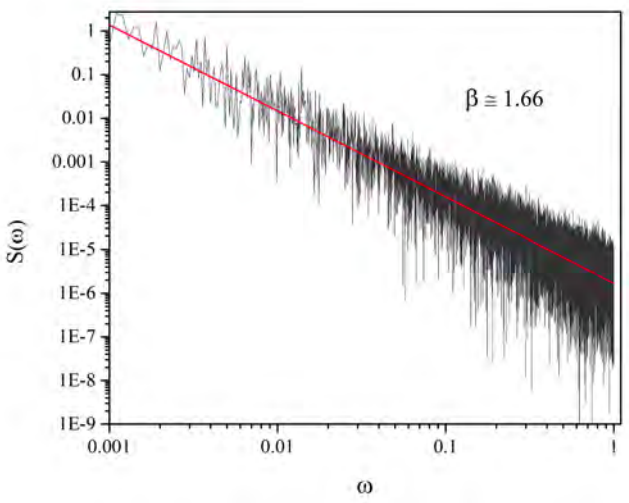

FIGURE 4.6. Spectrum of the fluctuations of $K(t)$ for $T = 1.5$, $\chi = 4$, $M = 100$.

time interval exists, $1/\lambda \ll t \ll 1/\Delta$, where $\psi \propto \frac{1}{t^{1+\alpha}}$, thereby yielding Eq. (4.16) and Eq. (4.17) when $\alpha = 0.3$. This structure is lost for $M = 25$, when temporal complexity is gone.

The most important reason for the use of Eq. (4.19) is that when an extended IPL emerges from it, the process is distinctly non-ergodic. The spectrum of the fluctuation in that case cannot be derived from the Wiener-Khintchine theorem, resting on the stationarity assumption. It is necessary to take into account that $\mu < 2$, $\mu = 1.3$ in this case, the average time interval between two consecutive events diverges, thereby making non-stationary the process driven by the crucial events. This anomalous condition yields [23]

$$S(\omega) \propto \frac{1}{L^{2-\mu}} \frac{1}{\omega^{\beta}}, \tag{4.20}$$

with

$$\beta = 3 - \mu. \tag{4.21}$$

In the case where the process yields a slow but stationary correlation function, we would have $\beta < 1$ [23]. Evaluating the power spectrum in this case becomes computationally challenging because, as shown by Eq. (4.20), the noise intensity decreases with increasing the length L of the time series. Nevertheless, the results of Fig. 8.6, yielding $\beta = 1.67$,

afford a satisfactory support to our claim that the origin crossings of ζ are renewal non-stationary events. In conclusion, the SOTC spontaneously generates the crucial events of criticality-induced temporal complexity.

4.6. Complexity Matching

It has to be stressed that the synchronization between two networks is not a form of chaos synchronization. It is due to the non-Poisson renewal events of the driving network exerting influence on the renewal events of the driven network, as pointed out in Ref. [27] (see also Aquino *et al* [26]). The non-Poisson renewal events are generated by criticality and in the composite network proposed here they are the result of a spontaneous process. In Fig. 4.7 we illustrate the remarkable synchronization between two identical self-organized complex networks, A and B, with $M = 100$. We select a random subgroup S_A of the network A, consisting of 5% of the units of A, and we assign to each of them the strategy of a unit of B, also randomly selected. We follow the same prescription with a subgroup S_B consisting of 5% of units of B following the strategy of randomly selected units of A. We see in Fig. 4.7 that a remarkable synchronization between the two networks is realized.

To establish the accuracy of this synchronization we apply the same procedure to two self-organized networks A and B with M changing from $M = 25$ to $M = 900$. We study the cross correlation $C(\tau)$ defined by

$$C(\tau) \equiv \frac{\int_0^{L-\tau} dt\,(x(t)-\overline{x})\,(y(t+\tau)-\overline{y})}{\sqrt{\int_0^L dt\,(x(t)-\overline{x})^2 \int_0^L dt\,(y(t)-\overline{y})^2}}. \tag{4.22}$$

The numerical result is illustrated in Fig. (4.8). To understand the importance of this result, we must make a short digression to mention an important result recently reached in the field of evolutionary game theory [62]. This earlier paper stresses the connection between emergence of cooperation and memory. Our SOTC model based on the memory of the last two trades before making a decision about the degree of attention to the nearest neighbor may be related to the model of Ref. [62]. Fig. (4.8) seems to confirm this interesting relation insofar as it establishes that the cooperation-induced efficiency increases with decreasing the

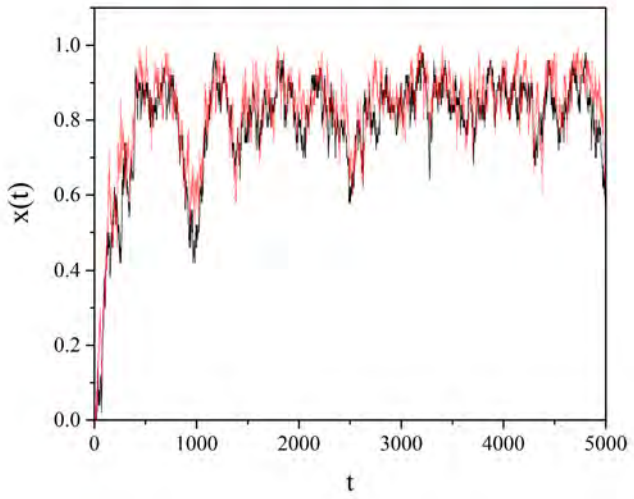

FIGURE 4.7. The mean field $x(t)$ of two identical self-organizing networks connected to each other according to text illustration. The self-organization is realized through the individual choice. We adopted the values: $T = 1.5$, $\chi = 4$, $M = 100$.

size of the interacting networks. However, Fig. (4.8) shows that there exists a small size, $M = 100$, at which the efficiency of information transport from one to another self-organizing network is maximal. The heuristic interpretation of this effect is that *temporal complexity* is a finite size property of intensity proportional to $1/\sqrt{M}$ [40], thereby explaining why the communication efficiency increases upon decreasing M. Temporal complexity is the signature of criticality that we adopt, rather than avalanche size, to reveal criticality in the case of self-organization as well as in the case of criticality generated by the fine tuning of the control parameter K. In the case of this work as we have earlier shown with the help of Fig. (4.1) and Fig. (4.3), the fluctuating field may be K itself, which, as we have seen in the case of individual choice fluctuates around $K \approx 1.8$, when $M = 100$. The length of this complexity time region decreases upon decreasing M. Therefore, it explains the interesting result that an optimal size exists, at which the efficiency of information transport becomes maximal. In fact, complexity matching depends on both the complexity index μ and the

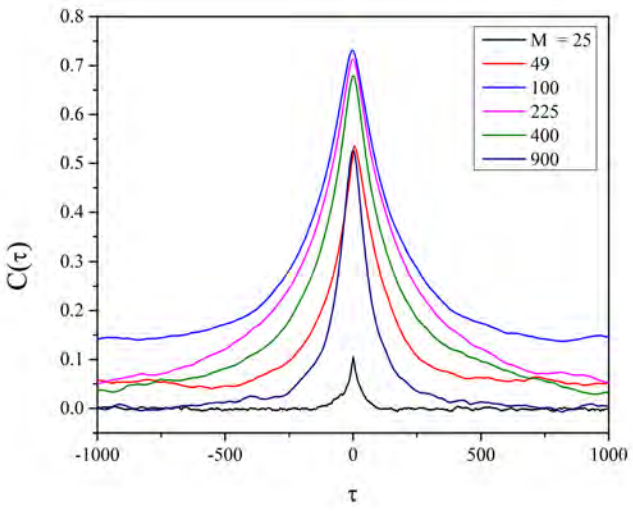

FIGURE 4.8. Cross correlation between two identical self-organizing networks with different size of size M. The different curves refer from top to bottom to: $M = 100, 225, 400, 49, 900, 25$. The self-organization is realized through the individual choice. We adopt for the cross-correlation the definition of Eq. (4.22) and the values: $T = 1.5$, $\chi = 4$.

fluctuation intensity. Decreasing M makes the fluctuation intensity increase (see Fig. 4.5) but it decreases the length of the time duration region characterized by the complex value of μ.

It is important to stress that $M = 100$ depends also on the parameters defining the Prisoners' Dilemma game. The weakening of cooperation with the increase of the number of players is a subject of interest, see [75] as well as [62], thereby generating the issue of establishing if there exists an optimal size of the number of interacting units [76]. We cannot rule out that a more refined treatment of the dependence on the parameters of the Prisoner's Dilemma game may lead to an optimal value of M much smaller than $M = 100$ of Fig. (4.8). However, the emergence of a waiting time PDF with IPL seems to prevent us from accounting for the results of the experimental investigation of Ref. [76], setting $M = 2$ as the optimal size for cooperation emergence.

4.7. Concluding Remarks

This reseaarch work has been stimulated by the manifesto of computational science [65] listing *scaling* and *criticality* as two crucial aspects of computational social science. Herein, criticality was not forced upon the networks by setting the suitable value K for the imitation strength, as done in earlier work [63, 54, 72]. The critical value of K is spontaneously reached without artificially enhancing altruism, but assuming that each unit selects the value of K assigning to themselves the maximal benefit.

It is important to notice that the SOTC condition is reached regardless of whether we adopt the individual or the global choice rules. The global choice rule implies the existence of a leader and consequently of intelligence driving the social system. The fact that criticality is spontaneously generated adopting also the individual choice rule is a compelling indication that the model of this work can be interpreted also as a spontaneous transition to the condition of *swarm intelligence*.

The connection between criticality and swarm intelligence was widely discussed in Refs. [29, 77]. Due to the criticality-induced long-range correlation a small number of lookout birds, perceiving the arrival of a predator and changing flying direction, thanks also to the simultaneous occurrence of crucial events, do succeed in exerting a strong influence on the swarm, enough to make the swarm change direction. This form of collective intelligence, due to the criticality-induced long-range space correlation is the intuitive explanation of the surprising fact that the local interaction between the single individuals and their four nearest neighbors generates the emergence of cooperation at the level of the whole network. This is due to the fact that the SOTC is equivalent to a spontaneous transition to the condition of swarm intelligence.

Notice that K in the earlier work of our group was interpreted as a form of blind imitation [36]. On the other hand the SOTC leads us to interpret K, the intensity of which is decided by the individuals on the basis of their benefit as the origin of intelligence and altruism, rather than a form of blind imitation. This model does not require to go through [1] to prevent the infiltration of defectors in cooperation clusters but it establishes the emergence

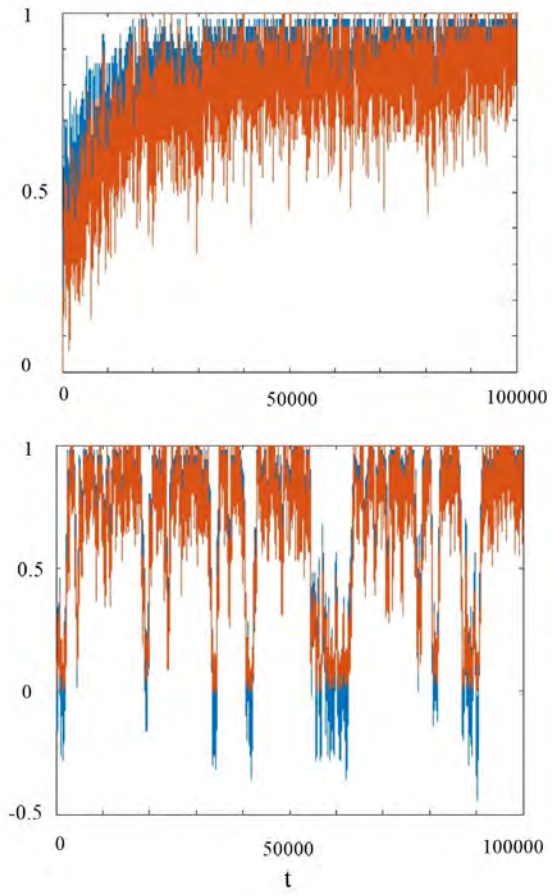

FIGURE 4.9. The blue curves denote the mean field $x(t)$. The red curves denote the ratio of number of cooperator units that are surrounded by 4 cooperators to the total number of units. The top panel refers to the individual choice and the bottom panel to the global choice. For both choices we adopted the parameters: $T = 1.5$, $\chi = 4$, $K(1) = 0.5$, $M = 100$.

of cooperation with the mere use of the Prisoner's Dilemma payoff thereby connecting the evolution of cooperation [32] with the search of agreement between the individuals and their nearest neighbors.

The global choice does not prevent the occurrence of organization collapses of the system, as clearly illustrated by Fig. (4.9). This figure indirectly evaluates the size of clusters of cooperators by counting the number of cooperator units surrounded by four cooperators. We see that the global condition is characterized by frequent collapses corresponding to the

fragmentation of the clusters of cooperators, whereas the individual self-organization is not affected by these collapses.

As mentioned earlier, the global choice rule is a form of top-down process, implying the action of a benevolent dictator [70, 71]. Thus, as earlier, the SOTC model strongly supports the conjectures of [70, 71].

We stress that the SOC model can also be interpreted as a contribution to evolutionary game theory explaining the origin of morality. Although morality is triggered by the macroscopic property of social prosperity as an effect of the bottom up process, it may be the source of a form of downward causality: we make the plausible conjecture that the action of morality on a social system under the influence of the individual SOC will have the effect of reinforcing the evolution towards social prosperity. This would not conflict with the observation made herein that the global choice rule is not as efficient as the global choice rule. We plan to study this reinforcement action in future work.

The SOTC model is highly simplified and ignores, for instance, the cost of the cooperation choice, which is explicitly taken into account, for instance, by Archetti and Scheuring [60]. We expect that the inclusion of the cost may have an effect equivalent to increasing the incentive to cheat and that this will affect the time scale for the emergence of cooperation. In other words, the transition to the complex fluctuations that in Fig. 4.1 is so fast as to be not visible in the scale of that figure,, may become significantly slower, without changing, however, the main properties of temporal complexity and complexity matching, illustrated here. We conjecture that this and other issues, including those of anthropological interest, may be included in the composite network without affecting the main conclusion that this form of SOTC has a general validity, ranging from the random growth of surfaces [73] to sociology. It is also important to stress that SOC is invoked by an increasing number of researchers in the field of complexity but its connection with the open field of phase transitions in systems of small size is not yet properly taken into account. This work affords a contribution to this still open research subject that hopefully may attract the attention of the researchers in the field of complexity, from biology to anthropology and from neurophysiology to sociology.

CHAPTER 5

RESOLVING THE PARADOX OF COOPERATION BETWEEN SELFISH UNINTS USING SELF-ORGANIZED TEMPORAL CRITICALITY

Ways to reconcile paradox have occupied the best scientific minds for centuries. Herein we contribute to the ongoing discussion regarding empirical paradox, using a social network model showing how individuals, acting solely in their own self-interest, can simultaneously maximize the benefit to society. We generalize the self-organized criticality (SOC) model to one of self-organized temporal criticality (SOTC). The SOTC model identifies the timing of events as a new mechanism with which to generate criticality, thereby establishing a way for the internal dynamics of the decision making process to resolve the conflict between the two poles of the paradox.

5.1. Introduction

Early in the twentieth century there existed a large body of empirical evidence establishing that light was a wave phenomenon. It was puzzling therefore that there also existed a significant amount of data establishing that light was a particle phenomenon. The fact that a particle is localized in space and a wave is extended in space thereby produced a physical paradox, that being, the existence of a given phenomenon possessing contradictory, or mutually exclusive, properties. Resolving this paradox led to wave-particle duality, the Copenhagen interpretation of quantum phenomena, with the result that the interpretation of what is observed is determined by the measurement that is made. It was resolved that light is neither a particle nor a wave, but paradoxically it is both, but one can only know its state by measurement, which produces either a particle or a wave at any given time, but never both simultaneously.

Herein we are interested in the notion of an empirical paradox (EP), a seemingly self-contradictory nature of two observed characteristics of a given phenomenon. This is different from a logical paradox, such as the sentence: I am a lair. The truth value of

the sentence switches with each reading and therein lies the paradox. This is separate and distinct from the EP found in a scientific theory, since nature has resolved the latter paradox by manifesting the contradictory traits in an observed phenomena. It is the logic of the explanatory theory that contains contradictory elements, and these contradictions lead to confusion. We investigate EP using a recently developed social network model [78], whose properties are shown to compliment and extend the understanding reached by others. This in itself is not surprising, since we incorporate some aspects of existing theory, with modification, into the new model that had previously been used independently to study contradictory characteristics of social behavior. What is surprising is the emergence of properties that did not appear when the modeling pieces were applied separately, as we subsequently disucuss.

There always exists a tension between the short term needs of individuals and the long term needs of the organized group to which they belong that address the challenges of the future**;** the delicate balance between stability and change. We take a networked-based approach to modeling in order to capture the emergence of the difference in behavior of the group from that of the individual. It is determined that the individual in our model recognizes that inconsistency is often necessary, even if not desirable, being capable of holding conflicting views, and is able to transition from *either/or*-thinking to *both/and*-thinking [79].

Computational social science relies on the recognition that criticality, such as reaching consensus, is a consequence of self-organization. A number of investigators have devised mathematical models by which to quantify critical phenomena and are reviewed by Sornette [80]. These models can be widely separated into two groups: those that achieve criticality through the external tuning of a control parameter, such as changing the temperature to induce physical phase transitions among gases, fluids and solids, contrasted with those in which criticality emerges due to internal dynamics, without adjusting an external control parameter. The former is the less interesting for our purposes here. The latter has acquired the name self-organized criticality (SOC) and has been applied in multiple biological and social, as well as, physical contexts [66].

5.2. On Modeling

We introduce a two-level dynamic network model of decision making, having criticality as an emergent property, and show how such a model can drive the social group, through the selfish behavior of individuals within the group, to spontaneously achieve maximum social benefit. Previous models attempted resolution by placing the good of the individual and the good of society in competition, with a clear winner and a loser. The self-organized temporal criticality (SOTC) model [78], or two-level dynamic network, introduced in the next section, shows that an individual can consistently act in their own self-interest, while simultaneously producing social benefit of their decisions. This benefit occurs independently of any specific physical, social or biological mechanism. The mathematics demonstrates that the intellectual conflict in an EP is mitigated when treated dynamically. The SOTC model reveals that what is good for society need not be purchased at the cost of what is good for the individual. In other words, the resolution of EP is not an either/or choice between absolutes.

The decisions made by individuals within the SOTC model are herein assumed to be consistent with the criterion of bounded rationality [81], which were expanded by Kahneman [82], and more recently discussed from the perspective of evolutionary game theory [83, 84]. Rand and Nowak [83] acknowledge the tension between what is good for the individual, what is good for society and they discuss it in the language of evolutionary game theory. Without reviewing the long history of studies on the nature of cooperation and defection, we note the meta-analysis of 67 empirical studies of cognitive-manipulation of economic cooperation games by Rand [84]. He concluded from his meta-analysis that all the experimental data could be explained using a dual-purpose heuristic model of cooperation; a model consisting of a balance between deliberation and intuition. Deliberation is considered to be a rational process that always favors non-cooperation, whereas intuition is treated as an irrational process that can favor cooperation or non-cooperation, depending on the individual.

Herein we adapt these linked concepts of intuition and deliberation by constructing a dynamic two-level network model [78]. One subnetwork (level) is based on the decision

making model (DMM) [36] and leads to strategy choices made by the individuals under the influence of the choices adopted by their nearest neighbors. The other subnetwork (level) quantifies these choices using the payoffs of the Prisoner's Dilemma Game (PDG). The interaction between the two levels is established by making the imitation strength K increase or decrease, according to whether the average difference of the last two payoffs increases or decreases, in accordance with the corresponding changes in K. Although the value of the imitation strengths is selected selfishly at each point in time, which is to say the individual choices of imitation strengths are always made in the best interest of the individual making the decision, the social system is driven by the resulting internal dynamics towards the state of cooperation, which has the greatest social benefit. In this way the EP is resolved by means of the internal dynamics of the two-level network.

5.3. Two-Level Network Model

The intuition mechanism proposed by Rand is realized through the dynamics of one subnetwork through the DMM [36]. The DMM on a two-dimensional lattice is based on individuals imperfectly imitating the majority opinion of their four nearest neighbors, thereby biasing the probability of deciding to transition from being a cooperator (C) to being a defector (D):

$$g_{CD}^{(r)} = g_0 \exp\left\{-K_r \frac{N_C^{(r)} - N_D^{(r)}}{N}\right\}, \tag{5.1}$$

where $N_C^{(r)}$ is the number of nearest neighbors to individual r that are cooperators, $N_D^{(r)}$ the number of defectors, and each individual on the simple lattice has $N = 4$ nearest neighbors. In the same way the probabilistic transition rate from defectors to cooperators $g_{DC}^{(r)}$ is give by Eq.(7.3) by interchanging C and D. The unbiased transition rate is taken to be $g_0 = 0.01$ throughout the calculations, and $1/g_0$ defines the time scale for the process. The original DMM assigns to all the individual imitation strengths K_r the same value K, a single parameter. This constant imitation parameter has been shown [36] to have a critical value that makes this theory undergo critical phase transitions and to be a member of the Ising

universality class. At criticality all the members of the network act cooperatively, depending on the magnitude of K. In the present two-level model the individual imitation parameters K_r can all be different. This decision making process is fast, emotional and does not involve any reasoning about a payoff.

The connection with self-interest, according to the slow thinking mechanism of Kahneman [82] is established by a second subnetwork that determines the payoff for the choices made. To define the payoff we adopt rules based on the PDG [30] so that the second subnetwork becomes a realization of Rand's deliberative mechanism within the two-level network model. In the second subnetwork, two players interact and receive a payoff from their interaction adopting either the defection, or the cooperation strategy. The PDG is based on the crucial payoffs $T > R > P > S$. Note that their choices are made continuously as the network dynamics unfold. We adopt the choice of parameter values made by Gintis [30], set $R = 1, P = 0, T - R = 0.9$ and $S = 0$ and evaluate the social benefit for the single individual, as well as, for the community as a whole as follows. The payoff P_r is defined for individual r as the average over the payoffs from the interactions with its four nearest neighbors. If both players of a pair are cooperators, the contribution to the payoff of the individual r, is $B_r = 2$. If one of the two playing individuals is a cooperator and the other is a defector, the contribution to the payoff of r is $B_r = T$. If both players are defectors the contribution to the payoff of r is $B_r = 0$. The payoff P_r to individual r is the sum over the four B_r's.

Each individual receives a total payoff from the play with the four nearest neighbors and adjusts their present imitation strength based on their two previous payoffs as follows:

$$K_r(t) = K_r(t - \Delta t) + \chi \frac{P_r(t - \Delta t) - P_r(t - 2\Delta t)}{P_r(t - \Delta t) + P_r(t - 2\Delta t)}, \tag{5.2}$$

where the parameter χ determines the intensity of interest of the individuals to the fractional change in their payoffs in time and is taken to be unity in the calculations. Consequently, the imitation strength of the individual in the DMM network is responsive to the recent history

of the payoffs determined by the PDG network, through this coupling. Note that in the limit of vanishing time intervals that Eq.(5.2) relates the time rate of change of an individual's imitation strength to the time rate of change of the logarithm of the local payoff to that individual. In this way the individual's DMM dynamics is not responsive to the absolute level of the payoff received, but instead responds to the relative change in the payoff over time, just as Daniel Bernoulli postulated in 1738 marking the beginning of utility theory.

In the two-level network simulation we work with a society of M individuals. On the global scale, the mean benefit to society of all the individuals is given by the average over all the individual payoffs $P_r\,(t)$:

$$\Pi(t) = \frac{1}{M}\sum_{j=1}^{M} P_r(t), \tag{5.3}$$

whereas the mean imitation strength is given by the average over all the individual imitation strengths $K_r(t)$:

$$K(t) = \frac{1}{M}\sum_{j=1}^{M} K_r(t). \tag{5.4}$$

The internal dynamics generated by the interaction of the two subnetworks as prescribed by inserting Eq.(5.2) into the expression for the rate of transition given by Eq.(7.3), drives the mean imitation strength, as well as, the mean social benefit to the fluctuating plateau values shown in the next section. The emergence of the maximum mean social benefit corresponds to the network evolving towards a majority of cooperators, thereby requiring the definition of the mean field $X(t)$ given by

$$X(t) = \frac{1}{M}\sum_{j=1}^{M} \xi_r(t), \tag{5.5}$$

where $\xi_r(t)$ is the state of individual r and is either $+1$ or -1.The condition $X(t) = 1$ corresponds to a social group consisting entirely of cooperators. The calculation shows

however that the mean field is a stochastic dynamic variable confined to the interval $-1 \leq X(t) \leq 1$.

In the absence of interaction with the PDG ($\chi = 0$), the DMM for the case of a regular two-dimensional lattice with $M = 100$ would achieve criticality at the value $K_C \approx 1.45$. At criticality the mean field $X(t)$ fluctuates around zero and the time interval between consecutive zero-crossings is described by a markedly non-exponential waiting-time probability density function (PDF) $\psi(t)$, with the inverse power law (IPL) structure:

$$\psi(\tau) \propto \tau^{-\mu}, \tag{5.6}$$

where it is determined by numerical calculations that $\mu = 1.5$. In the sub-critical regime $K < K_C$ the interval between consecutive zero-crossings is exponential, as are the intervals in the super-critical regime $K > K_C$.

Criticality generates non-Poisson renewal events characterized by an IPL PDF. Critical behavior is manifest through crucial events, which have been shown to generate phase transitions, modeled by members of the Ising universality class, in the DMM [36]. The occurrence of a phase transition in a DMM network, with a finite number of interacting individuals, occurs at a critical value of the imitation parameter $K = K_C = 1.45$.

When $\chi = 1$ the calculation is done for a two-dimensional regular lattice (with periodic boundary condition) having $M = 100$ units, $g_0 = 0.01$ and $T = 1.9$, with the mean social benefit, mean imitation strength and mean field, all starting from zero. The mean field of the two-level network is driven toward criticality by its internal dynamics, where the time averaged value of the mean field, $\overline{X(t)}$, is different from zero, due to the fact that criticality in this case generates a majority of cooperators. To stress the occurrence of crucial events in a social system we adopt a method of event detection based on recording the times at which the mean variable crosses its time averaged value. Thus, there are fluctuations around $\overline{X(t)}$ and the IPL structure for the PDF is obtained by evaluating the distribution of time intervals between consecutive re-crossings of $\overline{X(t)}$. As shown by Figure 6.2, the time intervals between consecutive crucial events is given by an IPL with index $\mu \approx 1.3$, a property shared

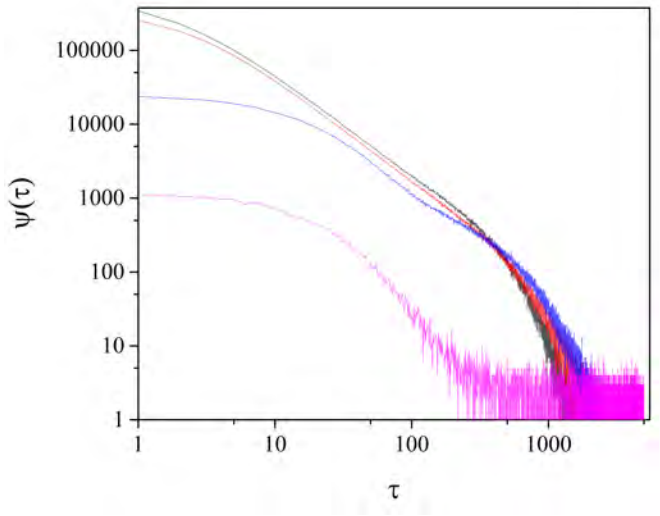

FIGURE 5.1. The black, red and blue curves are the waiting time PDF of the time interval between two consecutive crossings of $X(t)$, $K(t)$ and $\mathrm{K}_r(t)$ with their average values respectively. The pink curve is the waiting time PDF of the time interval between two consecutive crossings of $\mathrm{K}_r(t)$ with zero. The numerically determined PDF's have exponentially truncated IPL with an index of $\mu \approx 1.3$.

by other systems at criticality, see, for instance [29].

It is important to stress that in addition to $X(t)$ that the variables $K(t)$ and $K_r(t)$ are also characterized by the same property, namely, the waiting-time PDF of the time interval between consecutive crossings of $\overline{K(t)}$ by $K(t)$ and of $\overline{K_r(t)}$ by $K_r(t)$. These PDFs are graphed versus time on log-log graph paper in Figure 6.2, and yield an IPL index close to that of $X(t)$, which is, as written earlier, $\mu \approx 1.3$.

Notice that the regime of *intermediate asymptotics* [85] for $K(t)$ is as extended as that for $X(t)$, while the regime for the individual $K_r(t)$ is somewhat shortened. This shortening is a consequence of the fact that the behavior of the single individual is characterized by frequent collapses to zero and even negative values of $K_r(t)$. On the basis of the definition of the transition rates we can interpret these rare events as individuals turning into contrarians.

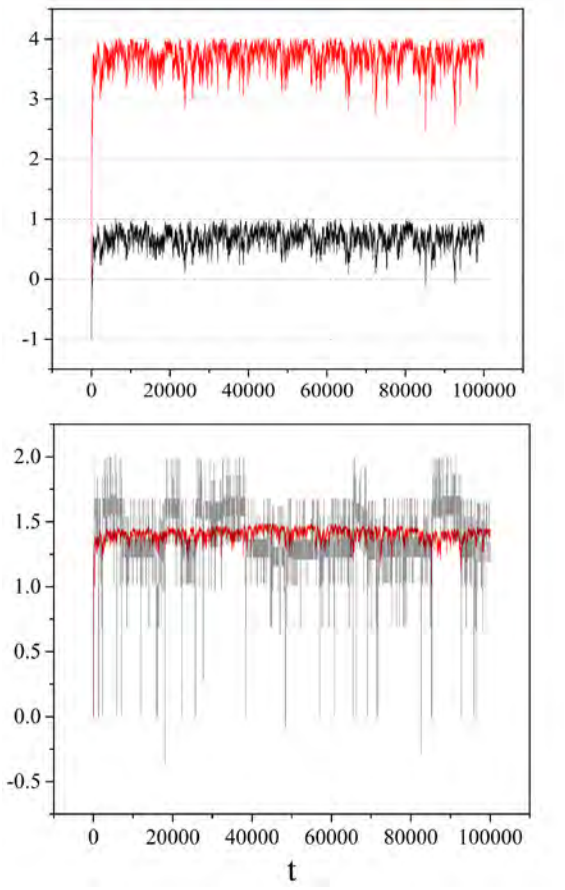

FIGURE 5.2. Top: The red and black curves are the time evolution of the mean social benefit $\Pi(t)$ and the mean field $X(t)$ respectively. Bottom: Red and gray curves are the time evolution of the mean imitation strength $K(t)$ and the imitation strength of one of the units $K_r(t)$ respectively. The mean field fluctuates around 0.7 which means about 85% of individuals are cooperators and 15% are defectors. A mean field of 1 has all individuals in the state of cooperation, and the maximum average social benefit reaches the value 4, because this is the number of nearest neighbors on the 2D lattice.

The calculations done yield: $\overline{X(t)} \approx 0.7$, $\overline{K(t)} \approx 1.4$ and $\overline{K_r(t)} \approx 1.4$ as depicted in Figure 5.2. This is the recently identified phenomenon of self-organized temporal criticality [78].

The quantity $K_r\,(t)$ is the value of imitation strength adopted by the generic individual r under the influences of the choices made by its four nearest neighbors, concerning

their selecting either the cooperation, or the defection, strategy. This value is not necessarily adopted by its four nearest neighbors, however, as distinct from the network reciprocity assumption of Nowak and May [1]. Consequently, the dynamics of the two-level network never reduce to the dynamics of the Nowak and May game theory network.

In other words, the imitation strength $K_r(t)$ is unidirectional and determines the interaction of r with all its nearest neighbors, but is not necessarily reciprocated. The lack of reciprocity is a consequence of the fact that each of the neighbors experiences a different set of nearest neighbors. The time-dependent imitation strength $K_r(t)$ changes from individual to individual, as well as in time and is depicted in Figure 5.2 along with the erratic time-dependence of the mean field $X(t)$, the mean social benefit $\Pi(t)$ and the mean imitation strength $K(t)$.

Figure 5.2 shows the self-organization of the social system as a result of individual choices of the separate individuals. The mean imitation strength $K(t)$ moves very quickly from its zero initial value, corresponding to no social interaction, towards a maximal value of $K \approx 1.4$, the critical value in this case. Notice that the mean social benefit $\Pi(t)$ at the top of this figure, which results from averaging over each of the individual payoffs obtained from the play of the PDG with their four nearest neighbors, also moves very quickly from its negligible initial value to a fluctuating plateau. The rate of the transition to the SOTC plateau is controlled by the parameter χ of Eq. (5.2) and it does occur, either sooner or later, for any positive value of χ.Thus, a smaller parameter indicates a weaker response to the change in payoffs, thereby slowing the transition to the plateau of the asymptotic state.

5.4. Discussion

As pointed out by Nowak and Sigmund [86] the PDG is a leading metaphor for the evolution of cooperative behavior in populations of selfish agents. They introduced a protagonist, with a Pavlov strategy, into the PDG, which they determined to be more robust in establishing cooperative stability than the leading alternative strategies of the time. The modification of the imitation strength in the SOTC model, incorporates a memory

dependence of the behavior strategy of the individual, based on the utility of prior payoffs. This utility strategy is related to, but is not the same as, the Pavlov strategy, however this introduction of memory into the decision making process does achieve similar stabilizing results.

We emphasize that the SOTC model [78] is here interpreted as a contribution to evolutionary game theory, and provides a resolution of the conflict between cooperators and defectors, by replacing the *either/or* with a *both/and* strategy. This replacement suggests that the SOTC model might be useful in the resolution of a number of EPs, including one with a long history, the altruism paradox (AP). It was first recognized by Charles Darwin that some individuals in a number of species act in a manner that although helpful to others, may jeopardize their own survival and yet this property is often characteristic of that species. He identified such altruism as contradicting his theory of evolution [87]:

> It is extremely doubtful whether the children of such [altruistic] individuals would be reared in greater number than the children of selfish and treacherous members of the same tribe...Therefore it hardly seems probable...that the standard of their excellence could be increased through natural selection, that is, by the survival of the fittest.

The crux of the paradox lies in the distinction between what is best for the group to function as an adaptive unit resulting from interactions within the social group, compared with interactions between social groups. This failure of the group to achieve maximum fitness through the self-sacrifice of individuals within the group forms the AP. Darwin proposed a resolution to this problem by speculating that natural selection is not restricted to the lowest element of the social group, the individual, but can occur at all levels of a biological hierarchy, which constitutes multilevel selection theory, as paraphrased by Wilson and Wilson [88]:

> Selfish individuals might out-compete altruists within groups but internally altruistic groups out-compete selfish groups. This is the essential logic of what has become known as multilevel selection theory.

Theoretical inconsistency arose in sociobiology with the rejection of Darwin's multi-

level selection hypothesis in the 1960s and the subsequent ambiguities, contradictions, and confusion that framed the subsequent theoretical discussion of the next half century in terms of the individual. We do not believe we can improve on the detailed critique of the alternatives to multilevel selection theory presented by Wilson and Wilson, even though there are a few details with which we may not completely agree. However, going into that level of detail here does not support our major purpose, that being, to demonstrate that the re-convergence of scientific consensus on the use of multilevel selection theory to resolve the AP in sociobiology is compatible with the results of the SOTC model shown herein.

We concur with the multilevel selection hypothesis of Darwin, but not necessarily with the biological requirement that there exist strictly altruistic individuals. Historically, the alternative theories to multilevel selection were based on the failure to make the altruistic actions of individuals compatible with the more universally accepted action of individual acting in their own self-interest. The SOTC model of decision making does not rely on such an either/or choice for the behavior of the individual on which AP is based. The two poles of the AP, selfishness and altruism, stand in such sharp contrast to one another that their incompatibility appears irrefutable. But if this logical incompatibility were not routinely resolved at the operational level, in the form of heroes, first responders, martyrs and other indicators of people caring for other people, often strangers, the need to resolve the AP would not be so compelling.

The SOTC model does not lead to the unrealistic condition of having a society with 100% cooperators, asymptotically. Note the fact, as shown by the black curve of top panel of Figure 5.2, that 15% of individuals remain defectors. The mean field increases to 0.7 and then fluctuates around this time average value. Some individuals may be converted to cooperation, but all individuals are equivalent and the conversion to cooperation is not permanent, meaning that no individual is a hero all the time, but neither are they perpetual scoundrels. As a consequence, 15% of each individual's time is spent in the defection condition. The gray curve of Figure 5.2 shows that while the mean value of the imitation strength K generates weak fluctuations around a mean value $K \approx 1.4$, the imitation strength of the

single individual may undergo collapses to a condition of total independence of the others.

Space limitations prevent us from making a proper comparison between the SOTC model and the vast literature on the subject of paradox. Consequently, we limit ourselves to noticing that most of the PDG work done along the lines of the pioneering work of Nowak and May [1] pointed out that the social activity of the single individual, which is described in the SOTC approach to EP, by adopting the DMM, has the effect of disrupting the benefits realized by the evolutionary PDG. Earlier work [63] presents the first attempt at making the behavior of individuals within the social network significantly reinforce, rather than disrupt, the benefits derived from the repeated use of the PDG. The DMM, on the other hand, has been discussed in detail [36] and the tendency to imperfectly imitate has been used for a variety of purposes, including the communication between the brains of two rats [89]. The SOTC model is based on the assumption that individuals may change imitation strengths, so as to maximize individual payoff and this extension of the DMM realizes a spontaneous transition to temporal criticality, meant as a sequence of unpredictable crucial events, which are non-ergodic and non-Poisson. These are the properties of living systems that must be made compatible with the traditional approaches to statistical physics, based on the adoption of stationary correlation functions [90]. The SOTC model successfully realizes this important task.

5.5. Concluding Remarks

Contradictions always exist in real world, complex, organized social groups, some of which form EPs that cannot be resolved by adopting to support one side of the paradox or the other. Both sides of the contradiction have value and a successfully organized group is one that can devise and implement enabling strategies to cope with paradox, without becoming doctrinaire. The resolution of EP entails that diametrically opposed alternatives be examined and consequently, such alternatives not only contradict one another, but also depend on one another. The dynamic stability of the SOTC model embraces EP, stability that emerges and then persists over time.

Using the terms adopted by Rand [83] we identified intuitive decision making with the choice of imitation strength and deliberative decision making with the direct adoption of the PDG. The resolution of EP and more specifically the AP made herein is accomplished by both $X(t)$ and $\Pi(t)$ simultaneously plateauing at their maximal values. This stabilization of the dynamics in SOTC is a consequence of scaling and criticality in the complex decision making process. In the SOTC model criticality is not forced upon the network, as it would be by externally tuning the imitation strength K to a critical value. The critical value of the imitation strength is spontaneously reached without artificially enhancing the level of altruism within the network, and is dynamically attained by assuming that each individual selects the value of K_r that assigns maximum benefit to themselves at each point in time.

Individuals weigh each and every decision they make, using the two subnetworks to adapt to the changing two-level network behavior. Note that the value of K used in earlier work was interpreted as a form of blind imitation [36]. But the SOTC model leads us to interpret K_r, the intensity of which is decided by the individuals on the basis of their own benefit, as the origin of cooperation, or altruism, rather than a form of blind imitation. The SOTC model does not require us to adopt the network reciprocity argument of Nowak and May [1] to prevent the infiltration of defectors in cooperation clusters, but instead establishes the emergence of cooperation by the mere use of the PDG payoff, thereby connecting the evolution of cooperation with the search for agreement between individuals and their nearest neighbors.

The dynamics of the SOTC model establishes the kind of dynamic steady state that balances the tension generated by the conflicting characteristics of an EP. This tension is inherent and persistent within EP typical of complex organizations, as discussed qualitatively by Smith and Lewis [91] for organizations within a business context. In Figure 5.2 we see the fluctuations in the dynamic steady state that are a consequence of the finite size of the social network and has nothing to do with the thermal fluctuations observed in physical phenomena, see [36] for a more complete discussion.

The SOTC model presented herein is illustrated using the simple prescription of the

PDG to take into account the incentive to cheat. More complex games may be used, see, for instance the work of Archetti and Scheuring [92, 60]. Also other issues, including those of anthropological interest, may be dealt with in the composite network without affecting the main conclusion that this form of SOTC has general validity, ranging from macro-evolution to sociology.

CHAPTER 6

SELF-ORGANIZED TEMPORAL CRITICALITY: BOTTOM-UP RESILIENCE VERSUS TOP-DOWN VULNERABILITY

In this chapter we propose a social model of spontaneous self-organization generating criticality and resilience, called Self-Organized Temporal Criticality (SOTC). The criticality-induced long-range correlation favors the societal benefit and can be interpreted as the social system becoming cognizant of the fact that altruism generates societal benefit. We show that when the spontaneous bottom-up emergence of altruism is replaced by a top-down process, mimicking the leadership of an elite, the crucial events favoring the system's resilience are turned into collapses, corresponding to the falls of the leading elites. We also show with numerical simulation that the top-down SOTC lacks the resilience of the bottom-up SOTC. We propose this theoretical model to contribute to the mathematical foundation of theoretical sociology illustrated in 1901 by Vilfredo Pareto to explain the rise and fall of elites.

6.1. Introduction

The recent book of Haidt [93] aims at explaining the psychological reasons for the conflicts between parties with arguments ranging from psychology to evolutionary biology and from religion to theoretical sociology. There exists a connection between these conflicts and the societal resilience that is supposed to be sufficiently robust as to prevent either societal collapses or rapid social changes. These important sociological issues were addressed in 1901 by Vifredo Pareto [94], who discussed the capability that elites should develop in order to adapt themselves to changing circumstances. The main goal of the present work is to contribute to the discussion on the resilience issue, with a simplified model that was recently

This chapter was adapted from Mahmoodi, Korosh and West, Bruce J and Grigolini, Paolo, "Self-Organized Temporal Criticality: Bottom-Up Resilience versus Top-Down Vulnerability", published on 26 March 2018 in Complexity, Vol. 2018, 8139058, Open access.

proposed by our group to resolve the altruism paradox, namely the emergence of cooperation from the social interaction of individuals who make their choice between cooperation, C, and defection, D, on the basis of their self interest [78].

The new model of spontaneous organization [78] is based on the conjecture that there are close connections between resilience and information transport, resilience and consciousness, as well as bewteen consciousness and criticality.

6.1.1. Criticality and Temporal Complexity

Phase transitions and critical phenomena occur frequently in nature and have been widely studied by physicists, see for instance [68]. The Ising model [95] originally introduced to explain ferromagnetic phase transition is well known, and the exact solution found by Onsager [96] for the occurrence of phase transition in the two-dimensional case is widely recognized as an example of outstanding theoretical achievement. In the last few years some scientists have used the Ising model to shed light on biological and neurophysiological collective processes [97, 98, 99, 100]. More precisely, the authors of [97] used the Ising model to explain the collective behavior of biological networks and the authors of [98, 99, 100] adopted the Ising model for the purpose of supporting their hypothesis that the brain works at criticality, but without establishing a clear distinction between phase transition and self-organized criticality [101]. Finally, we have to mention that the Ising model is frequently used, see for instance [102, 103], to model neurophysiological data subject to the constraint of maximal entropy. The term criticality is used to denote the physical condition corresponding to the onset of a phase transition, generated by the adoption of a suitable value of the control parameter K.

The Decision Making Model (DMM) [36], which is used in Section 6.2 and in Section 6.3, was proved [54] to generate phase transition as a function of its control parameter K identical to that of the Ising model, where the control parameter is the temperature. In other words, the DMM belongs to Ising universality class [36].

At criticality, namely, when the dynamics of the system are determined by the control

parameter generating phase transition, the mean field $x(t)$, which is defined as the ratio of the difference between the number of cooperator and the number of defectors to the total number of units, fluctuates around the vanishing value. The occurrence of a vanishing value is a *crucial event*. The crucial events are defined as follows. The time interval between consecutive crucial events is described by the waiting-time probability density function (PDF) $\psi(\tau)$ that in the long-time limit $\tau \to \infty$ has the inverse power law (IPL) structure:

$$\psi(\tau) \propto \frac{1}{\tau^{\mu}}, \tag{6.1}$$

with $\mu < 3$. The crucial events are renewal thereby making the correlation function $< \tau_i \tau_j >$ vanish if $i \neq j$.

In the case of the brain dynamics there is wide consensus on the connection between consciousness and criticality. See, for instance, [99], [17], [104], [105] and the recent review paper [46]. The electroencephalogram (EEG) signals are characterized by abrupt changes, called rapid transition processes (RTP), which are proved [106] to be renewal non-Poisson events, with $\mu \approx 2$. This means that the brain in the awake state is a generator of crucial events.

The crucial events are responsible for the information transport from one system at criticality to another system at criticality [77]. Furthermore, the emergence of crucial events requires that the size of the complex system is finite. M is the total number of units within the system. The intensity of the fluctuations of the mean field $x(t)$ obey the general prescription

$$\Delta\zeta \propto \frac{1}{M^{\nu}}, \tag{6.2}$$

where

$$\Delta\zeta = A(t) - \overline{A} \tag{6.3}$$

When working with DMM at criticality, A is the mean field x, with $\overline{x} = 0$, $\nu = 0.25$ [40]. In the case of SOTC [78], with $A = K$, see Section 6.2, we find $\nu = 0.5$. These criticality-

induced fluctuations, becoming visible for finite values of M, are referred to as an expression of *temporal complexity*.

6.1.2. Swarm Intelligence and Resilience

We may afford an intuitive interpretation of crucial (complex) events, using the example of a flock of birds flying in a given direction, as an effect of self organization. A crucial (complex) event is equivalent to a complete rejuvenation of the flock that after an organizational collapse may freely select any new flying direction. An external fluctuation of even weak intensity can force the complex system to move in a given direction, if it occurs at the exact instant of the free will of the SOTC model system. It is important to stress that the organizational collapse is not the fall of an elite, which will be discussed subsequently, because the flock self-organization occurs spontaneously and does not rest on the action of a leader. The choice of a new flying direction is thus determined by an external stimulus of even weak intensity occurring at the same time as the collapse, thereby implying the property of *complexity matching* between the perturbed and the perturbing complex system [36].

As mentioned earlier, the crucial events favor the transport of information from one complex system to another [77]. Crucial events are generated by criticality and consequently the transport of information becomes maximally efficient at criticality [41].

However, criticality may also be Achilles' heel of a complex system, if criticality is generated by a fine tuning control parameter. In fact, committed minorities acting when a crucial event occurs in the case of DMM can make the system jump from the state C to the state D [55]. Herein we show that this lack of resilience is not shared by the bottom-up approach to SOTC modeling, in fact, starting from the bottom generates a very resilient social organization.

6.1.3. From Criticality Generated by the Fine Tuning of a Control Parameter to Self-Organization Temporal Criticality

The model of [78] is a form of spontaneous transition to criticality, revealed by the emergence of events with the temporal properties of crucial events, thereby explaining the adoption of the name Self-Organized Temporal Criticality (SOTC) to define it. We show that the bottom-up SOTC modeling is resilient and that the top-down SOTC modeling is not.This SOTC model may help to contribute to the discussion of the sociological issues of Haidt [93] with the tools of Complexity Science. In fact, Haidt emphasized that the political conflict between conservatives and liberals is due to cultural and religious influences that have the effect of creating divisions. The top-down SOTC approach may be used to model these cultural influences. This is an extremely difficult problem, made even more difficult by the philosophical controversies on definition of morality [107]. According to the brilliant picture of Haidt, the philosophy of Hume and Menciu may be compatible with the bottom-up origin of cooperation, while the hypothesis that *morality transcends human nature*, an interpretation moving from Plato to Kant [93], may justify a top-down perspective. We make the extremely simplified assumption that the top-down SOTC, undermining social resilience, explains the fall of elites, if they represent only limited groups, a phenomenon that may be explained by noticing that "our minds were designed for groupish righteousness" [93]. The source of social conflict seems to be that cultural evolution differs from life evolution. These culturally-induced conflicts may overcome the biological origin of cooperation.

6.1.4. Bottom-Up Versus Top-Down Approach to Morality

For clarity in Section 6.2 and Section 6.3 we provide a review of the SOTC model [78], while stressing some properties of SOTC model that were not discussed. For instance, the behavior of single units with their frequent regression to the condition of independence of the other units, for the bottom-up process and the Pareto cycles of the top-down version of the model. The original results of this work indicated a lack of resilience of the top-down SOTC model and a robustness of the bottom-up SOTC model, which are illustrated in Section

6.4. Section 6.5 is devoteed to balancing the results of the present work against the open problems that we propose to study in future research.

6.2. Bottom-Up Approach to Self-Organized Temporal Criticality

The decisions of single individuals in our model are made in accordance with the criterion of bounded rationality [108, 81], expanded by Kanheman [82] and more recently discussed from within the perspective of evolutionary game theory (EGT) [83], [84]. The non-rational component of the decision making process is stressed also by the work of Gigerenzer [109]. Herein individuals make decision using DMM. The individuals of the social network aim at increasing their payoff make the control parameter K_r, for individual r, evolve towards criticality, thereby creating an intelligent group mind [34]. As we shall see, the time evolution of K_r is slow, because it depends on the payoffs of the individual at earlier time, corresponding to the slow thinking mechanism discussed by Kanheman [82].

6.2.1. The Intuitive and Emotional Level

We use the DMM on a two-dimensional lattice of size L, with $M = L \times L$ individuals, and we set $L = 10$. The DMM is based on individuals imperfectly imitating the majority opinion of their four nearest neighbors, thereby biasing the probability of making a transition from being a cooperator (C) to being a defector (D):

$$g_{CD}^{(r)} = g_0 \exp\left\{-K_r \frac{\left(N_C^{(r)} - N_D^{(r)}\right)}{N}\right\}, \tag{6.4}$$

where $N_C^{(r)}$ is the number of nearest neighbors to individual r that are cooperators, $N_D^{(r)}$ the number of defectors, and each individual on the simple lattice has $N = 4$ nearest neighbors. In the same way the transition rate from defectors to cooperators $g_{DC}^{(r)}$ is

$$g_{DC}^{(r)} = g_0 \exp\left\{K_r \frac{\left(N_C^{(r)} - N_D^{(r)}\right)}{N}\right\}. \tag{6.5}$$

The unbiased transition rate is $g_0 = 0.01$ throughout the calculations, and $1/g_0$ defines the time scale for the process. The DMM has been shown [36] to undergo critical phase transitions and to be a member of the Ising universality class in which all the members of the network can act cooperatively, depending on the magnitude of the interaction strength K [36]. However, this important result is obtained by assigning to all the individuals the same degree of attention to the opinions of their nearest neighbors, called K. Herein each individual may have a different degree of attention and this degree of attention does not fit the reciprocity principle. The degree of attention that the individual r devotes to the individual r' may differ from the degree of attention that the individual r' devotes to the individual r. To explain how the individual r is influenced by her nearest neighbors, let us consider for instance Eq. (6.4). The individual we are considering is a cooperator and Eq. (6.4) establishes the rate of her transition to the defection state. If $N_C^{(r)} > N_D^{(r)}$ the rate decreases and will vanish in the extreme limit $K_r = \infty$. Of course, this will have the effect of favoring the cooperation state.

6.2.2. The Rational Level

This decision making process is fast, emotional and does not involve any direct reasoning about the payoff. The connection with the self-interest, according to the slow thinking mechanism disscussed by Kanheman [82] is established over a more extended time scale, where the single individual exerts an influence on the process aiming at maximizing her payoff. To define the payoff we adopt the Prisoner's Dilemma Game (PDG) [30]. Two players interact and receive a payoff from their interaction adopting either the defection or the cooperation strategy. If both players select the cooperation strategies, each of them receives the payoff R and their society receives the payoff $2R$. The player choosing the defection strategy receives the payoff T. The temptation to cheat is established by setting the condition $T > R$. However, this larger payoff is assigned to the defector only if the other player selects cooperation. The player selecting cooperation receives the payoff S, which is smaller than R, If the other player also selects defection, the payoff for both players is P, which is

smaller than R. The PDG is based on the crucial payoffs $T > R > P > S$ and $S + T < 2R$.

We adopt the choice of parameter values made by Gintis [30] and set $R = 1$, $P = 0$ and $S = 0$. The maximal possible value of T is 2, and we select the value $T = 1.9$, which is a very strong incentive to cheat. We evaluate the social benefit for the single individual, as well as for the community as a whole as follows. We define the payoff P_r for individual r as the average over the payoffs from the interactions with its four nearest neighbors. If both players of a pair are cooperators, the contribution to the payoff of the individual r, is $B_r = 1$. If one of the two playing individuals is a cooperator and the other is a defector, the contribution to the payoff of r is $B_r = T$. If both players are defectors the contribution to the payoff of r is $B_r = 0$. The payoff P_r to individual r is the sum over the four B_r's.

Each individual receives a total payoff from the game with the four nearest neighbors and adjusts her imitation strength as follows:

$$K_r(t) = K_r(t - \Delta t) + \chi \frac{P_r(t - \Delta t) - P_r(t - 2\Delta t)}{P_r(t - \Delta t) + P_r(t - 2\Delta t)}, \tag{6.6}$$

where the parameter χ determines the intensity of interest of the individuals to the fractional change in their payoffs in time. The key equation (6.6) is based on the assumption that the intuitive decision making process is so fast that at both time $t - \Delta t$ and $t - 2\Delta t$ is possible to evaluate the corresponding payoffs on the basis of fast decisions made by each individual and by her 4 nearest neighbors. The decision of adjusting the social sensitivity $K_r(t)$ requires the time interval $2\Delta t$, while the intuitive decision is virtually instantaneous.

The second term on the right-hand size of Eq. (6.6) is the ratio between two quantities that for special cases vanish. In these cases we set the condition

$$K_r(t) = RK_r(t - \Delta t), \tag{6.7}$$

with $R < 1$. We selected $R = 0$ but for other values we get the same result. When $K_r(t)$ goes to negative values we set it equal to zero.

Note that in the limit of vanishing time intervals Eq.(6.6) relates the time rate of change of an individual's imitation strength to the time rate of change of the logarithm of

the local payoff to that individual. On the global scale, the mean benefit to society of all the individuals is given by the average over all the P_r's:

$$\Pi(t) = \frac{1}{N}\sum_{r=1}^{N} P_r(t), \tag{6.8}$$

whereas the mean imitation strength is given by the average over all the $K_r(t)$:

$$K(t) = \frac{1}{N}\sum_{r=1}^{N} K_r(t). \tag{6.9}$$

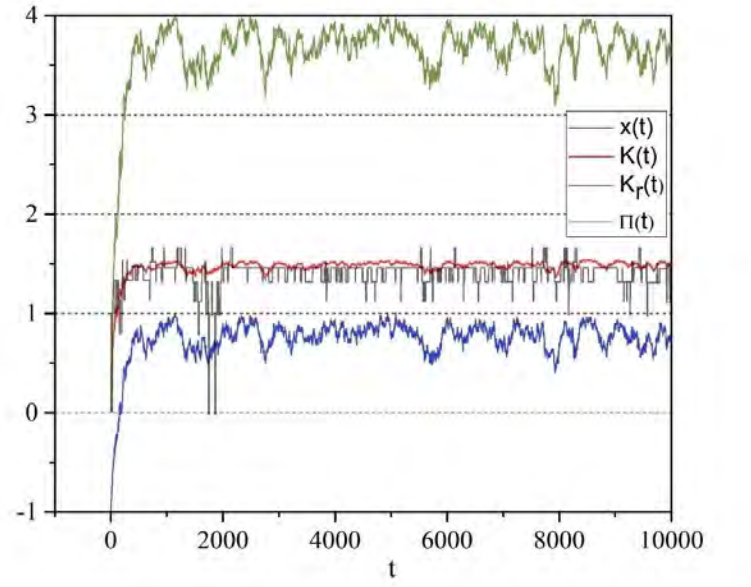

FIGURE 6.1. For the bottom-up SOCT: Time evolution of the average social benefit $\Pi(t)$, the average imitation strength K(t), the mean field x(t) and the imitation strength of one of the units $K_r(t)$ plotted versus time. The mean field fluctuates around 0.8 which means about 90 percent of individuals are cooperators and 10 percent are defectors. Mean field of 1 has all individuals in the state of cooperation, and the maximum average social benefit has the value 4, because this is the number of nearest neighbors on the two-dimensional lattice.

For the bottom-up case discussed in this section, the calculation is done with the parameters $M = 100$, $g_0 = 0.01$, $T = 1.9$ and $\chi = 1$, with the social benefit, imitation strength and mean field starting from zero.

The results of Figure 6.1 are used to establish the bottom-up origin of altruism, rather than interpreting it, as it is frequently done, to be the result of a religion-induced top-down process. The calculations show that the top-down process generating altruism weakens the system's resilience, whereas the genuinely bottom-up approach makes the emergence of altruism robust against external perturbation. Figure 6.1 shows that the time evolution of the individual social sensitivity K_r is characterized by abrupt jumps that from time to time may also bring the single individual back to a behavior totally independent of the choices made by her nearest neighbors. This is a healthy social condition that has the effect of making the global properties $x(t)$, $K(t)$ and $\Pi(t)$ host crucial events favoring the transmission of information between different social systems, either countries or parties.

To stress the occurrence of crucial events in a social system resting on the bottom-up emergence of altruism, we have to extend the method used for criticality generated by the fine tuning of the control parameter K. In that case, at criticality the mean field fluctuates around the vanishing value and the crucial events correspond to the occurrence of this vanishing value [54, 40]. We follow [110] and evaluate the fluctuations around the proper non-vanishing mean value of $K = 1.5$. To explain this choice notice that in the conventional case of criticality, generated by the choice of a proper control parameter K, with $M = 100$, $K = 1.5$ is the value at which the onset of phase transition occurs. This is the value making the mean field $x(t)$ of the conventional DMM fluctuate around $x = 0$ with complex fluctuations and which generates criticality-induced intelligence [29, 58]. In the case of the SOTC model this condition of criticality-induced intelligence, with fluctuations of $K(t)$ around 1.5 is spontaneously generated. When the criticality condition is reached the complex fluctuations of $x(t)$ do not occur any longer around $x = 0$, but around a positive value of the order of 0.8. The time intervals τ between consecutive crossings of the 1.5 level are monitored and the corresponding waiting-time PDF $\psi(\tau)$ is illustrated in Fig. 6.2.

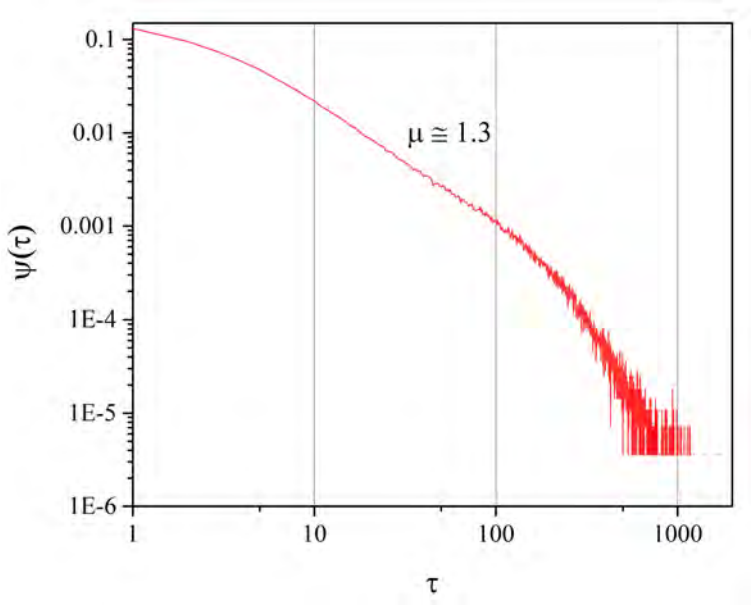

FIGURE 6.2. For bottom-up SOTC: the waiting time PDF of the time interval between two consecutive crossings of the average value of the mean value of $K(t)$, which is ≈ 1.5, is graphed. $\psi(\tau)$ is exponentially truncated and has an intermediate asymptotic regime with an index of $\mu \approx 1.3$. This figure was taken from [78] with permission.

Figure 6.2 is taken from [78] and illustrates the effects of perturbation (see Fig. 6.4). We limit ourselves to noticing that temporal complexity shows up in the intermediate asymptotics regime [78] and it is characterized by the IPL index $\mu = 1.3$, a property shared by other systems at criticality, see, for instance, [77]. This is evidence that the spontaneous transition to criticality also generates the crucial events responsible for information transport. Earlier work [78] confirms that the crucial events facilitate the transport of information from one complex social system to another, if the two systems are at criticality as a result of the spontaneous process of self-organization.

In spite of the exponential truncation that may lead to the misleading conclusion that the Poisson-like character of the long-time regime quenches the manifestations of complexity, the transport of information is determined by the intermediate asymptotics. In the earlier work of Ref. [78] we studied the efficiency of transport of information from one bottom-up

SOTC to another identical SOTC and we found that the maximal efficiency of the information transport corresponds to about $M = 100$, which is the condition studied here. The explanation of this interesting effects is the following. The intensity of fluctuations generating crucial events decreases with the size increase, according to the formula (see Eq. (14) of Ref. [78])

$$\Delta\zeta \propto \frac{1}{M^{\nu}}, \tag{6.10}$$

with $\nu = 0.5$. Note that $\Delta\zeta$ denotes the intensity of the fluctuations of the variables K, Π and $x(t)$ around their mean values. Therefore the systems with $M > 100$ have crucial fluctuations of smaller intensity, thereby explaining the reduction of the process of information transport. For values $M < 100$, the role of the exponential truncation becomes more important and the time extension of the complex intermediate asymptotics is reduced and eventually the intermediate asymptotics regime vanishes, turning the system into a Poisson system, with no complexity. This has the effect of significantly reducing the efficiency of the process of information transport. As far as the resilience of the bottom-up SOTC is concerned, the theory of this work rests on the connection between resilience and the efficiency of information transport. As a consequence the results on the resilience of the bottom-up SOTC for $M = 100$ automatically correspond on the condition of maximal resilience [111].

6.3. Top-Down Approach to Self-Organized Temporal Criticality

The top-down approach to self-organization is done using again Eq. (6.4) and Eq. (6.5). The adoption of the top-down perspective is realized by replacing Eq. (6.6) with

$$K(t) = K(t - \Delta t) + \chi \frac{\Pi(t - \Delta t) - \Pi(t - 2\Delta t)}{\Pi(t - \Delta t) + \Pi(t - 2\Delta t)}. \tag{6.11}$$

The top-down origin of this process is made evident by the fact that all individuals in the network are forced to adopt the same time-dependent imitation strength. Furthermore, rational choice is made on the basis of the collective payoff $\Pi(t)$, using PDG. The conceptual difference with the bottom-up approach of Section 6.2 is impressive. In fact, with Eq.

(6.11) all the individuals of this society must change their social sensitivity at the same time and the information about the increase or decrease of the global payoff implies that all the individuals are given this information from a central source such as the government, suggesting that a form of organization already exists and is not created by the interaction between the individuals. In Ref. [78] the assumption was made that a benevolent dictator exists and leads such a process. Using Pareto's social theory we make the assumption that this process implies the leadership of an elite [94].

The second term on the right-hand size of Eq. (6.11) is the ratio between two quantities that, similarly to the bottom-up model, for special cases vanish. In these cases, as done in Section 6.2, we set the condition

$$K_r(t) = RK_r(t - \Delta t), \tag{6.12}$$

with $R < 1$. We selected $R = 0$. When $K_r(t)$ goes to negative values we set it equal to zero.

For the top-down case discussed in this section, the calculation is done with the parameters $M = 100$, $g_0 = 0.01$, $T = 1.9$ and $\chi = 4$, with the social benefit, imitation strength and mean field starting from zero. χ is chosen to be larger than in the bottom-up case because of the fact that transition to criticality in the top-down case is much slower (see Fig. 6.1 and Fig. 6.3).

Under the leadership of an elite, see Figure 6.3, the control parameter $K(t)$ shows a behavior totally different from that of Figure 6.1. In this Section we focus on the behavior of $K(t)$ in the absence of perturbation and discuss the effects of perturbation in Section 6.4. With no perturbation there is a transient from $t = 0$ to $t \approx 40000$, after which time a sequence of rises and falls occur. The value of K adjusts according to Eq.(6.11) from small values around 0.2 to a maximal value of 1.8, which is known to correspond to a supercritical condition in the case of the conventional DMM. When using the fine tuning control parameter approach we set $K = 1.8$ the social system is far from the intelligence condition that according to a widely accepted opinion [99, 17, 104, 105, 46] requires criticality. The mean field $x(t)$ has very fast fluctuations around a mean value close to 1, but these

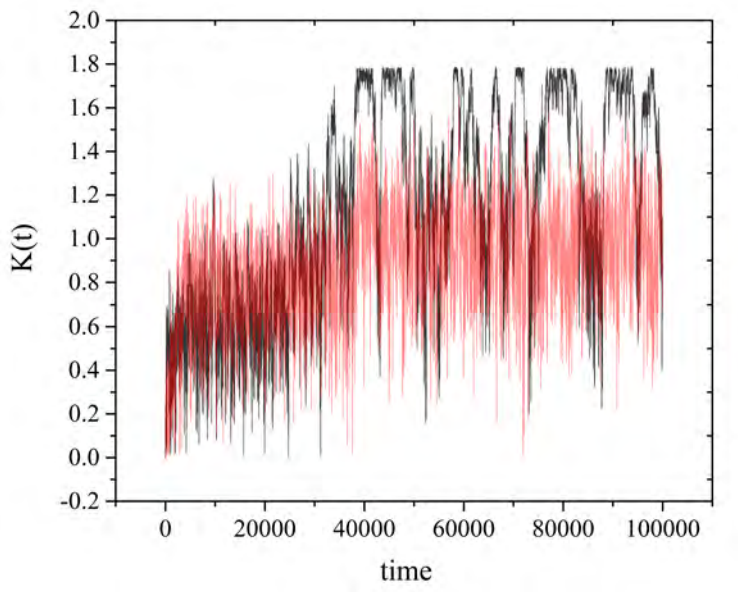

FIGURE 6.3. Black line: The time evolution $K(t)$ of Eq. (6.11) for the same regular two-dimensional network of Figure 6.1; Red line: The time evolution of $K(t)$ of the self-organized system described by the black under the influence of the weak noisy perturbation described in Section 6.4.

fluctuations are Poisson and the conventional DMM system loses its complexity [77].

The falls to the small values of K are interpreted as falls of elites. The subcritical condition, as well as the supercritical, is characterized by a lack of intelligence. We have to remark also that values of K significantly smaller than $K \approx 1.5$ indicate that there are many units with $K_r = 0$, like the single unit of Figure 6.1 at a time close to $t \approx 2000$. In conclusion, both small and maximal values of K are affected by a lack of consciousness, and the transitions through $K \approx 1.5$ are too fast for the social system to benefit from the intelligence of the critical condition. This lack of intelligence is responsible for the lack of resilience. The sojourn times in the supercritical state correspond to the time durations of elites. We do not have to confuse the fluctuations of $K(t)$ with those of the mean field $x(t)$ that are not shown here. The fluctuations of $x(t)$ are always Poisson, around mean values close to 1, when $K(t)$ is close to 1.8 and around the vanishing mean value when $K(t)$ drops.

It is interesting to notice that also the time interval between consecutive falls of elite

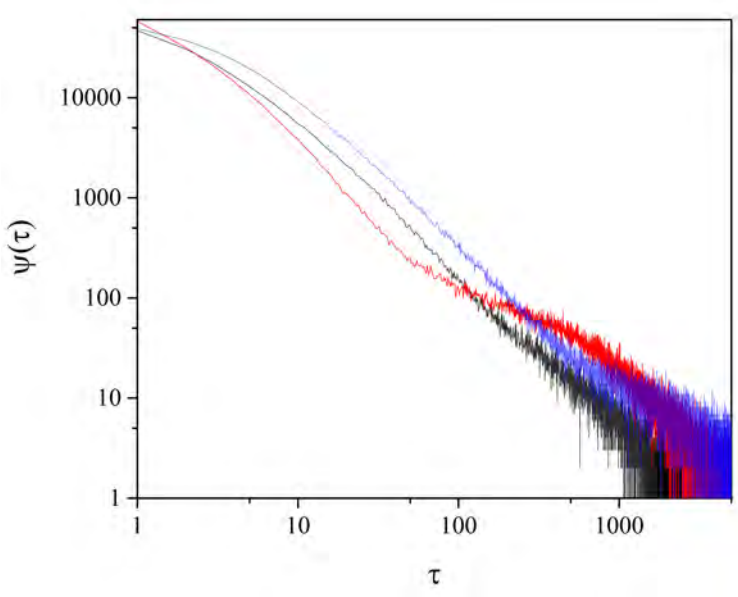

FIGURE 6.4. For bottom-up SOTC, the waiting time PDF of the time intervals between two consecutive crossings of the horizontal line with $K = 0.7$ (black and red line) and $K = 1.7$ (blue line) for the top-down SOTC. The blue and the black lines describe the unperturbed case and the red line describes the perturbation described in Section 6.4.

is a complex dynamical process characterized by an IPL, with $\mu \approx 2$ in this case, as shown by Figure 6.4. However, the system is not resilient. The sojourn in a supercritical state with a K significantly larger than $K \approx 1.5$ is characterized by fast Poisson fluctuations and an external perturbation can easily affect the time duration of this regime [112]. In fact, the big difference between Poisson events and crucial events is that the former events obey conventional linear response theory and any forms of perturbation can deeply affect their dynamics, thereby undermining the social resilience, as we show in the next section.

6.4. Perturbing the Self-Organized Society

To substantiate the arguments of the earlier section with the results of a numerical simulation we devote this section to illustrating some numerical experiments on the effects of a perturbation on the process of societal self-organization.

First of all let us define two different sources of perturbation, the *independent* and the *committted* minorities. We assume that a minority of independent individual exists. An independent individual is a unit that is characterized by $K_r = 0$. As a consequence this unit does not adopt Eq. (6.6) and is completely insensitive to the connection between individual and societal benefit that yield the emergence of cooperation [78]. The perturbing nature of this independent individual is realized by the fact that, while the independent keeping $K_r = 0$ is completely independent of the choices made by the other units, her nearest neighbors are influenced by the choices of the independent through the DMM and through the evaluation of the payoff $P_r(t)$ of Eq. (6.6).

In the top-down SOTC model the independent influences the process through his vanishing contribution to $K(t)$ and through his contribution to the global payoff of Eq. (6.11). The perturbation of independents is made more devastating when the independents are allowed to move randomly through the social network.

The other kind of perturbation, that produced by committed minorities, has already studied studied elsewhere [55]. These are minorities that keep selecting the state D. The committed minorities are also called zealots and have been the subject of many publications, see [113] for a wide set of references. These publications emphasize the dramatic consequences that the zealots have on their societies, thereby implying that their models of organization are not resilient. The experiment on the perturbation of zealots done herein shows that the top-down SOTC model shares the lack of resilience observed in these earlier studies on the social influences of zealots. The bottom-up SOTC model seems to be the only fully resilient model.

Let us discuss first the strongest source of perturbation, the randomly moving independents. At any time step one of the $M = 100$ is randomly selected to play the role of independent, namely we force her to adopt the value $\xi = 1$ or the value $\xi = -1$, with equal probability. In the case of the bottom-up SOTC this perturbation does not have significant effect on the time evolution of $K(t)$, as shown by Figure 6.5.

In the case of the top-down SOTC the effects of this perturbation are impressive. The

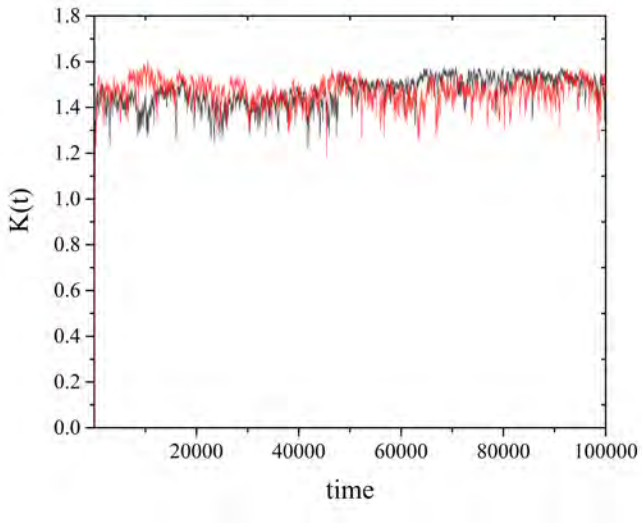

FIGURE 6.5. K(t) as a function of time for the bottom-up SOTC, in the no-perturbation (black line) and perturbed case (red line).

black line of Figure 6.3 shows the rise and the fall of an elite. The weak noisy perturbation makes $K(t)$ evolve as illustrated by the red line of the same figure, which shows that the sojourn times of unperturbed elites are filled with many falls that are a clear manifestation of the lack of societal resilience.

Important information on the lack of resilience of the top-down SOTC are afforded by Figure 6.4, showing $\psi(t)$ for different values of the threshold used to find the statistics of crucial events. When the threshold is 1.7, close to the top super-critical region reached by the system the intermediate asymptotics has a power index $\mu \approx 1.45$, larger than that of the bottom-up SOTC. The adoption of the threshold $K = 0.7$ as an effect of the collapse of elites cancels the intermediate asymptotic temporal complexity, and favor the birth of a Poisson shoulder. The noisy perturbation of independents makes this behavior even more pronounced. This strong exponential shoulder is a signature of the death of dynamical complexity and of the transition from non-Poisson to Poisson behavior [78].

The perturbing action of independents is weaker if the independent individuals do not move. This response to this form of perturbation is illustrated in Fig. 6.6, showing that

even in this case the bottom-up SOTC model is more robust than the top-down.

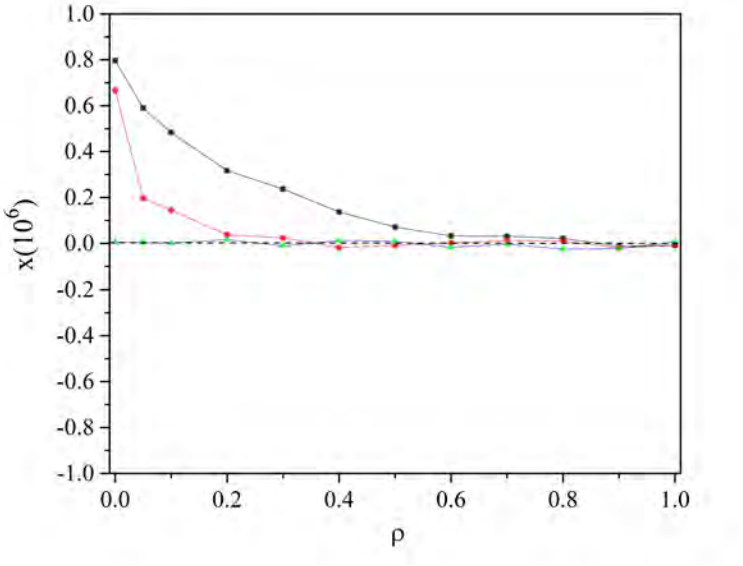

FIGURE 6.6. Dependence of mean field (at time 10^6) on the ratio ρ of independent units (which are fixed on the lattice) for the bottom-up SOTC modell (black line), top-down SOTC model (red line) and ordinary DMM with tuned control parameter $K_c = 1.5$ (green line). Ensemble average is done over 10 experiments.

We establish the perturbation of independent individuals in a different way. We assume that all the units are independent for a fraction η of their time. The results are depicted in Figure 6.7. It is clear from the figure that the bottom-up SOTC model is more resilient than the two-down, even to this most violent form of disruption.

Finally in Figure (6.8) we show the action of committed minorities. We see that only the bottom-up SOTC model is resilient. The top-down SOTC model shares the same lack of resilience shown by ordinary DMM at criticality.

6.5. Concluding Remarks

It is remarkable that according to SOTC the crucial events may be harmful as well as beneficial. If the global parameter $K(t)$, fluctuating around the long-range correlation

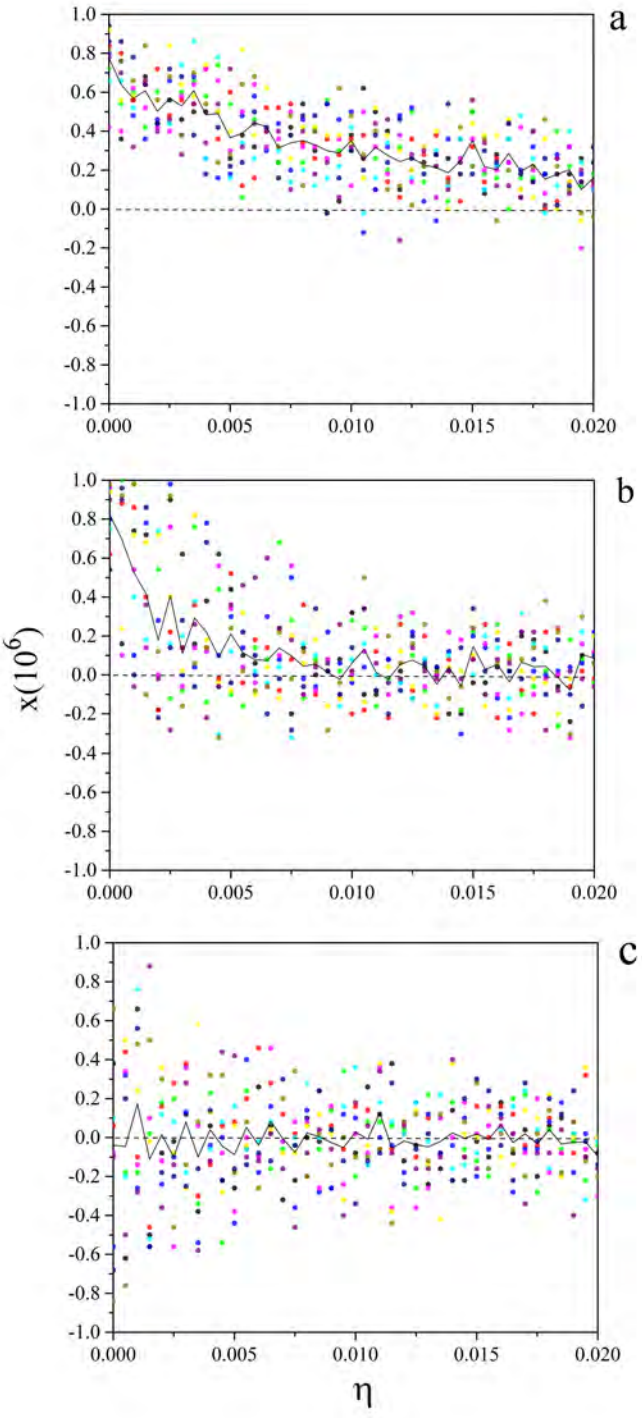

FIGURE 6.7. Dependence of mean field (at time 10^6) on η (the ratio oftime in which units behave individually) for bottom-up SOTC model (a), top-down SOTC model (b) and for ordinary DMM with tuned parameter $K_c = 1.5$ (c). Each set of colored dots is correspond to one experiment and the black solid lines are the average of them.

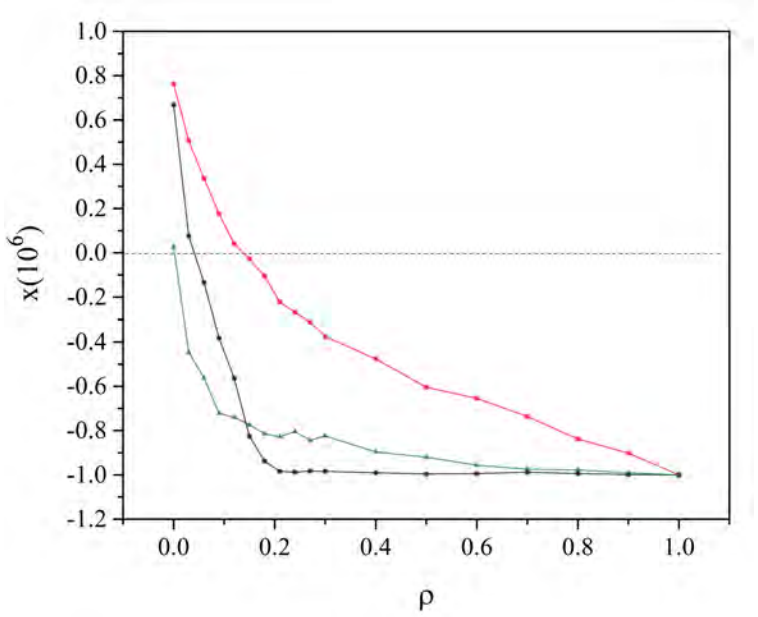

FIGURE 6.8. Dependence of mean field (at time 10^6) on the ratio ρ of fanatics (having fixed position on the lattice) for the bottom-up SOTC model (red line), Top-down SOTC model (black line) and ordinary DMM with tuned control parameter $K_c = 1.5$ (green line). Ensemble average is done over 10 experiments.

generating mean value, return to the vanishing value, the temporary collapse is turned into a societal disaster. The collapse into $K = 0$ would correspond to a new initial condition and, as shown by Figure 6.1, $K(t)$ would start increasing again generating a new organization led by a new elite [94]. However, the genuinely bottom-up process leading the time evolution illustrated by Figure 6.1 is expected to keep forever the social system in the condition of weak fluctuations around $K \approx 1.5$. In other words, there is an impressive difference between the crucial events hosted by the weak fluctuation around $K \approx 1.5$ and the regressions of $K(t)$ to values of $K \ll 1.5$, generated by the adoption of a top-down process led by an elite.

The main conclusion of this part concerning resilience is that criticality is necessary for resilience, but it is not sufficient. The top-down SOTC model generates criticality, but it is not resilient. Therefore information transport from one top-down SOTC model system to another top-down SOTC model system is expected to occur by means of complexity

matching, in spite of the fact that the two systems are not resilient and the information transport may be easily quenched by stray perturbing noises.

An attractive interpretation of the resilient nature of the bottom-up SOTC model is that the ideal condition of full democracy is the most robust form of social organization.

Here the social payoff is evaluated using the PDG [30]. The prisoner's dilemma game is frequently used in the field of EGT [32, 1]. EGTs aim at solving the altruism paradox using the concept of network reciprocity [1]. A game is played many times on a network where each individual is surrounded by a set of nearest neighbors and adopts the strategy of the most successful nearest neighbor. Since the clusters of cooperators are richer than the clusters of defectors it is plausible that the most successful nearest neighbor is a cooperator. However, this attempt at mimicking the action of a collective intelligence failed because the social activity of the units, being subcritical, disrupts the beneficial effects of network reciprocity [63, 49]. We note that SOTC modeling represents an attempt to amend the field of EGT by the limitations preventing, for instance, the concept of network reciprocity from yielding a satisfactory resolution of the altruism paradox.

The human inclination to cooperate is the result of biological evolution and of the spontaneous evolution towards criticality. The time appear ripe to unify the models of biology and physics made necessary to reach the ambitious goal of achieving a rigorous scientific foundation of this important human characteristic [114, 115]. The spontaneous transition to criticality of SOTC contributes to bypassing the current limitations of the field of EGT. SOTC model can be adapted to take into account the top-down processes connected with the non-resilient action of elites. It is possible to supplement the non-rational decision making process based on Eq. (6.4) and Eq. (6.5) with self-righteous biases [93] taking into account the influence of religion or other polarizing influences. We expect that such generalizations of SOTC theory will lead to a lack of societal resilience. However, this is left as a subject for future research.

CHAPTER 7

ON SOCIAL SENSITIVITY TO EITHER ZEALOT OR INDEPENDENT MINORITIES

Individuals act in their own self-interest, but in so doing contribute to the observed wellbeing of society, as determined using the self-organized temporal criticality (SOTC) model. This model identifies the timing of crucial events as a new mechanism with which to generate criticality, thereby establishing a way for the internal dynamics of the decision making process to suppress the sensitivity of social opinion to either zealot or independent minorities. We find that the sensitivity to the influence of zealots is much smaller than in the case of criticality with a fine tuning control parameter and the action of independent minorities may affect temporal complexity so as to realize the condition of ideal $1/f$ noise.

The role played by committed minorities, *zealots* or *fanatics*, in the behavior adopted by large groups, whether it is in the apparently frivolous taking on of a fad or fashion, or the more serious adoption of new social conventions, has attracted the attention of a significant number of sociologists [116, 117, 118], physicists [55, 119], network scientists [120, 121, 122, 123], in addition to scientists working in many other disciplines. These investigators explore, using a variety of models from multiple vantage points, how in times of crisis, committed activists may produce political, or other, changes of significant importance to society, in spite of their relatively small number. A common feature of these models is criticality, at which point the aggregate of individuals becomes a collective with a single purpose, and under the right conditions the zealots can leverage the organized behavior to redirect the collective. We observe that in a system of finite size the global consensus state is not permanent and times of crisis occur when there is an ambiguity concerning a given social issue. The correlation function within the cooperative system becomes similarly extended

This chapter was adapted from Mahmoodi, Korosh and West, Bruce J and Grigolini, Paolo, "On social sensitivity to either zealot or independent minorities", published on 20 March 2018 in Chaos, Solitons & Fractals, Vol. 110, 185, Open access.

as it is observed at criticality. This combination of independence (free will) and long-range correlation makes it possible for very small, but committed minorities to produce substantial changes in social consensus, see *e.g.* [36].

On the other hand, fluctuations are assumed to be generated by the same form of self-organization that brought the system to criticality in the first place. This assumption is frequently made by researchers studying the dynamics of the human brain [124, 125, 126, 127] leaving open, however, the origin of criticality in this context. Allegrini et al. [128] emphasized that the intermittent nature of these fluctuations, according to the prediction that the inverse power-law (IPL) spectrum:

$$S(f) \propto 1/f^{\beta}, \tag{7.1}$$

with the IPL index,

$$\beta = 3 - \mu, \tag{7.2}$$

should lead to the ideal $1/f$ - noise condition $\beta = 1$ for $\mu = 2$. The IPL index μ labels the time intervals between crucial events [36] at the tipping point (critical point of a phase transition); the three dimensional Ising model [129] generates $\mu = 1.55$, whereas the decision making model (DMM) [55] yields $\mu = 1.5$ at criticality.

Xie *et al.* [130] studied the influence of inflexible individuals on social behavior, using the Naming Game to model the social interaction, and found that when the committed minority reaches a threshold of 10% of the population the opinion of the entire social network can be reversed to conform to that of the minority. The theoretical results were shown to be supported by laboratory experiment [116]. The theoretical influuence of the minority was also shown to be largely independent of the structure of the interactions within the social model, but can be determined by as much as 10% to as little as 4% for a sparse network [131]. The percentage at which the tipping point occurs is clearly model dependent and can vary from 4% to 15% [132, 133].

Here we consider also another kind of minority, the minority of *independents*. An independent is an individual who makes her choices with no influence from her nearest

neighbor. In the long-time scale the behavior of the independent looks erratic and she exerts an influence on society, because their nearest neighbors make their choice taking into account also the erratic choices of the independent.

The analysis herein is based on the form of self-organization, called Self-Organized Temporal Criticality (SOTC) recently proposed in [78]. The individuals of this society have to make a choice between cooperation and defection. This research shows that the bottom-up form of spontaneous organization described by SOTC strongly reduces the efficiency of the committed minority in redirecting the behavior of society. We show that the SOTC model also disrupts the action of independents, paying however the price of changing the IPL index μ that provides a measure of the system's complexity.

In Section 7.1 we adapt the linked concepts of intuition and deliberation by constructing a dynamic two-level network model, where single individuals are located at the two-dimensional lattice nodes of a composite network. The composite network consists of two interacting subnetworks. One subnetwork is based on the decision making model (DMM) [36] and leads to strategy choices made by the individuals under the influence of the choices of their nearest neighbors. The other subnetwork measures the Prisoner's Dilemma Game (PDG) payoffs of these choices [30]. The interaction between the two subnetworks is carried out by increasing or decreasing the individual imitation strength K_r according to the history of payoffs to that individual. This is a generalization of the self-organized criticality (SOC) model [66], called the self-organized temporal criticality (SOTC) model [78].

In the SOTC model the decisions made by individuals are assumed to be consistent with the criterion of bounded rationality [81], which were expanded by Kahneman [82], and more recently discussed from the perspective of evolutionary game theory [83, 84]. Rand and Nowak [83] acknowledge the tension between what is good for the individual, what is good for society and they discuss the tension between them in the language of evolutionary game theory. Without reviewing the long history of studies into the nature of cooperation, defection, and the theoretical strategies that people may adopt to overcome their selfish urges, we note the meta-analysis of 67 empirical studies of cognitive-manipulation of eco-

nomic cooperation games by Rand [84]. He concluded from his meta-analysis that all the experimental data could be explained using a dual-purpose heuristic model of cooperation, a model consisting of a dynamic interaction between deliberation and intuition. Deliberation is considered to be a rational process that always favors non-cooperation, whereas intuition is treated as an irrational process that can favor cooperation or non-cooperation, depending on the individual.

In Section 7.1 we present numerical results built on those presented earlier [78] to determine the social sensitivity to the uncompromising behavior of a small number of individuals holding either inflexible opinions or changing their opinion with no influence from their nearest neighbors. The committed minority individuals are assigned the state D and do not change their opinion. The independent change their choices in random way. In both these cases the minorities are totally independent of their nearest neighbors but their nearest neighbors are influenced by them according to the DMM rules. The remarkable result is that the SOTC approach to criticality turns out to be much less sensitive to the influence of these minorities that in the case of criticality is obtained by a fine tuning of the control parameter K. It is also remarkable that the independent minority does succeed in affecting the temporal complexity making it possible to realize $\mu = 2$, the condition that generates $1/f$ noise, produced by the brain in the wakefulness state.

7.1. Two-Level Network Model

The dynamics of the model of interest consists of the interaction between two distinct subnetworks. The behavior of one subnetwork consists of decisions made by individuals influenced by their nearest neighbors and realized by the DMM [36]. The second subnetwork assesses the choice made by the individual and assigns a payoff based on the PDG model. The interaction between the two subnetworks is established by making the individual's imitation strength K_r increase or decrease, according to whether the average difference of the last two payoffs increase or decrease, in accordance with the corresponding changes in K_r. Although each of these imitation strengths is selected selfishly, which is to say the individual choices

of imitation strengths are made in the best interest of the individual making the decision at that time, the social system is driven by the resulting internal dynamics towards the state of cooperation, which has the greatest social benefit, which is a unique property of the SOTC. The individuals of the two-level network are located at the nodes of a regular two-dimensional network, denoted by the symbol r, which is equivalent to the double index (i, j).

7.1.1. The DMM Subnetwork

The intuition mechanism proposed by Rand [84] is realized through the dynamics of one subnetwork through the DMM. The DMM on a two-dimensional lattice is based on individuals imperfectly imitating the majority opinion of their four nearest neighbors, thereby biasing the probability of deciding to transition from being a cooperator (C) to being a defector (D):

$$g_{CD}^{(r)} = g_0 \exp\left\{-K_r \frac{N_C^{(r)} - N_D^{(r)}}{N}\right\}, \tag{7.3}$$

where $N_C^{(r)}$ is the number of nearest neighbors to individual r that are cooperators, $N_D^{(r)}$ the number of defectors, and each individual on the simple lattice has $N = 4$ nearest neighbors. In the same way the transition rate from defectors to cooperators $g_{DC}^{(r)}$ is obtained from Eq.(7.3) by interchanging indices. The unbiased transition rate is $g_0 = 0.01$ throughout the calculations, and $1/g_0$ defines the time scale for the process.

To realize SOTC, as we shall explain in Section (7.1.3), the imitation strength of the single individual changes in time, according to the interaction with the PDG subnetwork. The goal of this work, as mentioned in Section 7, is to discuss the influence on the SOTC organization of a fraction ρ of individuals that do not fit the bottom-up approach to cooperation. These individuals are *zealots* (fanatics) or *independent* individuals. The zealots are individual who do not change their choice. In this work they always select defection. The independent individuals exert a random perturbation on the SOTC organization. These

individuals have an imitation strength $K_r = 0$, which does not change in time. Furthermore to enhance their random nature we assign to them $g_0 = 0.5$.

The DMM in isolation, with neither zealots nor independent individuals either, assigns to all the individual imitation strengths K_r the same value K, a control parameter that has been shown to make this theory undergo critical phase transitions and to be a member of the Ising universality class in which all the members of the network can act cooperatively, depending on the magnitude of K [36]. In the present two-level model the K_r can all be different. This decision making process is fast, emotional and in its original form does not involve any reasoning about payoff.

To denote the effect of imitation we assign to the units selecting the cooperation state the value $\xi_r = 1$ and to the units in the defection state the value $\xi_r = -1$. To establish whether cooperation or defection is selected by the social system we use the mean field $x(t)$ defined by

$$x(t) = \frac{1}{M}\sum_{r=1}^{M}\xi_r(t). \tag{7.4}$$

For the isolated DMM if imitation strength K is less than the critical value $K < K_C$ the mean field vanishes, but at criticality, when $K = K_C$, the social system can select either the cooperation, or the defection, branch yielding for $K \gg K_C$, either the value $x = 1$ or $x = -1$. The same situation arises when the DMM is allowed to interact with the PDG, but the critical value of the imitation strength shifts to a new value. The critical value of the imitation parameter K is $K_C = 1$ in the all-to-all coupling configuration and $K_C = 1.5$ (for $M = 30 \times 30$) in the configuration of a regular two-dimensional lattice, with nearest neighbor coupling.

7.1.2. The PDG Subnetwork

The connection with self-interest, according to the slow thinking, cognitive, mechanism of Kahneman [82] is established by a second subnetwork that determines the payoff for the choices made. To define the payoff we adopt rules based on the PDG [30], so that

the second subnetwork becomes a realization of Rand's deliberative mechanism within the two-level network model.

Two players interact and receive a payoff from their interaction adopting either the defection or the cooperation strategy. If both players select the cooperation strategies, each of them receives the payoff R and their society receives the payoff $2R$. The player choosing the defection strategy receives the payoff T. The temptation to cheat is established by setting the condition $T > R$. However, this larger payoff is assigned to the defector only if the other player selects cooperation. The player selecting cooperation receives the payoff S, which is smaller than R. If the other player also selects defection, the payoff for both players is P, which is smaller than R. The game is based on the crucial payoffs $T > R > P > S$. Note that their choices are made continuously as the network dynamics unfold.

We adopt the choice of parameter values made by Gintis [30] and set $R = 1, P = 0, T - R = 0.9$ and $S = 0$. We evaluate the social benefit for the single individual, as well as, for the community as a whole as follows. We define first the payoff P_r for individual r as the average over the payoffs from the interactions with its four nearest neighbors. If both players of a pair are cooperators, the contribution to the payoff of the individual r, is $B_r = 2$. If one of the two playing individuals is a cooperator and the other is a defector, the contribution to the payoff of r is $B_r = T$. If both players are defectors the contribution to the payoff of r is $B_r = 0$. The payoff P_r to individual r is the sum over the four B_r's.

We work with a society of M individuals, so that on the global scale, the mean benefit to society of all the individuals is given by the average over all the payoffs P_r's:

$$\Pi(t) = \frac{1}{M}\sum_{r=1}^{M} P_r(t), \tag{7.5}$$

whereas the mean imitation strength is given by the average over all the imitation strengths $K_r(t)$:

$$K(t) = \frac{1}{M}\sum_{r=1}^{M} K_r(t). \tag{7.6}$$

7.1.3. The Interaction

It is important to notice that K_r , the value of imitation strength adopted by the typical unit r to pay attention to the choices made by its four nearest neighbors, about selecting either the cooperation or the defection strategy, is not necessarily adopted by its four nearest neighbors. In other words, the imitation strength $K_r(t)$ is unidirectional and it determines how r reacts to all its nearest neighbors. The imitation strength $K_r(t)$ changes from individual to individual, as well as in time, and it is consequently very different from the control parameter K of the conventional DMM phase transition processes, where K has a single value throughout the entire network.

Each member of the present network is assigned a vanishing initial imitation strength, corresponding to complete independence of the choices made by its nearest neighbors. At each time step the units play the PDG and independently change their imitation strengths making the implicit assumption that the increase (decrease) of their individual payoff in the last two time steps makes it convenient for them to increase (decrease) their imitation strength. More precisely, they adopt the following rule. As stated earlier, time is discrete and the interval between two consecutive time events is $\Delta t = 1$. The imitation strength of the individual r changes in time according the individual choice rule as follows:

$$K_r(t) = K_r(t - \Delta t) + \chi \frac{[P_r(t - \Delta t) - P_r(t - 2\Delta t)]}{[P_r(t - \Delta t) + P_r(t - 2\Delta t)]} \tag{7.7}$$

where the parameter χ determines the intensity of interest of the individuals to the fractional change in their payoffs in time and is set to one in the calculations presented herein. The second term on the right-hand size of Eq. (7.7) is the ratio between two quantities that for

special cases vanish. In this case we set the condition

$$K_r(t) = RK_r(t - \Delta t), \tag{7.8}$$

with $R < 1$. We select $R = 0.5$ but for other values $R < 1$ we get the same result.

The internal dynamics generated by the interaction of Eq.(7.7), that is between the two subnetworks, drives the average imitation strength and social benefit to the fluctuating plateau values shown in Section 7.2.

7.2. Results

In the case when a phase transition is generated by fine tuning of the control parameter, criticality generates non-Poisson renewal events characterized by an IPL probability density function (PDF) [36]. Critical behavior is manifest through events generating phase transitions, modeled by members of the Ising Universality class, as is the DMM. The occurrence of phase transition in a DMM network, with a finite number of interacting individuals, occurs at a critical value of the imitation parameter $K = K_C$. At criticality the mean field $x(t)$ fluctuates around zero and the time interval between two consecutive zero-crossings is described by a markedly non-exponential waiting-time PDF $\psi(t)$, with the IPL structure

$$\psi(\tau) \propto \frac{1}{\tau^{\mu}}, \tag{7.9}$$

where $\mu = 1.5$.

Here we activate SOTC for a two-dimensional regular lattice (with periodic boundary condition) having $M = 30 * 30$ units and we set $g_0 = 0.01$ and $T = 1.9$, with the mean social benefit, mean imitation strength and mean field starting from zero. The mean field of the two-level network is driven by internal dynamics toward criticality, where the time averaged value of $x(t)$, $\overline{x(t)}$, does not vanish, due to the fact that criticality in this case generates a majority of altruists. Before the interaction with either the zealot or independent minorities is turned on, the mean field reaches a critical state with $\overline{x(t)} = 0.7$, which is to say the social

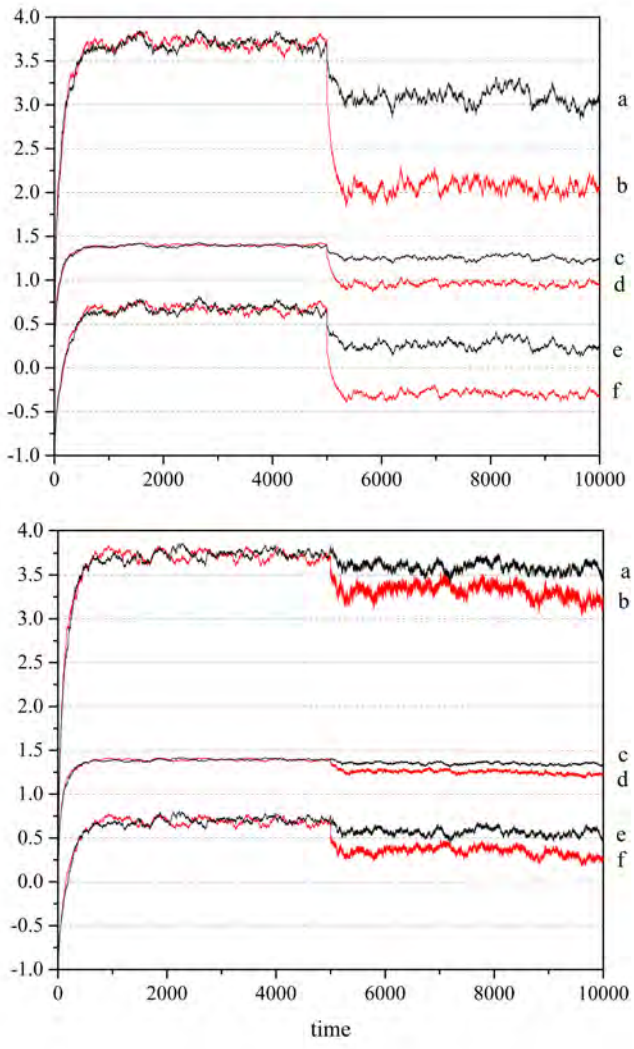

FIGURE 7.1. Effect of fanatics (top) and Independents (bottom) on the 1D SOTC DMM system. At time $5 * 10^4$ fanatics/independents started to act. Black and red correspond $\rho = 0.1$ and $\rho = 0.3$ respectively. (a) and (b) refer to Π; (c) and (d) refer to K; (e) and (f) refer to x.

network has a steady state consisting of 85% altruists or cooperators, as depicted in Figure 7.1.

At time $t = 5 \times 10^4$ after the calculation has been started, a number of individuals are selected at random positions on the lattice and their behavior is modified. In the top panel of Figure 7.1, these randomly chosen individuals are zealots and they are assigned the

opinion state D and not allowed to change, although in every other way they interact with their nearest neighbors as usual. In the bottom panel the randomly selected individuals are independent. Their random behavior is totally independent of the choices of their nearest neighbors, but the choice of their nearest neighbors are influenced by them according to the rules defining the interaction between the two networks.

The two panels show the mean field $x(t)$, the mean global benefit $\Pi(t)$ and the mean imitation strength $K(t)$.

The black curve has $\rho = 0.1$ of the society selected at random to be fanatics, whereas for the red curve $\rho = 0.3$. There is a precipitous drop in the mean field once the modified behavior is introduced, falling from 0.7 to 0.35 and to -0.15 respectively. The dependence on the fraction of fanatics is remarkable.

In the lower panel of this figure we examine the influence on the mean field, not by individuals who do not change their opinion, but by independent individuals who capriciously change their opinions at random. The influence of this cohort group lacks the coherence of the fanatics and may be barely perceptible even at $\rho = 0.3$.

The mean field of the two-level network is driven toward criticality by its internal dynamics, where the time averaged value of the mean field $\overline{x(t)}$ does not vanish, due to the fact that criticality in this case generates a majority of altruists. To stress the occurrence of crucial events in a social system we adopt a method of event detection based on recording the times at which the mean variable crosses its time averaged value. Thus, there are fluctuations around $\overline{x(t)}$ and the IPL structure of Eq. (7.9) is obtained by evaluating the time distance between two consecutive re-crossings of $\overline{x(t)}$. As shown by Figure 7.2, the time intervals between two consecutive crucial events is given by an IPL with index $\mu \approx 1.35$, a property shared by other systems at criticality, see, for instance [29].

It is important to stress that in addition to $x(t)$ also the variables $K(t)$ and $K_r(t)$ are characterized by the same property, namely, also the waiting time PDF of the time interval between two consecutive crossings by $K(t)$ of $\overline{K(t)}$ and by $K_r(t)$ of $\overline{K_r(t)}$, graphed versus time on log-log graph paper, yield an IPL index close to that of $x(t)$ [78]. This is a

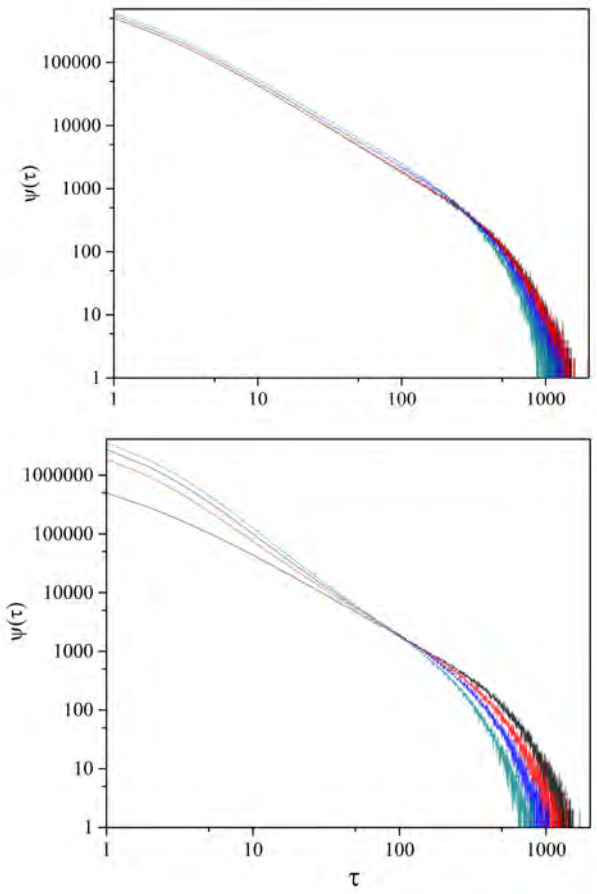

FIGURE 7.2. Effect of fanatics (top) and independents (bottom) on complexity of the SOTC model system. Black, light blue, red, dark blue and purple correspond to $\rho = 0$, 0.1, 0.2, 0.3 and 0.4 fanatics/independents respectively. In top figure the slopes are approximately 1.35 and in the bottom figure slopes (from top to bottom) are approximately 1.35, 1.66, 1.81, 1.91 and 2.17.

consequence of the fact that the behavior of the single individual is characterized by frequent collapses to vanishing and even negative values of $K_r(t)$. On the basis of the form of the transition rate given by Eq. (7.3) we interpret K_r negative as a single individual turning into a contrarian. The calculations done here and elsewhere [134] yields: $\overline{x(t)} \approx 0.7$, $\overline{K(t)} \approx 1.4$ and $\overline{K_r(t)} \approx 1.4$. This is the new phenomenon of self-organized temporal criticality.

Here again we are interested in the changes in the IPL PDF induced by the committed

minorities in the social network. In the upper panel of Figure 7.2 we see essentially no change in the slope of the IPL PDF of approximately 1.35, even though the calculation has been done with the behavior of $\rho = 0$, 0.1, 0.2 and 0.3 assigned the permanent opinion D. The four calculation deviate slightly as the asymptotic exponential region is approached, since the finite number of individuals contributing to the exponential tempering of the IPL decreases as the number of fanatics increases. Note that this measure of sensitivity does not register the strength of the response to the change in the number of fanatics that the amplitude of the mean field records in Figure 7.1.

The curves in the lower panel tell a different story. The slope for the IPL of unmodified network is 1.35, whereas when $\rho = 0.1$, 0.2 , 0.3 and 0.4 ratio of the randomly selected individual change their opinion choices to noise the slopes denoting the IPL indices become 1.66, 1.81, 1.91 and 2.17 respectively. So, there exist a ρ between 0.3 and 0.4 with IPL index $\mu = 2$, thereby realizing according to Eq. (7.2) the ideal $1/f$ noise that is expected to correspond to the dynamics of the brain in the awake state [128]. Thus, the significance of the behavior modification depends on the measure employed. The mean field is relatively insensitive to a noisy minority, as depicted in the lower panel of Figure 7.1, whereas the statistics of the mean field is quite sensitive to the noisy behavior as depicted in Figure 7.2.

It is interesting to determine how the social response changes with the fraction of aberrant individuals is increased. In Figure 7.3 the top panel records the asymptotic percentage of cooperators as a function of the fraction of randomly located fanatics within the social network. There is a monotonic decrease from a mean field of 0.7 with no fanatics to 1.0 with a 100% fanatics, with the mean field crossing the zero axis at approximately 20% fanatics. Note that the sensitivity of the social response is greatly suppressed compared to that of previously considered models in which a 10% contamination brought about a complete reversal of behavior.

The lower panel of Figure 7.3 shows the effect of increasing the percentage of individuals who make random choice. It is necessary to force all the individuals to make random

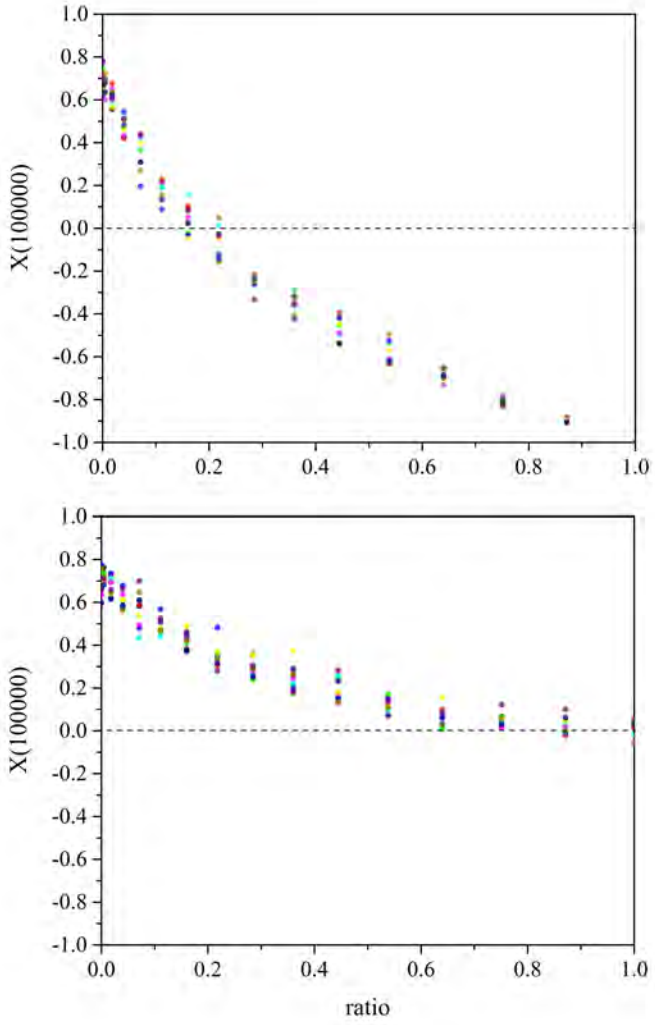

FIGURE 7.3. The mean field of the SOTC model at time 10^5 versus the ratio of fanatics (top) and independent minorities (bottom) which was turned on at time 5×10^4.

choice to totally disrupt the social organization generated by the SOTC bottom up approach. The maximum disruption of the social order is a reduction to subcritical behavior, where the individuals act independently of one another, which is to say they cease to act as a social group.

7.3. Concluding Remarks

In the SOTC model criticality is not forced upon the network by setting the individual imitation strength to a critical value. The critical value of the imitation strength is spontaneously reached without artificially enhancing the level of altruism within the network, but is dynamically attained by assuming that each individual selects the value of the imitation strength that assigns maximum benefit to themselves at a given time. The SOTC model does not require us to adopt the network reciprocity argument of Nowak and May [1] to prevent the infiltration of defectors in cooperation clusters, but instead establishes the emergence of cooperation by the mere use of the PDG payoff, thereby connecting the evolution of cooperation with the search for agreement between individuals and their nearest neighbors.

We think that the theoretical perspective advocated in this work may afford a scientific perspective to address a debate on the failure of liberalism [135]. According to Brook [136]:

> The difficulties stem not from anything inherent in liberalism but from the fact that we have neglected the moral order and the vision of human dignity embedded within liberalism itself. As anybody who has read John Stuart Mill, Walt Whitman, Abraham Lincoln, Vaclav Havel, Michael Novak and Meir Soloveichik knows, liberal democracy contains a rich and soul-filling version of human flourishing and solidarity, which Deneen airbrushes from history.

Herein we have presented the SOTC model, which shows that the bottom-up approach to cooperation (solidarity) is the fundamental ingredient for the resilience of an organized society.

CHAPTER 8

EMERGENCE OF MULTIFRACTALITY AS A RESULT OF COOPERATION

This chapter is devoted to the discovery of renewal events, hidden in the computed dynamics of a multifractal metronome. We show that metronome simply has the properties of a SOTC system which also has complex-periodicity, for example heart or the brain. Multifractal analysis helps us to study homeodymamics. We also study the multifractality of the DMM model which at criticality is equaelent to a SOTC system. We find conditions in which transfer of information could occur between two metronomes as well as two DMM systems. We establish that the phenomenon of complexity matching, which is the theme of an increasing number of research groups, has two distinct measures. One measure is the sensitivity of a complex system to environmental multifractality; another is the level of information transfer, between two complex networks at criticality. The cross-correlation function is evaluated in the ergodic long-time limit, but its delayed maximal value is the signature of information transfer occurring in the non ergodic short-time regime. It is shown that a more complex system transfers its multifractality to a less complex system while the reverse case is not possible.

8.1. Introduction

The central role of complexity in understanding nonlinear dynamic phenomena has become increasingly evident over the last quarter century, whether the scientific focus is on ice melting across the car windshield, stock prices plummeting in a market crash, or the swarming of insects [134]. It is remarkable, given its importance in modulating the behavior of dynamic phenomena, from the cooperative behavior observed in herding, schooling, and consensus building, to the behavior of the lone individual responding to motor control response tasks, that defining complexity has been so elusive.

The work of Ref. [134] affords theoretical arguments on the phenomenon of *complexity matching* that is frequently interpreted as transport of multifractality from the perturbing to

the perturbed network. The main purpose of this part is to draw the attention of the investigators in this field of research that multifractality may be the signature of crucial events, hereby defined in Section 8.1.2, generated by the processes of self-organization to criticality. This connection may be of significant importance, given the fact that mulifractality is well known in many areas of research, whereas criticality-induced crucial events are not widely known, in spite of the fact that they are generators of multifractality.

8.1.1. A Short Review of Multifractality in Physiological Dynamics

Multifractality has been revealed by the analysis of human heartbeat dynamics [137, 138, 139]. It is interesting to notice that Ref. [138] associates multifractality to the $1/f$ noise. Ref. [140] also devotes some attention to $1/f$ noise. The theory of present work connects multifractality to $1/f$ noise, showing however that this form of noise is due to crucial events rather than to Fractional Brownian Motion (FBM). The connection between FBM $1/f$ noise and multifractality would create a conflict with the conjecture made in the 2002 work of [141] that the multifractality of healthy subjects may be a signature of crucial events. The papers [142] and [143] are of remarkable interest for their possible contribution to bypass this conflict. The key results of Refs. [142, 143], emphasizing the role of magnitude for the emergence of multifractality allow us to focus on the crucial events approach to $1/f$ noise, since the FBM sub-diffusion associated to the study of sign fluctuations is proved to not yield significant contributions to multifractality.

In fact, splitting the analysis of time series into the analysis of magnitude fluctuations and sign alternation shows that the analysis of signs yields a form of anti-correlation, suggesting FBM sub-diffusion, but not significant contribution to multifractality. Note that the conjecture of the connection between crucial events and multifractality has been fully supported by the later work of our group [144]. In conclusion, thanks to the results of Ref. [142] and [143] we feel free to focus on the $1/f$ noise induced by crucial events rather than on FBM $1/f$-noise.

Further interesting examples of multifractality in complex biological systems are af-

forded by Refs. [145, 146, 140]. Of remarkable interest is the connection with the biological rhythms [145, 146]. Although in principle the biological rhythm may be mimicked by the multifractal metronome of this work, we decided to leave the study of rhythm and complexity as subject of investigation for future research work.

8.1.2. Complexity Management

The focus of this part is on experimental psychology. As Delignières and Marmelat [147] point out, a complex system consists of a large number of infinitely entangled elements, which cannot be decomposed into elementary components. They go on to provide an elegant, if truncated, historical review of complexity, along with its modern connection to fluctuations and randomness. They provide a working definition for complexity, as done earlier by West *et al* [134], as a balance between regularity and randomness.

In order to sidestep the impasse of providing an absolute definition of complexity, West *et al.* [134] introduced the *complexity matching effect* (CME). This effect details how one complex network responds to an excitation by a second complex network, as a function of the mismatch in the measures of complexity of the two networks. An erratic time series generated by a complex network hosts *crucial events*, namely events characterized by the following properties. The time distance τ between two consecutive events has a probability density function (PDF), $\psi(\tau)$, that is inverse power law (IPL) with IPL index $\mu < 3$. Different pairs of consecutive times correspond to time distances with no correlation, renewal property. The measure of complexity is taken to be the IPL index μ. Aquino *et al.* [26] show that a complex network S with IPL-index $\mu < 2$, has no characteristic time scale, and in the long-time limit is insensitive to a perturbation by a complex network with a finite time scale, including one having oscillatory dynamics. It is important to notice that when $\mu < 2$, the first moment of $\psi(\tau)$ is divergent, thereby generating a condition of perennial aging, while the condition $\mu < 3$, making the second moment of $\psi(\tau)$ divergent, generates non-stationary fluctuations that become stationary in the long-time limit. The spectrum of these fluctuations in the region $2 < \mu < 3$ can be evaluated using the ordinary Wiener-Khintchine

theorem, whereas the region of perennial aging, $\mu < 2$, requires the adoption of a generalized version of this theorem [23].

The network S is expected to be sensitive to perturbations having the same IPL index. This observation generated the plausible conjecture that a complex network, with a given temporal complexity, is especially sensitive to the influence of a network with the same temporal complexity, this being, in fact, a manifestation of CME.

The crucial events are generated by complex systems at criticality [148]. On the basis of this property, Turalska *et al.* [28] afforded strong numerical support to the CME, showing that a network at criticality is maximally sensitive to the influence of a identical network also at criticality. In this case, the IPL-index of both the perturbed network, μ_S, and the IPL-index of the perturbing network, μ_P, must be identical, because the perturbing and the perturbed network are identical systems in the same condition, that being the criticality condition. It is known [40] that at criticality $\mu_S = \mu_P = 1.5$, thereby implying that the two systems share the same temporal complexity, with the same lack of a finite time scale. The CME was subsequently generalized to the *principle of complexity management* (PCM), where the network response was determined when both the perturbing and responding networks have indices in the interval $1 < \mu < 3$. This latter condition was studied by means of ensemble averages [26, 149] and time averages [27], leading to the discovery that in the region of perennial aging $1 < \mu < 2$ the evaluation of complexity management requires special treatment. This conclusion is based on the observation that renewal events are responsible for perennial aging, with the occurrence of the renewal events in the perturbed network being affected by the occurrence of the renewal events in the perturbing network. A careless treatment, ignoring this condition may lead to misleading observations characterized erratic behavior making it impossible to realize the correlation between the perturbed and the perturbing signal [27]. This is where the adoption of the multifractal perspective adopted by the authors of [150] to study CME may turn out to be more convenient that the adoption of the method of cross-correlation functions.

There is a growing literature devoted to the interpretation that $1/f$-noise is the sig-

nature of complexity, where the spectra of complex phenomena are given by $1/f^{\nu}$. The complexity in time series is generically called $1/f$-noise or $1/f$-fluctuations, even though empirically the IPL index lies in the interval $0.5 < \nu < 1.5$. The $1/f$-behavior can be detected by converting the underlying time series into a diffusion process. This conversion of data allows us to determine the corresponding Hurst exponent H for the diffusion process, which is well known to be related to the dimension of fractal fluctuations [151]. Consequently, we obtain for the scaling index of the spectrum

$$\nu = 2H - 1, \tag{8.1}$$

It is important to remark that this approach rests on the Gaussian assumption requiring some caution when dynamical complexity is incompatible with the Gaussian condition. It has been observed [152] that the condition $\mu > 2$ generates a diffusion process that, interpreted as Gaussian, yield the Hurst scaling

$$H = \frac{4 - \mu}{2}, \tag{8.2}$$

which plugged into Eq. (8.1) yields

$$\nu = 3 - \mu. \tag{8.3}$$

Eq. (8.3) is valid also for $\mu < 2$, but in this case it requires a theoretical derivation taking into explicit account the condition of perennial aging [23]. It is important to stress that $\nu > 1$ is consequently a sign of the action of crucial events. The spectrum of a complex network at criticality with crucial events with IPL index $\mu < 2$, expressed in terns of the frequency $\omega = 2\pi f$, is [23]:

$$S(\omega) \propto \frac{1}{L^{2-\mu}} \frac{1}{\omega^{3-\mu}}, \tag{8.4}$$

where L is the length of the observed time series. Here we shall use this expression to prove that the multifractal metronome used by the authors of Ref. [150] is driven by crucial events responsible for CME [134] and complexity management PCM [26].

Fractal statistics appear to be ubiquitous in time series characterizing complex phenomena. Some empirical evidence for the existence of $1/f$-noise within the brain and how it relates to the transfer of information, helps set the stage for the theoretical arguments given below. The brain has been shown to be more sensitive to $1/f$-noise than to white noise [153]; neurons in the primary visual cortex exhibit higher coding efficiency and information transmission rates for $1/f$-signals than for white noise [154]; human EEG activity is characterized by changing patterns and these fluctuations generate renewal events [155]; reaction time to stimuli reveals that the more challenging the task, the weaker the cognitive $1/f$-noise produced [24]. Of course, we could extend this list of brain-related experiments, or shift our attention to other complex systems, but the point has been made.

Here we stress that according to the analysis of [156] the brain dynamics is a source of ideal $1/f$-noise being characterized by crucial events with $\mu \approx 2$ in accordance with an independent observation made by Buiatti *et al* [157] of IPL index μ ranging from 1.7 to 2.3. It is interesting to notice that heartbeat dynamics of healthy patients were proved to host crucial events with μ close to the ideal condition $\mu = 2$ [141] and that the recent work of Bohara *et al* [144], in addition to confirming this observation lends support to interpreting the meditation-activated brain-heartbeat synchronicity [158] as a form of CME of the same kind as that observed by Deligniéres and co-workers [150], namely, as a transfer of multifractality.

8.1.3. Experiments, Multifractality and Ergodicty Breaking

With the increase in geopolitical tensions between states, the enhanced social media connectivity between individuals along with the rapid progress of neurophysiology, societal behavior has become one of today's more important scientific topics, forcing researchers to develop and adopt new interdisciplinary approaches to understanding. As pointed out by Pentland [159], even the most fundamental social interaction, that being the dialogue between two individuals, is a societal behavior involving psychology, sociology, information science and neurophysiology. Consequently, we try and keep the theoretical discussion outside any one particular discipline and focus our remarks on what may apply across disciplines.

Consequently, the same issue of dyadic interaction can be studied from the theoretical perspective of the Science of Complexity, which we interpret as an attempt to establish a fruitful interdisciplinary perspective. This view recognizes that the interaction between phenomena from different disciplines requires the transfer of information from one complex system to another. The adoption of this interdisciplinary perspective naturally leads us to use the previously introduced notion of *complexity matching* [6, 147, 134]. On the other hand, the transition in modeling from physics to biology, ecology, or sociology, gives rise to doubts concerning the adoption of the usual reductionism strategy and establishes a periodicity constraint that is often ignored by physical theories [160].

The observation of the dynamics of single molecules [161], yields the surprising result that in biological systems the ergodic assumption is violated [162]. On the basis of real psychological experiments, for instance the remarkable report on the response of the brain to the influence of a multifractal metronome [163], complexity matching has been interpreted as the transfer of a scaling PDF from a stimulus to the brain of a stimulated subject. More recent experimental results [150] confirm this interpretation, based on the transfer of global properties from one complex network to another, termed *genuine complexity matching*, while affording suggestions on how to distinguish it from more conventional local discrete coupling.

We notice that the PCM [134] relies on the crucial role of criticality and ergodicity breaking, in full agreement with the concept of the transport of global properties from one complex network to another. This agreement suggests, however, that a connection exists, but has not yet been established, between multifractality and ergodicity breaking, in spite of the fact that current approaches to detecting multifractality are based on the ergodicity assumption [164]. Note that multifractality is defined by a time series having a spectrum of Hurst exponents (fractal dimensions), which is to say the scaling index changes over time [165], resulting in no single fractal dimension, or scaling parameter, characterizing the process. In psycho-physical experiments, for example, a person is asked to synchronize a tapping finger in response to a chaotic auditory stimulus, and complexity matching is interpreted as the transfer of scaling of the fractal statistical behavior of the stimulus, to

the fractal statistical response of the stimulated subject's brain. This response of the brain, in such a motor control task, when the stimulus is a multifractal metronome, has been established [163].

Experimental results [150] confirm this interpretation, based on the transfer of global properties from one complex network to another. In these latter experiments the multifractal metronome generates a spectrum of fractal dimensions $f(\alpha)$ as a function of the average singularity strength of the excititory signal and it is this dimensional spectrum that is captured by the brain response simulation. The multifractal behavior manifested by the unimodal distribution provides a unique measure of complexity of the underlying network.It is worth noting that the same displacement of the metronome spectrum, from the body response spectrum, is observed for walking in response to a multifractal metronome.

The main purpose of the present work is to establish that the multifractal arguments advanced by many advocates of complexity matching must be compatible with data displaying ergodicity breaking. The dynamical model that we use to establish this connection is the multifractal metronome [163], described by the periodically driven rate equation with delay:

$$\dot{x} = -\gamma x(t) - \beta sin\left(x(t-\tau_m)\right). \tag{8.5}$$

This model, originally introduced by Ikeda and co-workers [166, 167], was adopted by Voss [168] to illustrate the phenomenon of anticipating synchronization. In the present work, we adopt Eq. (8.5) to mimic the output of a complex network, generating both temporal complexity [40] and periodicity [169]. More precisely, setting $\gamma = 1$, we use Eq. (8.5) with only two adjustable parameters; the amplitude of the sinusoidal driver β and the delay time τ_m, to determine the nonlinear dynamics of a metronome with a multifractal time series. We should use this simple equation to study the joint action of renewal events and periodicity, which may have the effect of either annihilating or reducing the renewal nature of events. This is, however, a challenging issue that we plan to discuss in future work. In this work, on purpose, we establish a time separation between temporal complexity and periodicity and

we establish the accuracy of this separation by means of the aging experiment.

We show that this simple equation, with a careful choice of the parameters β and τ_m, generates the same temporal complexity as that produced at criticality by a large number of interacting units in a complex network [40], yielding ergodicity breaking. This earlier work shows that in the long-time regime the nonlinear Langevin equation, yielding ergodicity breaking in the short-time regime, becomes equivalent to an ordinary linear Langevin equation. Herein we use this theory to establish the cross-correlation between a perturbed network S and a perturbing network P, identical to the network S, when both networks are at criticality. Using the important property that in the long-time limit the non-linear Langevin equation becomes identical to an ordinary Langevin equation, we find an exact analytical expression for the cross-correlation between S and P. We prove that the mulltifractal metronome, with a suitable choice of the parameters γ, β and τ_m generates crucial events and that the temporal complexity of these events is identical to that a complex network at criticality, more precisely the complex network of Section 8.2. On the basis of this equivalence we predict that the cross-correlation function between the metronome equivalent to the network S and the metronome equivalent to the metronome P should be identical to the analytical cross-correlation function between network S and network P. This prediction is supported with a surprising accuracy by the numerical results of this work.

The strategy of replacing the output of a complex network with the time series solution to a multifractal metronome equation yields the additional benefit of avoiding numerically integrating the equations of motion for a complex dynamic network, involving the interactions among a large number of particles in a physical model, people in a social model, or neurons in a model of the brain. Although the interplay between complexity and periodicity is an issue of fundamental importance [169], herein we focus on the IPL complexity, hidden within the dynamics of Eq. (8.5); complexity that was overlooked in earlier research on this subject.

As pointed out earlier, with our arguments about the generalization of the Wiener-Khintchine theorem in the case of perennial aging we prove numerically that the spectrum $S(\omega)$ of the metronome fits very well the prediction of Eq. (8.4). On the other hand, we

prove directly that a network at criticality is the source of the broad multifractal spectrum used in Ref. [150] to discuss CME.

8.1.4. Outline

Section II shows that a complex network at criticality generates a distinct multifractal spectrum. We devote Section III to detecting the renewal events hidden within the dynamics of Eq.(8.5) and we establish the equivalence between the multifractal metronome and a complex network at criticality. In Section IV we find the analytical expression for the cross-correlation between two complex networks at criticality and we prove numerically that the two equivalent multifractal metronomes generate the same cross-correlation. Section V illustrates the transfer of the multifractal spectrum from a complex to a deterministic metronome. Finally, to support the equivalence between criticality-induced long-range correlation in a model with local-interaction and a model with no-local interaction, in Section VI we recover a qualitative agreement with the results of Section II, based on a model with local interaction, by analyzing the time evolution of a mean field of a non-local model. We use this equivalence to support the concluding remarks of this last Section.

8.2. Criticality, Decision Making Model and Multifractality

8.2.1. Multifractality of the Decision Making Model

As an example of criticality we adopt the Decision Making Model (DMM) widely illustrated in the earlier work of Refs. [148, 28, 40, 28, 54, 56, 58]. For a review please consult the book of Ref. [36]. To clarify the connection between criticality and multifractality, we use the DMM. This model rests on a network of N units that have to make a choice between two states, called C and D. The state C corresponds to the value $\xi = 1$ and the state D corresponds to the value $\xi = -1$. The transition rate from C to D, g_{CD}, is given by

$$g_{CD} = g_0 exp\left[-K\left(\frac{M_C - M_D}{M}\right)\right] \tag{8.6}$$

and the transition rate from D to the C, g_{DC}, is given by

$$g_{DC} = g_0 exp\left[K\left(\frac{M_C - M_D}{M}\right)\right]. \tag{8.7}$$

The meaning of this prescription is as follows. The parameter $1/g_0$ defines a dynamic time scale and we set $g_0 = 0.1$ throughout. Each individual has M neighbors (four in the case of the regular two-dimensional lattice used in this article). The cooperation state is indicated by C and the defection state by D. If an individual is in C, and the majority of its neighbors are in the same state, then the transition rate becomes smaller and then the individual sojourns in the cooperation state for a longer time. If the majority of its neighbors are in D, then the individual sojourns in the cooperator state for a shorter time. An analogous prescription is used if the individual is in the defection state.

We run the DMM for a time t and we evaluate the mean field

$$x(t) \equiv \frac{\sum_i^N \xi_i}{N}, \tag{8.8}$$

where $\xi_i = 1$ or $\xi_i = -1$, according to whether the $i - th$ individual is in the state C or in the state D, respectively. For values of the control parameter much smaller than the critical values K_c, which depends on the network topology, the mean field x fluctuates around the vanishing mean values. For values of K significantly larger than K_c the mean field $x(t)$ fluctuates around either 1 or -1. It is important to stress that for values of K in the vicinity of the critical value K_c, the fluctuations of the mean field have large intensity and the largest intensity corresponds to the critical value K_c. The exact value of K_c depends also on the number of units [56]. Here we limit ourselves to notice that in the case of a regular two-dimensional network K_c, with $N = 100$ is around 1.5 . The adoption of an irregular networks with a distribution of links departing from the condition of an equal number of links for each unit may have the effect of significantly reducing the value of K_c. A scale-free distribution of links was found [58] to make K_c very close to $K_c = 1$, which corresponds to the ideal case where each unit is linked to all the other $N-1$ units. The PDF of the time intervals between two consecutive re-crossings of $x = 0$ in the sub-critical condition $K < K_c$ is exponential. At $K = K_c$ the PDF becomes an IPL with power index $\mu = 1.5$. In the supercritical state, the

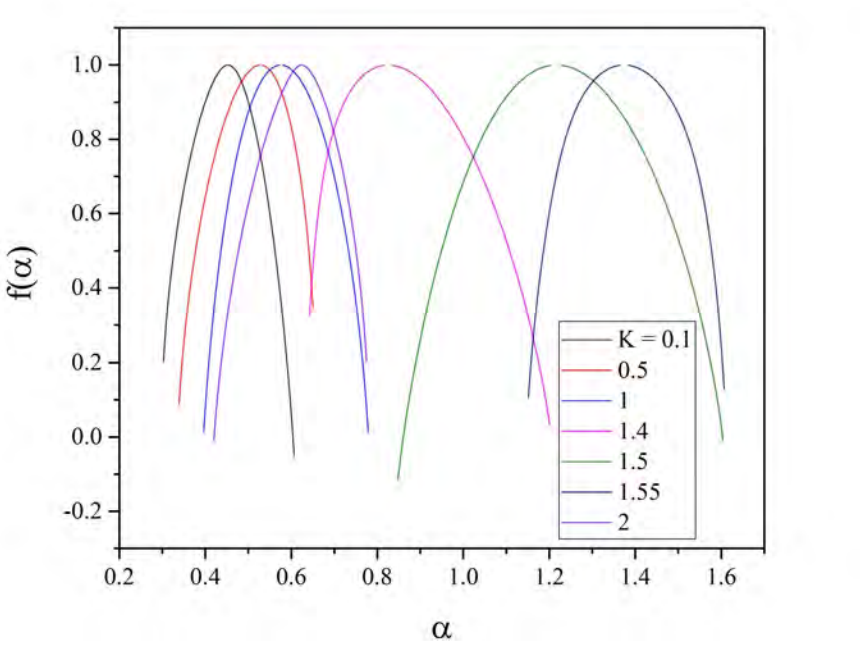

FIGURE 8.1. Multifractal spectrum of the DMM network for different values of the control parameter K. Note the non-monotonic behavior of the location of the peak , as well as, the width of the distribution, with the value of K.

mean field fluctuates around a non-vanishing mean field. For $K \gg K_c$ the PDF of the time intervals between two consecutive re-crossing of this non-vanishing mean field again becomes exponential. The purpose of this Section is to give the readers a better understanding of the role crucial events, namely non-Poisson renewal events with power index μ fitting the condition $1 < \mu < 3$. Here we limit ourselves to illustrate the connection between criticality and multifractal spectrum.

Following Delignières and co-workers [150] we apply to the time series $x(t)$ the multifractal method of analysis proposed in 2002 by Kantelhardt *et al* [170]. The method of Ref. [170] is an extension of the popular technique called Detrended Fluctuation Analysis (DFA) of Ref. [171] originally proposed to determine the Hurst coefficient H. The results depicted in Fig. 8.1 show that the inverted parabola $f(\alpha)$ becomes broadest at criticality. It is interesting to observe that in the sub-critical regime, where the fluctuation of the mean field of Eq. (8.8) generates ordinary diffusion with Hurst coefficient $H = 0.5$, the spectrum is much

sharper and is centered around $\alpha = 0.5$. Increasing the value of the control parameter has the effect of shifting the barycenter of the inverted parabola towards larger values of α with no significant effect on the parabola's width. The dependence of $f(\alpha)$ on K is dramatically non-linear. In fact, with K going closer to K_c the barycenter of the inverted parabola jumps to the vicinity of $\alpha = 1.2$ and the parabola, as stated earlier, reaches its maximal width. Moving towards higher values of K, supercritical values, has the effect of further shifting to the right the parabola's barycenter. However, the parabola's width becomes much smaller, in line with earlier arguments about the super-critical condition being less complex than the critical condition. It is impressive that with $K = 2$ the parabola's barycenter jumps back to the left, suggesting that for even larger values of K complexity is lost, in a full agreement with [77, 29].

The work of [144] suggests that the spectrum $f(\alpha)$ is made broader by the action of crucial events activated by the criticality of the processes of self-organization [78]. The numerical results of this Section confirms this property. In fact, as remarked earlier, Fig. 8.1 shows that the multifractal spectrum becomes broadest at criticality, while it becomes sharper in both the supercritical and sub-critical condition, where according to [77] the time interval between two consecutive events has an exponential PDF. This result suggests that, as done by Delignières and co-workers [150] it may be convenient to measure CME observing the correlation between the multifractal spectrum of the perturbed network S and the multifractal spectrum of the perturbing network P rather than the cross-correlation between the crucial events of S and the crucial events of P. This method, although more closely related to the occurrence of crucial events is made hard by ergodicity breaking [27], even when the crucial events are visible, not to speak about the fact that usually crucial events are hidden in a cloud of non-crucial events [141].

8.2.2. Transfer of Multifractality from One DMM to Another DMM Network

In this Section we want to discuss an experiment similar to that of Ref. [150]. We do that with two DMM networks, the perturbing network playing the role of metronome

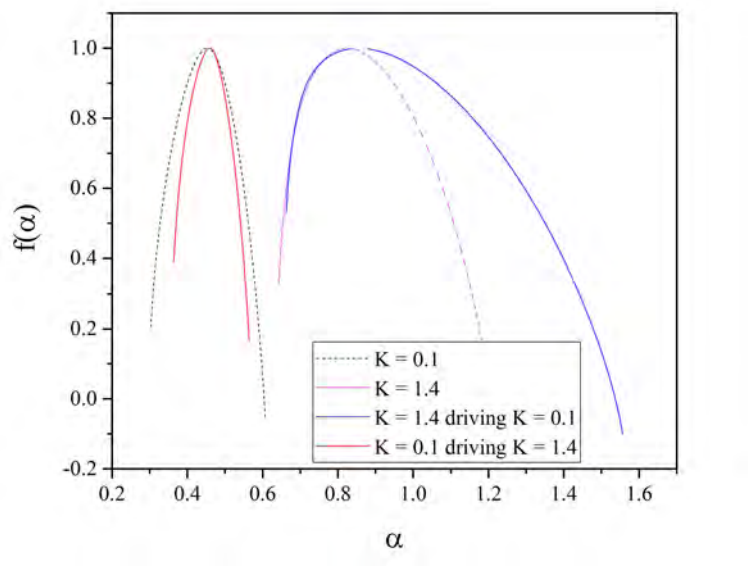

FIGURE 8.2. The dashed black curve is the multifractal spectrum of the system A with $K = 0.1$ and the dashed pink curve denotes the multifractal spectrum of the system B, with $K = 1.4$. One network perturbs the other, as described in the text, with 5% of its units adopting the state C or D according to whether the perturbing system has a positive or a negative mean field. The blue curve is the multifractal spectrum of the network B under the influence of network A and the red curve is the multifractal spectrum of A under the influence of B.

and the perturbed network playing the role of participants. The complex network A has the control parameter $K = 0.1$, namely, it is a system in the subcritical condition and the network B has the control parameter $K = 1.4$, close to criticality. We explore two opposite conditions. In the first the system A perturbs the system B and in the second the system B perturbs the system A. The perturbation is done as follows. 5% of the units of the perturbed system adopt either the state C or D, according to whether the perturbing system has a positive or a negative mean field. We see that when the system B with broader spectrum perturbs A, with a a sharper spectrum, it forces A to get a much broader spectrum ,even broader the spectrum of B. When A, with a sharper spectrum than B perturbs B it has

the effect of making B adopt a spectrum as sharp as that of the perturbing system. This result can be compared to that of the earlier work of Ref. [28], where 2% of the units of the perturbed network adopted the choice made by the perturbing network. In that case no correlation was detected between S and P but in the case where both networks being at criticality. This suggests that the correlation between the multifractal spectrum $f(\alpha)$ of S and the multifractal spectrum $f(\alpha)$ of P may be a more proper way to study CME.

8.3. Detecting Renewal Events

We devote this Section to establish the equivalence between the dynamics of metronome and those of a DMM network at criticality. We make a suitable choice of the parameters β and τ_m of Eq. (8.5) so as to make it possible to establish this statistical equivalence.

8.3.1. Renewal Character of Re-Crossings

As done in earlier work [40, 28] attention is focused on events corresponding to zero-crossings, that is, to the time intervals between succesive crossings of $x = 0$. Successive zero-crossings are used to generate a first time (FT) series $\{\tau_i\}$, where $\tau_i = t_{i+1} - t_i$ is the time interval between two consecutive events, that is, zero-crossings. An important question about this FT series is whether a non-zero two-time correlation, between different events, exists or not. The events are identified as renewal if all two-time and higher-order correlations are zero.

The renewal nature of the events generated using the metronome equation is determined by using the aging experiment [172]. The method, originally proposed by Allegrini *et al.* [172], was for the purpose of proving that each zero-crossing of a time series is an isolated event, with no correlation with earlier events. The lack of correlation implies that when an event occurs, the occurrence of the next event is completely unrelated and unpredictable; the occurrence of an event can be interpreted as a form of rejuvenation of the system. Ergodicity breaking [162] is closely connected to the occurrence of renewal events, as can be intuitively

understood by assigning to the waiting-time PDF $\psi(\tau)$ the IPL form

$$\psi(\tau) \propto 1/\tau^{\mu}. \tag{8.9}$$

In the case $\mu < 2$ the mean waiting time is infinite,

$$\langle \tau \rangle = \int_0^{\infty} \tau \psi(\tau) d\tau = \infty,$$

and the longer the total length of the time series under study, the greater the maximum value of the waiting-time τ detected. In fact, although a very short time interval can be drawn immediately after a very long one is drawn, due to the renewal nature of the process, it is impossible that the largest value of τ found, within a sequence of length L_1, remains the maximum in examining a sequence of length $L_2 > L_1$. This would conflict with the $\langle \tau \rangle = \infty$ condition.

To assess whether the FT series $\{\tau_i\}$ generated by Eq. (8.5) is detected to be renewal, we generate a second, auxiliary, time series by shuffling the FT series. We refer to the latter as the shuffled time series. We apply the aging experiment algorithm to both the original and the shuffled sequence: We adopt a window of size t_a, corresponding to the age of the network that we want to examine. Locate the left end of the window at the time of occurrence of an event, record the time interval between the right end of the window and the occurrence of the first event, emerging after the end of the window. Note that adopting windows of vanishing size corresponds to generating ordinary histograms. The histograms generated by t_a produce different decision-time distribution densities, and these distribution densities, properly normalized, generate survival probabilities, whose relaxation can be distinctly different from that of the ordinary survival probability.

A non-ergodic renewal process is expected to generate a relaxation that becomes slower and slower as t_a increases. This lengthening of the relaxation time occurs because the method leads to a truncated time series. However, the truncation affects the short time intervals more than it does the long time intervals, thereby reducing the weight of $\psi(\tau)$ for short times, while enhancing the weight of long time intervals. We have, of course, to take

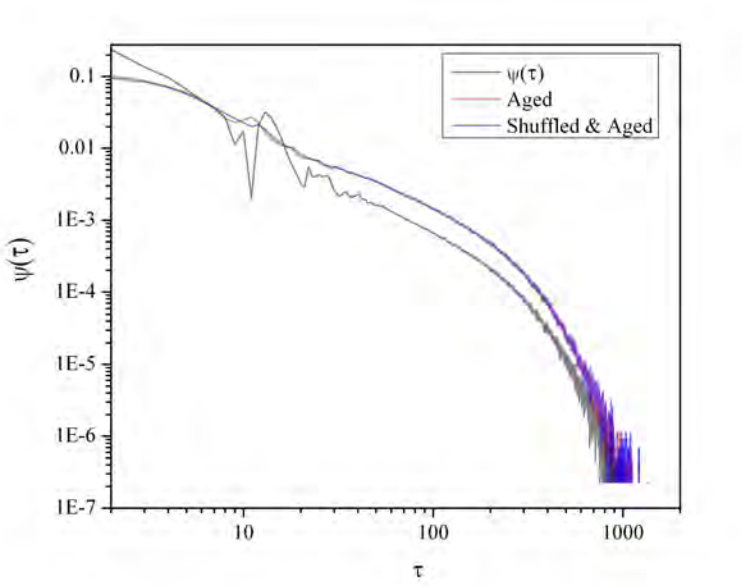

FIGURE 8.3. (Color online) Waiting-time PDF for $\gamma = 1$, $\beta = 200$, $t_m = 10$, $L = 10^7$ and $\tau_a = 10$.

into account that we adopt normalized histograms. A process is renewal if the aging of the non-shuffled FT series is identical to the aging of the shuffled time series.

Let us discuss the results of the aging experiment applied to the time series $\{\tau_i\}$ generated by the multifractal metronome data of Eq. (8.5). In Fig. 8.3 the shuffled time series is seen to yield a slight deviation from the non-shuffled time series of approximate magnitude $\tau \sim 10$. This is a consequence of setting the delay time to $\tau_m = 10$, thereby establishing a periodicity interfering with temporal complexity. On the other hand, Fig. 8.4 shows that the shuffled data curve virtually coincides with the non-shuffled data curve throughout the entire time region explored by the multifractal metronome.

8.3.2. Long-Time Ergodic Behavior

Note that the data curves in both Fig.8.3 and Fig.8.4 are characterized by long-time exponential truncations. In the intermediate time regions, both conditions show an IPL behavior with IPL-index $\mu = 1.5$. This property reinforces the conviction that the metronome dynamics and that of a network of interacting units at criticality are equivalent. In fact,

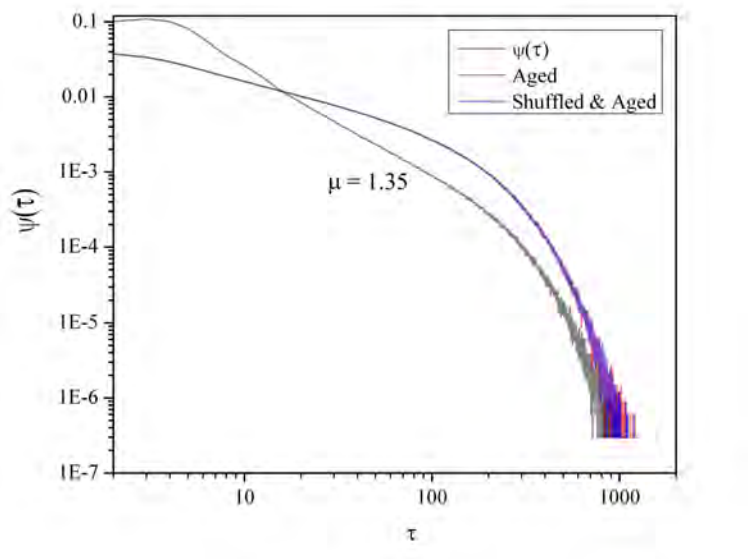

FIGURE 8.4. Waiting-time PDF for $\gamma = 1$, $\beta = 1000$, $\tau_m = 1000$, $L = 10^7$ and $\tau_a = 100$.

in the absence of exponential truncation, the complex network would generate perennial non-ergodic behavior. The latter behavior would make the network dynamics incompatible with multifractality, which, as pointed out by Juzba and Korbel [164], requires a condition of thermodynamic equilibrium.

The recent work of Beig et al. [40] shows that the mean field of a complex network at criticality generates a mean field $x(t)$, which is well described by the nonlinear Langevin equation:

$$\dot{x}(t) = -ax(t)^3 + f_x(t), \tag{8.10}$$

with $f_x(t)$ being a random noise generated by the finite size of the network, whose intensity is proportional to $1/\sqrt{N}$, and N is the number of the interacting units. Eq.(8.10) describes the over-damped motion of a particle within a quartic potential, which has a canonical equilibrium distribution. However, a particle moving from the initial condition $x(0) = 0$, undergoes a virtual diffusional process for an extended time T_{eq}. The order of magnitude of

this time is given by

$$T_{eq} \propto \sqrt{\frac{N}{a}} \tag{8.11}$$

For times $t \ll T_{eq}$ the network's dynamics are non-ergodic, but they become ergodic asymptotically for $t \gg T_{eq}$.

The zero-crossings are well described by a waiting-time PDF given by Eq.(8.9) for times $\tau \ll T_{eq}$. This PDF, however, is exponentially truncated, and as a consequence of this truncation the renewal aging is not perennial. As a result of aging the IPL index of the PDF changes from μ to $\mu - 1$, making the decay slower in the intermediate time region, as shown in Fig. 8.4. However, the aging process has also the effect of extending the exponential truncation. In the case of the complex network at criticality, this corresponds to the existence of a thermodynamical equilibrium emerging from the adoption of a large time scale of the order of T_{eq}. It is known [40] that the normalized auto-correlation function of the mean field x, to a high degree of approximation, becomes

$$A(\tau) = exp\left(-\Gamma|\tau|\right) \tag{8.12}$$

with the relaxation rate given by [40]

$$\Gamma \propto a \left\langle x^2 \right\rangle_{eq}. \tag{8.13}$$

Note that the theory of Ref. [40] proves that this auto-correlation function is obtained by replacing the non-linear Langevin equation of Eq. (8.10) with the following linear Langevin equation

$$\dot{x}(t) = -\Gamma x(t) + f_x(t). \tag{8.14}$$

In Section 8.4 we shall use these arguments to prove that the strong-anticipation of the multifractal metronome may be closely related to the complexity matching observed by stimulating a complex network at criticality, with the mean field of another complex network at criticality, see Lukóvic *et al* [77] for more details. The authors of the latter article studied a network of N units, with a small fraction of these units, called lookout birds because of

the context of the discussion, or more generally labeled perceiving units, are sensitive to the mean field of another network of N units in a comparable physical condition. The units in both networks are decision making individuals, who have to make a dyadic choice, between the yes, $+1$, and no, -1, state. The perceiving units adopt the $+1$ state, if the mean field perceived by them is positive, $y > 0$, or the -1 state, if they perceive $y < 0$. The cross-correlation between the mean field $x(t)$ of the driven network and the mean field $y(t)$ of the driving network attains maximal intensity when both networks are at criticality. It turns out that the cross-correlation function is identical to the auto-correlation function of $x(t)$, with a significant shift, namely, the cross-correlation function $\langle x(t+\tau)y(t)\rangle$ gets its maximal value when $\tau = \Delta$, where the delay Δ represents a delay in transmitting information from the perturbing to the perturbed complex network.

An intuitive interpretation of the above time delay is that the information perceived by the lookout birds must be transmitted to all the units of their network. Lukovic *et al* [77] adopted a different interpretation of this important delay time. To vindicate their view they studied the all-to-all coupling condition, where the preceptors are coupled to all the other units in their network. Even in this case the cross-correlation function is characterized by a significant time delay, with respect to the unperturbed correlation function of $x(t)$. The reason for the delay is that the group, in the case discussed by [77, 29], a flock of birds, can follow the direction of the driving network only when a significantly large number of zero-crossings occur. A zero-crossing corresponds to a free-will condition, where the whole network, can be nudged by an infinitesimally small fluctuation, to select either the positive or the negative state. Thus, the renewal nature of the zero-crossing events becomes essential for the emergence of such cooperative behavior as cognition [29], as in changing one's mind for no apparent reason. The zero-crossing is the time at which the network is most sensitive to a perturbation, so the more zero-crossings the shorter the interval between a perturbation and response.

8.3.3. Beyond Ordinary Diffusion

We note that the waiting-time PDF of Fig. 8.4 is given by

$$\mu \approx 1.35 \tag{8.15}$$

This does not conflict with the earlier arguments on the exponential nature of the infinitely aged regime. In fact, on the basis of a theoretical approach based on the observation of random growth of surfaces [73] it is argued [78] that in all the organization processes the fluctuation of $x(t)$ around the origin are non-Poisson renewal events characterized by the following common property. Let us call $\Psi(t)$ the probability that no renewal non-Poisson event occurs at a distance t from an earlier event. The Laplace transform of $\Psi(t)$, $\hat{\Psi}(u)$, is given by

$$\hat{\Psi}(u) = \frac{1}{u + \lambda^{\alpha} (u + \Delta)^{1-\alpha}}. \tag{8.16}$$

On the basis of Fig. 8.3 we assume that there exists a wide time interval generating the PDF index $\mu = 1 + \alpha$, which is 1.35 in the case of that figure. This time interval is defined by

$$\frac{1}{\lambda} \ll t \ll \frac{1}{\Delta}. \tag{8.17}$$

This wide time interval in the Laplace domain becomes

$$\lambda \gg u \gg \Delta, \tag{8.18}$$

thereby turning Eq. 8.16 into

$$\hat{\Psi}(u) = \frac{1}{u + \lambda^{\alpha} u^{1-\alpha}}. \tag{8.19}$$

This is equivalent to the Laplace transform of the Mittag-Leffler function, which is known to be a stretched exponential in the time regime $t < 1/\lambda$ and the inverse power law $1/t^{\alpha}$ in the time regime $t > 1/\lambda$. Due to Eq. (8.17) we conclude that in that time interval

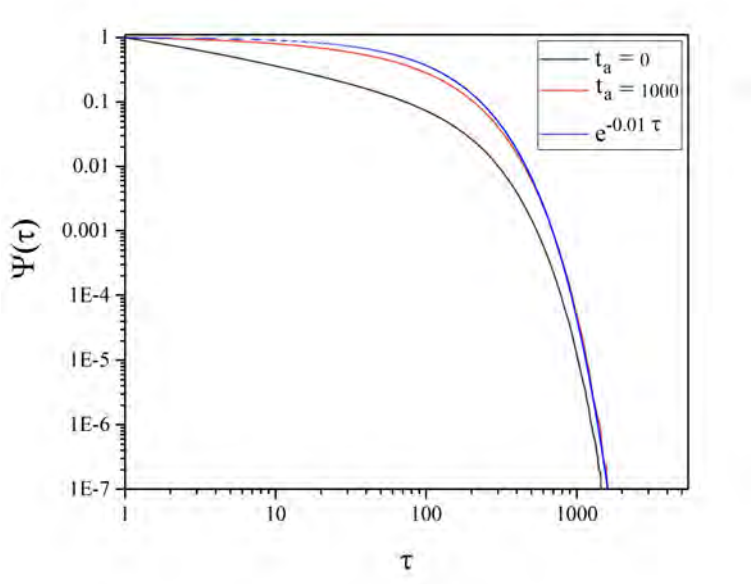

FIGURE 8.5. Survival probability of the crucial events of the metronome, compared to the exponential function corresponding to infinitely large age.The blue curve is the exponential function of Eq. (8.22).

the waiting time distribution density is an inverse power law with $\mu = 1 + \alpha$ while for times $t > 1/\Delta$

$$\psi(t) = \Gamma exp\left(-\Gamma t\right), \tag{8.20}$$

where

$$\Gamma \equiv \lambda^{\alpha} \Delta^{1-\alpha}. \tag{8.21}$$

Note that the corresponding survival probability, $\Psi(t)$, gets the form

$$\Psi(t) = exp\left(-\Gamma t\right) \tag{8.22}$$

and is identical an equilibrium correlation function with the same form as that of Eq. (8.12), with Γ given by Eq. (8.21).

In the example discussed in Section 8.4, where $\Gamma = 0.01$, we have $\Delta = 0.0078$ corresponding to the time $t = 129$.

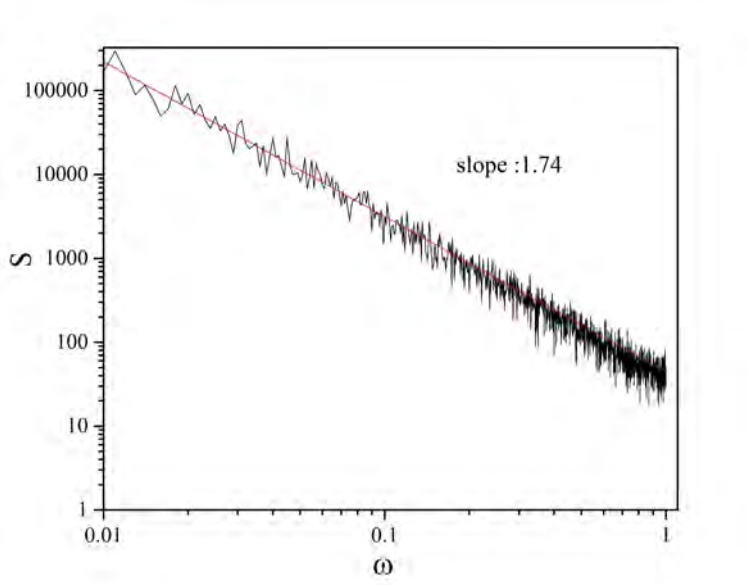

FIGURE 8.6. The spectrum $S(\omega)$ of the metronome in the condition of Fig. 8.4.

In Fig. 8.5 we make a comparison between the numerical results on the aging of the renewal events and the theoretical prediction of Eq. (8.22). The good agreement between numerical results and numerical prediction confirms that the metronome hosts crucial events therefore supporting our conviction that the multifractal properties of the metronome, stressed by the work of Deligniéres and coworkers [150], are a manifestation of the action of crucial events.

We afford a further support to this important property studying the spectrum $S(\omega)$ of the metronome in the condition corresponding to Fig. 8.4. According to the arguments illustrated in subsection 8.6, see Eq. (8.4), the $1/f$-noise generated by the metronome in this condition, with $\mu = 1.333$, should yield $\nu = 1.67$. Fig. 8.6 yields a satisfactorily agreement between theory and numerical results if we take into account the challenging numerical issue of evaluating the spectrum of a non-ergodic process with the density of crucial events decreasing upon increase of L.

8.4. Complexity Matching Between Two Multifractal Metronomes

In this Section we discuss the results of a numerical experiment done on the cross-correlation between two identical multifractal metronomes, in the condition illustrated by Fig. 8.4, which makes them, as shown in the earlier Section, equivalent to the complex networks at criticality of Ref. [40]. We stress that this equivalence rests on sharing the same temporal complexity, namely, the same non-Poisson renewal statistics for the zero-crossings. The results of this experiment of information transport from one to another identical multifractal metronome generates a qualitative agreement with the results of the earlier work of Ref. [77] on the information transport from a complex network at criticality to another complex network at criticality. However, we go much beyond this qualitative agreement. To do so, we use the theory of Ref. [40] to derive an analytical expression for the cross-correlation used to evaluate the information transport and compare it to the cross-correlation between the two equivalent multifractal metronomes done in this Section, and we find outstanding agreement.

The numerical calculations of this Section are based on the following set of coupled equations:

$$\dot{x} = -\gamma x(t) - \beta sin\left(x(t-\tau_m)\right) + \chi y, \tag{8.23}$$

where $x(t)$ is the mean field of the responding network and $y(t)$ is the mean field generated by the driving network

$$\dot{y} = -\gamma y(t) - \beta sin\left(y(t-\tau_m)\right). \tag{8.24}$$

This choice of equations is done to mimic the influence that perceptors (lookout birds) exert on their own network in response to an external network. The interaction term χy must be weak to mimic the influence of a very small number of perceiving units. For this reason we assign to the coupling coefficient χ the value $\chi = 0.1$.

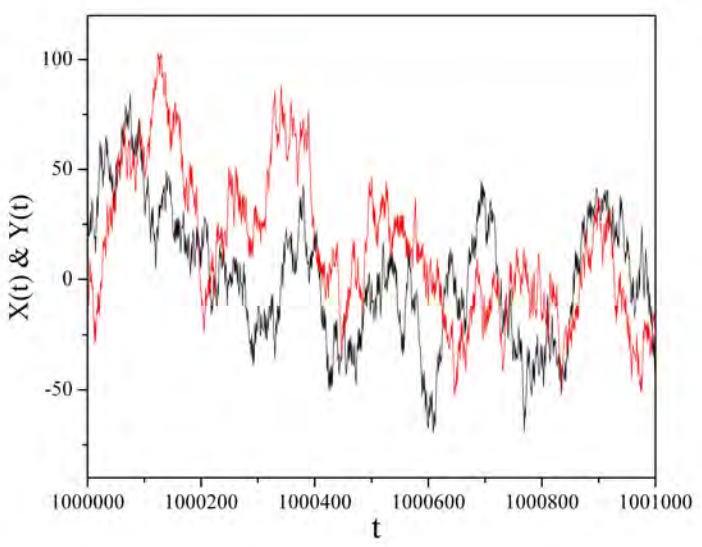

FIGURE 8.7. (Color online) Complexity matching between driven and driving metronome. The black curve is the driving system and red curve corresponds to the driven network.

In Fig. 8.7 we show that this weak coupling results in a remarkable synchronization of the driven metronome with the driving metronome. Let us now move a quantitative discussion. To make our results compatible with the observation of single complex systems, the brain being an example of unique system making it impossible for us to adopt the ensemble average method, we use the time average approach and we define the autocorrelation function $A(\tau)$ and the cross-correlation function $C(\tau)$ as follows:

$$A(\tau) = \frac{\int_0^{T-\tau} dt x(t+\tau)x(t)}{T-\tau} \tag{8.25}$$

and

$$C(\tau) = \frac{\int_0^{T-\tau} dt x(t+\tau)y(t)}{T-\tau}. \tag{8.26}$$

In both cases we set $T = 10^7$. The auto-correlation function of Eq. (8.36) is evaluated with $\chi = 0$, namely, when the metronome x is not perturbed by the metronome y.

The bottom panel of Fig. 8.8 shows that the cross-correlation function, as expected, is characterized by a significant delay, on the order of $\tau \sim 100$. The cross-correlation function

is asymmetric with respect to the shifted maximum. Notice that we have selected the value $\tau_m = 1000$, of Fig. 8.4 so as to reduce the influence of periodicity on the temporal complexity.

Let us now generate an analytical expression to match these numerical results. First of all let us stress that setting $T = 10^7$ is equivalent to make the numerical observation in the ergodic regime, where time and ensemble averages are expected to yield the same results. The adoption of ensemble averages make the calculations much simpler and for this reason, with no contradiction with the statement that we focus our attention on unique complex networks, we rest our theoretical arguments on ensemble averages.

The assumption that the time series generated by the multifractal metronome and that of the complex network are equivalent at criticality, and the arguments [40] proving the equivalence between Eq. (8.10) and Eq. (8.14) lead us to replace Eq. (8.23) and Eq. (8.24) with the linearized forms

$$\dot{x} = -\Gamma x(t) + f_x(t) + \chi y, \tag{8.27}$$

and

$$\dot{y} = -\Gamma y(t) + f_y(t), \tag{8.28}$$

where $f_x(t)$ and $f_y(t)$ are mutually uncorrelated Wiener noises. It is straightforward to show, using the lack of correlation between the two sources of noise, that the stationary cross-correlation function $C(\tau)$ is

$$C(\tau) \equiv \lim_{t\to\infty} \langle x(t+\tau)y(t)\rangle \tag{8.29}$$

and

$$\lim_{t\to\infty} \langle x(t+\tau)y(t)\rangle = \lim_{t\to\infty} \chi \int_0^{t+|\tau|} dt' e^{-\Gamma(t+|\tau|-t')} \langle y(t)y(t')\rangle \,. \tag{8.30}$$

In the absence of coupling, the two metronomes are characterized by the normalized auto-correlation functions

$$A_x(\tau) = A_y(\tau) = e^{-\Gamma|\tau|} \equiv A(\tau). \tag{8.31}$$

As a consequence

$$\langle y(t)y(t')\rangle = \left\langle y^2\right\rangle_{eq} e^{-\Gamma|t-t'|}. \tag{8.32}$$

By inserting Eq. (8.32) into Eq. (8.30), and taking into account that for $\tau > 0$, there are two distinct conditions, $t' < t$ and $t < t' < t + \tau$, we obtain

$$C(\tau) \equiv \lim_{t\to\infty} \langle x(t+\tau)y(t)\rangle = be^{-\Gamma|\tau|},\ \tau < 0, \tag{8.33}$$

and

$$C(\tau) \equiv \lim_{t\to\infty} \langle x(t+\tau)y(t)\rangle = be^{-\Gamma|\tau|}(1+2\Gamma\tau),\ \tau > 0. \tag{8.34}$$

Note that

$$b \equiv \frac{\left\langle y^2\right\rangle_{eq}\chi}{2\Gamma}. \tag{8.35}$$

It is important to stress that the normalized auto-correlation function of the multi-fractal metronome

$$A(\tau) \equiv \lim_{t\to\infty} \frac{\langle x(t)x(t+\tau)\rangle}{\langle x(t)^2\rangle} = e^{-\Gamma|\tau|} \tag{8.36}$$

is evaluated numerically and it is illustrated in the top panel of Fig. 5. We derive the value of Γ from this numerical treatment and its value $\Gamma = 0.01$ is used in Eq. (8.33) and in Eq. (8.34). As a consequence, to make a comparison between theoretical and numerical cross-correlation function we have only one fitting parameter, b, the intensity of autocorrelation function at $\tau = 0$. The bottom of Fig. 8.8 depicts the comparison between numerical and theoretical results and shows that the agreement between the two goes far beyond the qualitative. It is interesting to notice Eq. (8.33) yields for the time shift Δ of the cross-correlation function the following analytical expression

$$\Delta = \frac{1}{2\Gamma}. \tag{8.37}$$

This interesting expression shows that reducing Γ has the effect of increasing the time shift. On the other hand reducing Γ has the effect of making the non-ergodic time regime $t < T_{eq}$

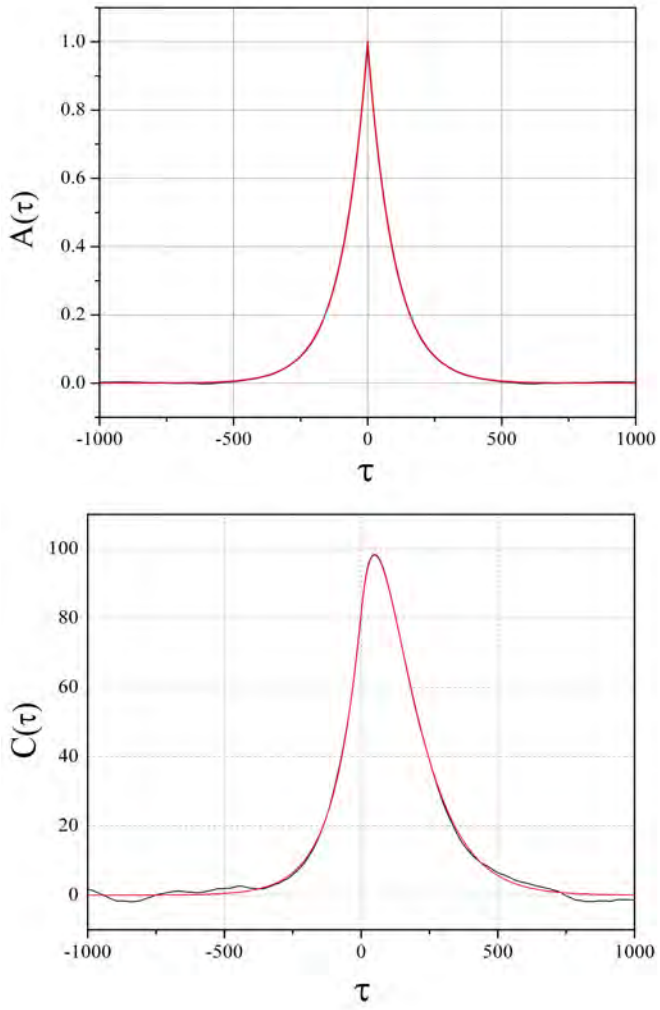

FIGURE 8.8. (Color online) Top panel: Numerical auto-correlation function $A(\tau)$ of Eq. (8.36). The numerical value of Γ is $\Gamma = 0.01$. Bottom panel: The black curve denotes the numerical result for the cross-correlation function with $\gamma = 1$, $\beta = 1000$ and $\tau_m = 1000$. The red curve is derived from Eq. (8.33) and Eq. (8.34) with the same Γ as in the top panel and the fitting parameter b with the value $b = 81.8$.

more extended, thereby suggesting a close connection between complexity matching and ergodicity breaking.

8.5. Transfer of Multifractal Spectrum from a Complex to a Deterministic Metronome

After illustrating the similarity between the metronome-metronome interaction and the DMM-DMM interaction when both DMM networks are at criticality, let us move to discuss the transfer of information from a complex metronome to a a deterministic metronome. On the basis of the PCM we should expect that in this case no significant transfer of information occurs. See, for instance, the earlier work of Ref. [28], as an example of a lack of information transport when the DMM driving network is at criticality and the driven DMM network is in the subcritical condition.

The field $x(t)$ of the driving network is illustrated by the top panel of Fig.8.9. The waiting time PDF between two consecutive regressions to the origin is of the same kind as that illustrated in Fig. 8.3, with an intermediate time region with the complexity $\mu = 1.35$, and an exponential truncation. The driven metronome in the absence of the influence of the driving metronome generates the field $x(t)$ illustrated by the middle panel of Fig.8.9. This is a fully deterministic condition corresponding to the choice of $\tau_m = 1$, which implies a lack of complexity. More precisely, Eqs. (8.23) and (8.24) has been changed into

$$\dot{x} = -\gamma x(t) - \beta sin\left(x(t - \tau_S)\right) + \chi y, \tag{8.38}$$

and

$$\dot{y} = -\gamma y(t) - \beta sin\left(y(t - \tau_P)\right), \tag{8.39}$$

respectively, where $\tau_S = 1$ and $\tau_P = 1000$.

The influence of the driving metronome on the driven one is illustrated by the bottom panel of Fig.8.9. It is evident that the driven metronome has absorbed the complexity of the driving metronome. This important property is made compelling from the results of Fig. 8.10. This figure was obtained by applying the multifractal algorithm of Ref. [170] to the time series $x(t)$ of the driven metronome moving under the influence of the driving metronome.

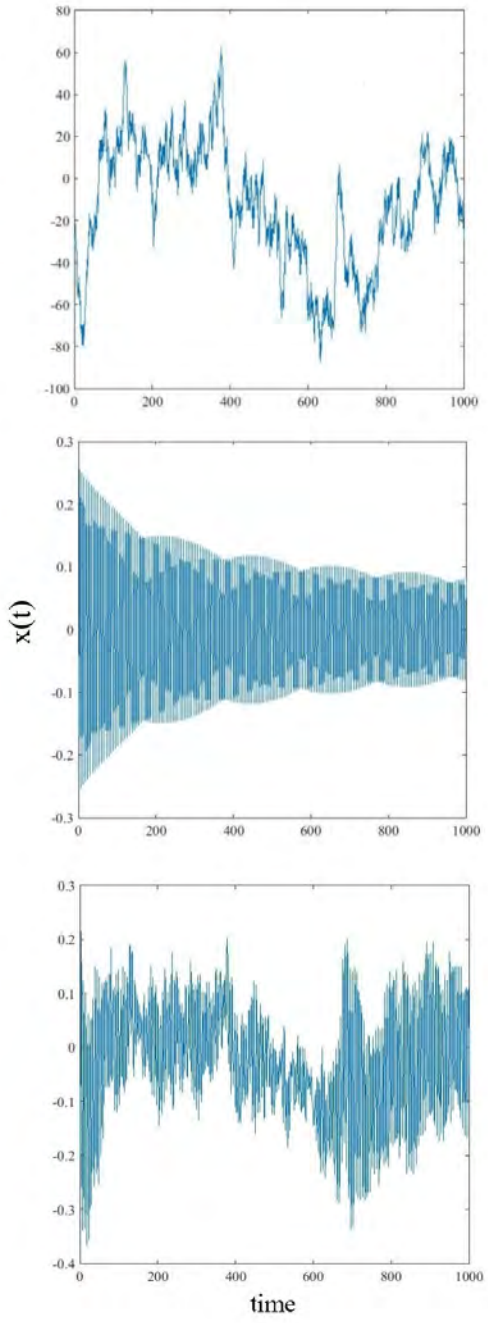

FIGURE 8.9. (Color online) Top panel: Time evolution of driving metronome with $\gamma = 1$, $\beta = 1000$ and $\tau_m = 1000$. Middle panel: Time evolution of driven metronome (before connection) with $\gamma = 1$, $\beta = 100$ and $\tau_m = 1$. Bottom panel: Time evolution of driven metronome (after connection, $\chi = 0.1$).

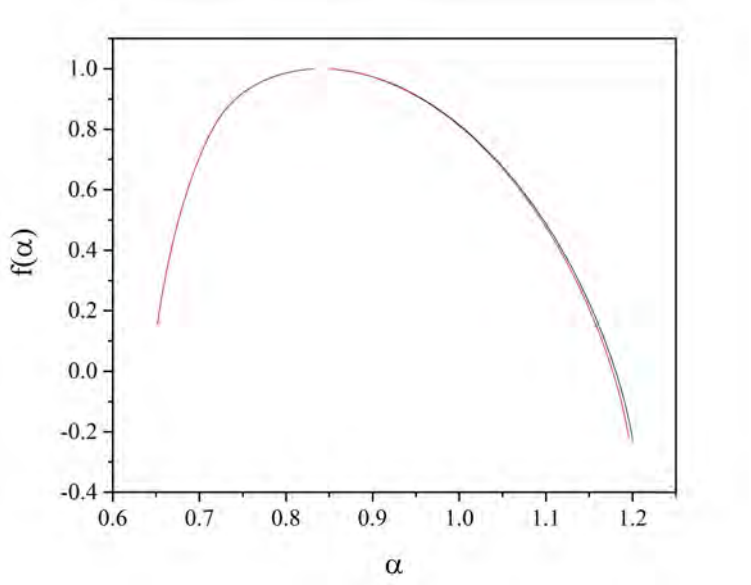

FIGURE 8.10. (Color online) Black curve: Parabola of driving metronome with $\gamma = 1$, $\beta = 1000$ and $\tau_m = 1000$. Red curve: Parabola of driven metronome with $\gamma = 1$, $\beta = 100$ and $\tau_m = 1$. $\chi = 0.1$.

How to explain this surprising result? The earlier dynamical work on complexity matching was based on the assumption that a complex network made complex by criticality is characterized by $K = K_c$ and a network with no complexity has a control parameter distinctly smaller than the critical value K_c. The crucial events of the driving network exert an influence on the time occurrence of crucial events of the driven network and consequently a form of synchronization takes place, when both networks are at criticality. However, the interaction between the two networks does not affect the values of their control parameters. If the driven network is in the subcritical regime, the statistics of its events remain of Poisson kind, thereby making it impossible to realize such a synchronization effect. The parameter τ_m apparently plays the same role as the control parameter K of the DMM network, but $\beta sin\,(x(t-\tau_S)) + \chi y$ of Eq. (8.38), with $\tau_S = \tau_m$ under the influence of perturbation is turned into $\beta sin\,(y(t-\tau_P))$. The multifractal metronome is more flexible than a DMM network in the subcritical regime.

The discussion on the origin of multifractality done in this work is far from being complete. Some attention should be devoted to the adoption of wavelet transform modulus maxima method (WTMM) [173, 174], which unmask singularities covered by higher order polynomial trends. The traditional $f(\alpha)$ method and the structure function method have limitations for negative moments, thereby leading to the development of WTMM. Another discussion of interest is about the role of large and small fluctuations for the different sides of the multifractal spectrum that correspond to positive and negative moments. We conjecture that the discussion of these issues and of the role of data length to estimate multifractality as well, should deserve a proper attention for a more rigorous theoretical foundation of criticality-induced multifractality.

In spite of these limitations, we state that the main results of this work are the following. The multifractal metronome used by Deligniéres and co-workers [150] is equivalent to a complex network at crititicality in the sense that it hosts crucial events. This establishes a connection between multifractal spectrum $f(\alpha)$ and crucial events. This result is in a qualitative accordance with the observation done in Fig. 8.1. The multifractal metronome is equivalent to a complex network at criticality, although its temporal complexity is characterized by $\mu = 1.35$ rather than $\mu = 1.5$, as for DMM [40]. The cross-correlation between two identical networks in the long-time limit is indistinguishable from that of two DMM networks at criticality, as shown by Fig. 8.8. Thus, we can conclude that the complexity matching established by Deligniéres and co-workers [150] is a process made possible by the influence that the crucial events of the metronome exert on the crucial events of the brain of the participants.

The adoption of $f(\alpha)$ as a measure of the response of S to P seems to be more powerful than the use of cross-correlation function. In fact, it is also of remarkable interest to notice that the correspondence between crucial events and broader distribution of $f(\alpha)$ makes it possible to establish the existence of a correlation between the perturbed network S and the perturbing network P in conditions far from the complexity matching of both

networks at criticality, where earlier work did not reveal any significant correlation [28]. The metronome in the physical condition making it equivalent to a network of interacting units at criticality exerts a strong influence on a network in the deterministic condition, see Fig. 8.9. Also in this case $f(\alpha)$ is a powerful indicator of correlation. Fig. 8.10 shows that the perturbed deterministic metronome inherits the spectral distribution $f(\alpha)$ of the perturbing metronome.

Complexity matching is a phenomenon closely connected to criticality that generates long-range correlation between the units of a complex network. The multifractal metronome with the delay $t-\tau$ generates a signal equivalent to that produced by a network at criticality which would require the interaction between a very large number of units and its influence is perceived by the brain that is a network of interacting neurons at criticality. Criticality generates long-range correlation and as a consequence a sort of interaction between different neurons [58], regardless of their Euclidean distance. In the case of DMM, at criticality the local interaction of each unit with its four nearest neighbors generates long-range correlation [58] with effects that are indistinguishable from real long-range interactions, thereby generating multifractality. The authors of Ref. [58] have afforded an intuitive explanation of the equivalence between long-range correlation and effective non-local interaction by adopting the concept of Hebbian learning, based on the assumption that a strong correlation between two units, regardless of their Euclidean distance, is replaced by a real link. They proved that this approach leads to establish a new scale free network, with a distribution of links $p(k) \propto \frac{1}{k^{\nu}}$ with $\nu \approx 1$. This criticality-induced network structure is virtually indistinguishable from an All-to-All coupling network. Running this network has the effect of making smaller the value of the control parameter K necessary to generate criticality, moving it from the value $K = 1.5$, used in Section II, to the value $K = 1$.

On the basis of this form of equivalence between criticality-induced long-range correlation and effective non-local interaction, leading to the conclusion that multi-fractality is connected to an effective non-local interaction, we make the plausible conjecture that a non-local model, based on the All-to-All coupling at criticality, generates a behavior quali-

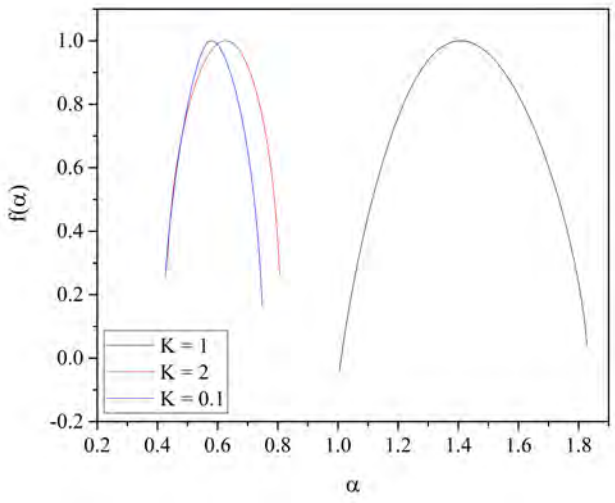

FIGURE 8.11. Multifractal spectrum of the DMM network in the case of All-To-All coupling, at criticality, $K = K_c = 1$, in the sub-critical regime, $K = 0.1$ and in the supercritical regime, $K = 2$. We use $g_0 = 0.1$.

tatively similar to that of Fig. 2. Hereby we prove that this conjecture is correct. The mean field x of DMM in the All-To-All case with a finite number of units N is described by [40]

$$\frac{d}{dt}x = g_0 sinh\left[K(x+\xi)\right] - g_0 x cosh\left[K(x+\xi)\right]. \tag{8.40}$$

Note that $\xi(t)$ is a random fluctuation of intensity proportional to $1/\sqrt{N}$, where N is the number of interacting units. We assume that

$$\xi = 0.1r, \tag{8.41}$$

where r is a random number getting the values $r = 1$ and $r = -1$. This simple numerical prescription serves the purpose of modeling the fluctuations ξ when the number of interacting units $N = 100$.

In the All-to-All coupling case criticality is realized by setting $K = K_c = 1$. In this condition Eq. (8.40) gets the form of the non-linear Langevin equation of Eq. (8.10). In the subcritical case, $K < 1$, it gets the form of an ordinary Langevin equation and in the

supercritical case, $K > 1$, it is again an ordinary Langevin equation, although the equilibrium value is not more $x = 0$ [40].

If the conjecture about the equivalence between criticality-induced long-range correlation and effective non-local interaction is correct, the application of the analysis of Kantelhard *et al* [170] to the time evolution of $x(t)$ of Eq. (8.40), non-local interaction, should yield results qualitatively equivalent to those illustrated in Fig. 2, which are obtained applying the same statistical analysis to the time evolution of $x(t)$ of Eq. (8.8), which is generated by a model of local interaction. We see that Fig. 8.11 qualitatively reproduces the results of Fig. 8.1, with a wider multifractal spectrum at criticality, and two sharper ones in both the sub-critical and supercritical condition, thereby proving that our conjecture is correct.

In this sense the genuine complexity matching is based on effective non-local interaction. The recent experiment described in [3] shows that the correlation between multifractal spectra could also arise from local corrections processes that have nothing to do with genuine complexity matching. This observation lends further support to the conclusions of this work that is, in fact, devoted to the discussion of genuine complexity matching.

CHAPTER 9

COMPLEXITY MATCHING AND REQUISITE VARIETY

9.1. Introduction

The theory that we use here should not be confused with chaos synchronization. In fact, our approach aims at establishing the proper theoretical framework to explain, for instance, brain-heart communication and there exists in the literature the increasing conviction that heart is not a chaotic system [175].

To deal with the ambitious challenge by Ashby [2] we adopt the theoretical perspective of subordination theory [176]. This theoretical perspective is closely connected to the Continuous Time Random Walk (CTRW) [177, 178], which is known to generate anomalous diffusion. We use this theoretical perspective to establish a satisfactory approach to explain the experimental results showing the remarkable oscillatory synchronization between different areas of the brain [22].

9.2. Modeling and Results

Consider a clock, whose hand regularly ticks and the time interval between two consecutive ticks, Δt, is assumed to be equal to 1. At any tick the angle θ of the clock rotates by the quantity $2\pi/T$, where T is an number corresponding to the number of ticks necessary to make a complete 2π rotation. We realize subordination by selecting for the time interval between consecutive ticks a value τ from the waiting -time PDF $\psi(\tau)$. This is a way of embedding crucial events into the periodic process. Notice that in the Poisson limit $\mu \to \infty$ the resulting rotation becomes virtually indistinguishable from that of the non-subordinated clock. Note that when $\mu > 2$, the mean waiting time $\langle \tau \rangle$ is finite. As a consequence, if T is the information on the frequency $\Omega = 2\pi/T$, this information is not completely lost. During the dynamical process the signal frequency fluctuates around Ω and the frequency Ω

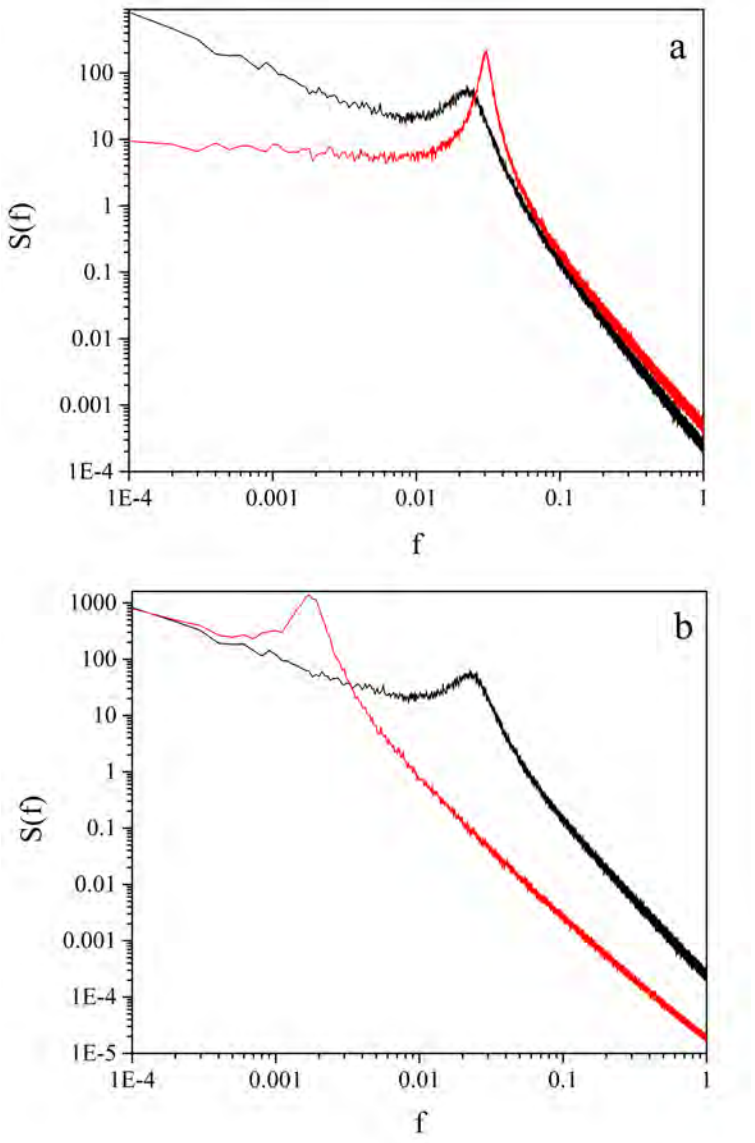

FIGURE 9.1. The spectrum $S(f)$ of four subordinations to the regular clock motion. Top panel: $\Omega = 0.06283$, $\mu = 2.1$ (black curve), $\mu = 2.9$ (red curve); bottom panel $\mu = 2.1$, $\Omega = 0.06283$ (black curve), $\Omega = 0.0006283$ (red curve).

is changed into

$$\Omega_{eff} = (\mu - 2)\Omega. \tag{9.1}$$

In fact, $\mu = 3$ is the border with the Gaussian region $\mu > 3$ where both the first and second moment of $\psi(\tau)$ are finite, and the average of the fluctuating frequencies is identical to Ω.

In the region $\mu < 2$ the process is non-ergodic, the first moment $< \tau >$ is divergent and the direct indications of homeodynamics vanish. The condition $2 < \mu < 3$ is compatible with the emergence of a stationary correlation function, in the long-time limit, with μ replaced by $\mu - 1$. Thus, using the result of earlier work [179] we get for the equilibrium correlation function exponentially damped regular oscillations, and, at the end of this oscillatory process, a power law tail proportional to $1/t^{\mu-1}$. This explains why $S(f)$ becomes proportional to $1/f^{3-\mu}$ for $f \to 0$. In conclusion, in a log-log representation, we get a curve with different slopes, $\beta = 3 - \mu$, at the left of the bump, and $\beta = 2$, at its right. $\beta = 2$ is a consequence of the exponentially damped oscillations. Fig. (9.1) illustrates the result of a numerical approach to subordination, confirming the theoretical prediction.

We interpret the time evolution of $x(t)$, the x-component of subordination to periodicity, as the result of a cooperative interaction between many oscillators. The inverse power law index μ is a sign of temporal complexity that is spontaneously realized as an effect of that interaction. To make system-1 drive system-2 we have to generalize the swarm intelligence prescription adopted in the earlier work of Ref. [28] and Ref. [29]. This generalization is necessary because the earlier work was based on the assumption that the single units of the complex systems, in the absence of interaction, undergo dichotomous fluctuations with no periodicity. In the absence of periodicity, the mean field $x(t)$ of the complex system can be written as $x(t) = (U(t) - D(t))/(U(t) + D(t))$, where $U(t)$ is the number of individual in the state $|+>$, $x > 0$, and $D(t)$ is the number of individuals in the state $|->$, $x < 0$. Using this notation (see supplementary material) we show that

$$x_2(t) - x_1(t) \propto K(t), \tag{9.2}$$

where

$$K(t) \equiv (1 - x_2(t))(1 + x_1(t)) - (1 + x_2(t))(1 - x_1(t)). \tag{9.3}$$

To take periodicity into account he have to notice that $x_1(t)$, has the structure

$$x_1(t) = cos(\Omega_1 n_1(t)). \tag{9.4}$$

System-2 has the same periodical structure

$$x_2(t) = cos(\Omega_1 n_2(t) + \Phi(t)), \tag{9.5}$$

where the phase $\Phi(t)$ is a consequence of the fact that the units of system-2 try to compensate the effects produced by the two independent self-organization processes. The number of clicks of system-1, $n_1(t)$, due to the occurrence of crucial events, tends to become increasingly different from the number of clicks of system-2, $n_2(t)$. The units of system-2, trying to imitate the choices made by the units of system-1, in addition to the process described by $K(t)$ of Eq. (9.3) must adjust also the phase $\Phi(t)$ of Eq. (9.5). This phase may either increase or decrease in accordance to the sign of the virtual sine corresponding to Eq. (9.5), $sin(\Omega_1 n_2(t) + \Phi(t))$. The intensity of this virtual sine establishes also a correction to the intensity established by $K(t)$ of Eq. (9.3). Thus we obtain the central algorithmic prescription of this work:

$$\Phi(t+1) = \Phi(t), \tag{9.6}$$

if at $t+1$) no crucial event occurs, and

$$\Phi(t+1) = \Phi(t) - r_1 K(t) sin\left(\Omega_2 n_2(t) + \Phi(t)\right), \tag{9.7}$$

if at $t+1$ a crucial event occurs. Note that the real positive number r_1, smaller than one, defines the proportionality factor left open by Eq. (9.2), or, equivalently, defines the strength of the perturbation that system-1 exerts on system-2.

Fig. (9.2) illustrates the significant synchronization between the driven and the driving system obtained for $\mu = 2.2$, close to the values of the crucial events of the brain dynamics [17]. This result can be used to explain the experimental observation of Delignières and coworkers [3] (see supplementary material).

The top panel of Fig. (9.3) shows that the system-2, with $\mu_2 = 2.9$, very close the Gaussian border, gets the higher complexity of system-1 with $\mu_1 = 2.1$, namely the complexity of a system very close to the ideal condition, $\mu = 2$, to realize $1/f$ noise.

In the bottom panel of Fig. (9.3) we see that a driving system very close to the Gaussian border does not make the driven system less complex, but it does succeed in

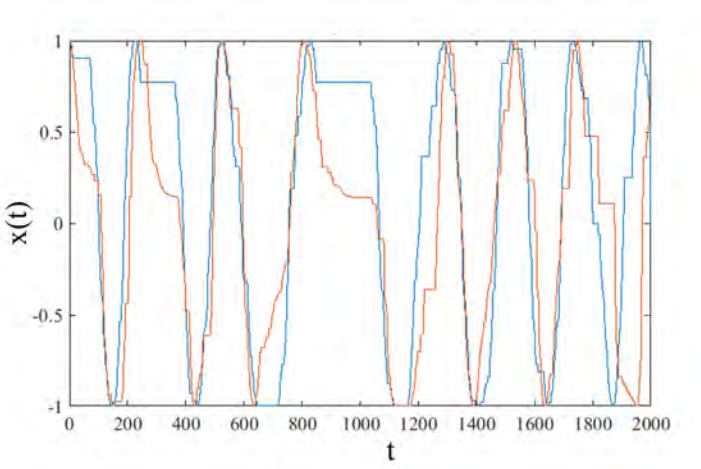

FIGURE 9.2. System-1 drives system-2, The two systems are identical: $\mu = 2.2$, $\Omega = 0.063$. $r_1 = 0.05$. The coupling is realized using Eq. (9.2) and Eq. (9.3).

forcing it to adopt the regulator's periodicity. Here we have to stress that the perturbing system is quite different from the external fluctuation that was originally adopted to mimic the effort generated by a difficult task [180]. In that case the complex system has to address a difficult task, a cognition problem making its power index μ depart from the $1/f$-noise condition [24].

The theory of this work substantiates the opposite effect of cooperation. It is straightforward to extend the treatment of this work to the case where system-1 is influenced by system-2 in the same way system-2 is influenced by system-1. To make this extension we have to introduce the new parameter r_2, which defines the intensity of the influence of system-2 on system-1. As a result of this back-to-back interaction, we have $\mu_1 \rightarrow \mu_1^{'}$ and $\mu_2 \rightarrow \mu_2$. When $\mu_1 < \mu_2$ we expect

$$\mu_1 < \mu_1^{'} < \mu_2^{'} < \mu_2. \tag{9.8}$$

Fig. 9.4 shows that $\mu_1^{'} \approx \mu_1$, thereby suggesting that the system with larger complexity drives the system with smaller complexity.

We interpret this result as an indication that the system with higher complexity does

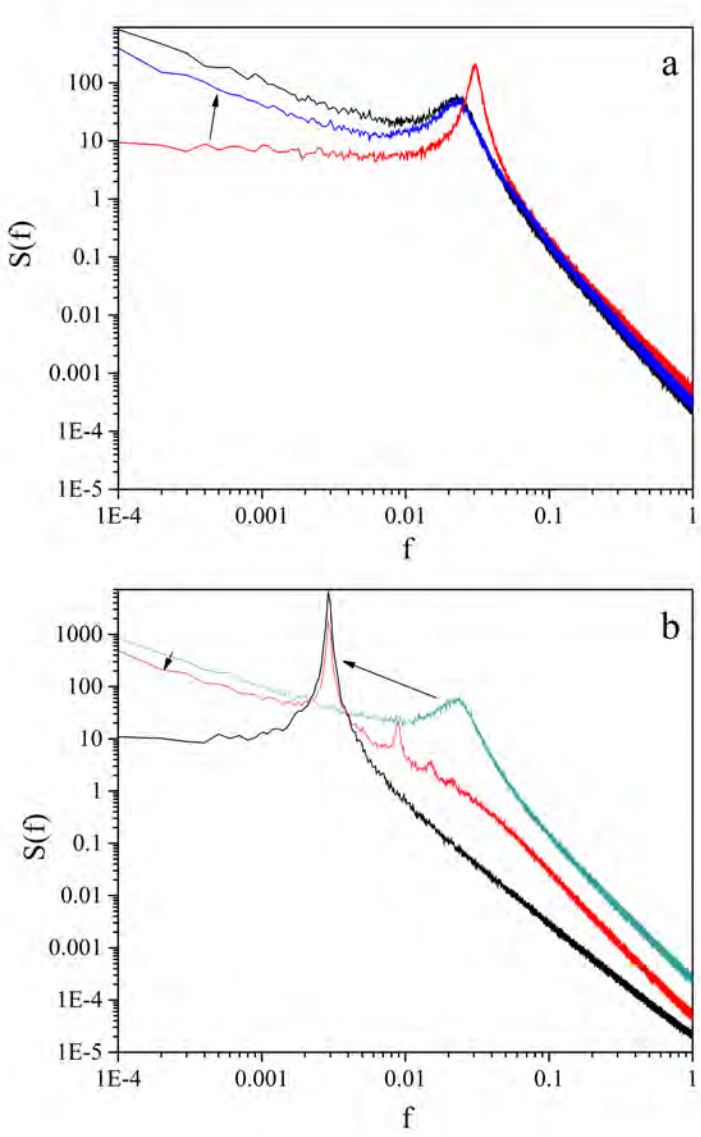

FIGURE 9.3. Top: Driven system: $\mu = 2.9, \Omega = 0.063$; driving system: $\mu = 2.1, \Omega = 0.063$. $r_1 = 0.1$. Bottom: Driving system: $\mu = 2.9, \Omega = 0.0063$; driven system: $\mu = 2.1, \Omega = 0.063$. $r_1 = 0.1$.

not perceive its interaction with the other system as a difficult task, while the less complex system has a sense of relief. We interpret this result as an important property that should be the subject of psychological experiments to shed light into the teaching and learning process. The theory of this work makes it possible to go beyond the limitation of the earlier work on

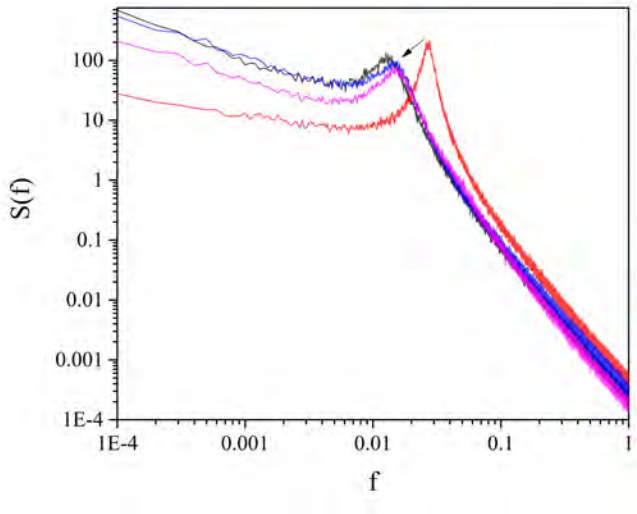

FIGURE 9.4. Two cooperating systems with different complexity. System-1: $\mu_1 = 2.2$, $\Omega_1 = 0.063$; system-2: $\mu_2 = 2.9$, $\Omega_2 = 0.063$; $r_1 = r_2 = 0.1$.

complexity management, as illustrated in the supplementary material.

9.3. Concluding Remarks

The term "intelligent" that we are using here is equivalent to assessing that a system is as close as possible to the ideal condition $\mu = 2$, corresponding to the ideal $1/f$ noise. Two very intelligent systems are the brain and heart that in the healthy condition share the property of a μ very close to 2. This work therefore explains the synchronization between heart and the brain. This work shows that the concept of resonance, based on tuning the frequency of the stimulus to the frequency of the system to perturb may not be appropriate for complex biological system. It seems more appropriate for a physical system where the resonance tuning has been adopted over the years for the transport of energy. This is expected to contribute a significant therapeutic advance yielding a proper use of bio-feedback methods [181].

CHAPTER 10

CONCLUSIONS

In this work we showed how Self-Organized Temporal Criticality can resolve Eempirical paradox of emergence of cooperation in society of selfish individuals. We also showed how systems with this new kind of criticality transfer information and multifractality. Based on properties of SOTC systems we aimed to bridge between physics and biology. The work of [60], based on the prisoners dilemma game and network reciprocity, is used by biologists to explain enzyme action, with an extremely good agreement between theory and experimental observation. However, it is well known that the adoption of non-equilibrium statistical physics shows that the conventional Transition State Theory requires such an impressively large reaction rate enhancement [182] as to lead us to consider this problem to be totally unsettled, on the basis of the current understanding of non-equilibrium statistical physics. An attempt made many years ago [183] at settling this problem through the assumption that the enzyme generates a fluctuating temperature, yields us to adopt the model proposed by Voss and Clarke for the origin of 1/f noise [184]. This model, however, is questionable, insofar as the physical origin of 1/f noise is still considered an unsettled problem. In this work we have seen that the subordination to regular oscillation is interpreted as a way of using SOTC applied to a set of interacting oscillators, and we have seen that this leads to 1/f noise. This is what we mean by moving from the cooperative properties of biological processes to establish a solid bridge . This dissertation shows that it is necessary to supplement the current field of non-equilibrium statistical physics with the cooperative properties of living systems.

BIBLIOGRAPHY

[1] Martin A Nowak and Robert M May, *Evolutionary games and spatial chaos*, Nature 359 (1992), no. 6398, 826.

[2] W Ross Ashby, *An introduction to cybernetics*, (1957).

[3] Zainy MH Almurad, Clément Roume, and Didier Delignières, *Complexity matching in side-by-side walking*, Human movement science 54 (2017), 125–136.

[4] Ruud JR Den Hartigh, Vivien Marmelat, and Ralf FA Cox, *Multiscale coordination between athletes: Complexity matching in ergometer rowing*, Human movement science (2017).

[5] Charles A Coey, Auriel Washburn, Justin Hassebrock, and Michael J Richardson, *Complexity matching effects in bimanual and interpersonal syncopated finger tapping*, Neuroscience letters 616 (2016), 204–210.

[6] Drew H Abney, Alexandra Paxton, Rick Dale, and Christopher T Kello, *Complexity matching in dyadic conversation.*, Journal of Experimental Psychology: General 143 (2014), no. 6, 2304.

[7] Vivien Marmelat and Didier Delignières, *Strong anticipation: complexity matching in interpersonal coordination*, Experimental Brain Research 222 (2012), no. 1-2, 137–148.

[8] Justin M Fine, Aaron D Likens, Eric L Amazeen, and Polemnia G Amazeen, *Emergent complexity matching in interpersonal coordination: Local dynamics and global variability.*, Journal of experimental psychology: Human Perception and Performance 41 (2015), no. 3, 723.

[9] Leonardo Zapata-Fonseca, Dobromir Dotov, Ruben Fossion, and Tom Froese, *Time-series analysis of embodied interaction: movement variability and complexity matching as dyadic properties*, Frontiers in psychology 7 (2016), 1940.

[10] Tom Froese, Hiroyuki Iizuka, and Takashi Ikegami, *Embodied social interaction constitutes social cognition in pairs of humans: a minimalist virtual reality experiment*, Scientific reports 4 (2014), 3672.

[11] Guillaume Dumas, Jacqueline Nadel, Robert Soussignan, Jacques Martinerie, and Line Garnero, *Inter-brain synchronization during social interaction*, PloS one 5 (2010), no. 8, e12166.

[12] Hanne De Jaegher, Ezequiel Di Paolo, and Shaun Gallagher, *Can social interaction constitute social cognition?*, Trends in cognitive sciences 14 (2010), no. 10, 441–447.

[13] Gert Pfurtscheller, Andreas R Schwerdtfeger, Annemarie Seither-Preisler, Clemens Brunner, Christoph Stefan Aigner, Joana Brito, Marciano P Carmo, and Alexandre Andrade, *Brain–heart communication: Evidence for central pacemaker oscillations with a dominant frequency at 0.1 hz in the cingulum*, Clinical Neurophysiology 128 (2017), no. 1, 183–193.

[14] Michael G Rosenblum, Arkady S Pikovsky, and Jürgen Kurths, *Phase synchronization of chaotic oscillators*, Physical review letters 76 (1996), no. 11, 1804.

[15] David J Schwab, Ilya Nemenman, and Pankaj Mehta, *Zipfs law and criticality in multivariate data without fine-tuning*, Physical review letters 113 (2014), no. 6, 068102.

[16] Aref Pariz, Zahra G Esfahani, Shervin S Parsi, Alireza Valizadeh, Santiago Canals, and Claudio R Mirasso, *High frequency neurons determine effective connectivity in neuronal networks*, NeuroImage 166 (2018), 349–359.

[17] P Paradisi, P Allegrini, A Gemignani, M Laurino, D Menicucci, and A Piarulli, *Scaling and intermittency of brain events as a manifestation of consciousness*, AIP Conference Proceedings, vol. 1510, AIP, 2013, pp. 151–161.

[18] Ralf Metzler, Jae-Hyung Jeon, Andrey G Cherstvy, and Eli Barkai, *Anomalous diffusion models and their properties: non-stationarity, non-ergodicity, and ageing at the centenary of single particle tracking*, Physical Chemistry Chemical Physics 16 (2014), no. 44, 24128–24164.

[19] David Lloyd, Miguel A Aon, and Sonia Cortassa, *Why homeodynamics, not homeostasis?*, The Scientific World Journal 1 (2001), 133–145.

[20] Takashi Ikegami and Keisuke Suzuki, *From a homeostatic to a homeodynamic self*, BioSystems 91 (2008), no. 2, 388–400.

[21] Mizuki Oka, Hirotake Abe, and Takashi Ikegami, *Dynamic homeostasis in packet switching networks*, Adaptive Behavior 23 (2015), no. 1, 50–63.

[22] Manfred G Kitzbichler, Marie L Smith, Søren R Christensen, and Ed Bullmore, *Broadband criticality of human brain network synchronization*, PLoS computational biology 5 (2009), no. 3, e1000314.

[23] Mirko Lukovic and Paolo Grigolini, *Power spectra for both interrupted and perennial aging processes*, The Journal of chemical physics 129 (2008), no. 18, 184102.

[24] Joshua Correll, *1/f noise and effort on implicit measures of bias.*, Journal of Personality and Social Psychology 94 (2008), no. 1, 48.

[25] Paolo Allegrini, Mauro Bologna, Leone Fronzoni, Paolo Grigolini, and Ludovico Silvestri, *Experimental quenching of harmonic stimuli: universality of linear response theory*, Physical review letters 103 (2009), no. 3, 030602.

[26] Gerardo Aquino, Mauro Bologna, Paolo Grigolini, and Bruce J West, *Beyond the death of linear response: 1/f optimal information transport*, Physical review letters 105 (2010), no. 4, 040601.

[27] Nicola Piccinini, David Lambert, Bruce J. West, Mauro Bologna, and Paolo Grigolini, *Nonergodic complexity management*, Phys. Rev. E 93 (2016), 062301.

[28] Malgorzata Turalska, Mirko Lukovic, Bruce J West, and Paolo Grigolini, *Complexity and synchronization*, Physical Review E 80 (2009), no. 2, 021110.

[29] Fabio Vanni, Mirko Luković, and Paolo Grigolini, *Criticality and transmission of information in a swarm of cooperative units*, Physical review letters 107 (2011), no. 7, 078103.

[30] Herbert Gintis, *The bounds of reason: Game theory and the unification of the behavioral sciences*, Princeton University Press, 2014.

[31] Martin A Nowak, *Five rules for the evolution of cooperation*, science 314 (2006), no. 5805, 1560–1563.

[32] Robert Axelrod and William Donald Hamilton, *The evolution of cooperation*, science 211 (1981), no. 4489, 1390–1396.

[33] Zhen Wang, Lin Wang, Attila Szolnoki, and Matjaž Perc, *Evolutionary games on multilayer networks: a colloquium*, The European physical journal B 88 (2015), no. 5, 124.

[34] Paolo Grigolini, Nicola Piccinini, Adam Svenkeson, Pensri Pramukkul, David Lambert, and Bruce J West, *From neural and social cooperation to the global emergence of cognition*, Frontiers in bioengineering and biotechnology 3 (2015), 78.

[35] Paolo Grigolini, *Emergence of biological complexity: Criticality, renewal and memory*, Chaos, Solitons & Fractals 81 (2015), 575–588.

[36] Bruce J West, Malgorzata Turalska, and Paolo Grigolini, *Networks of echoes: Imitation, innovation and invisible leaders*, Springer Science & Business Media, 2014.

[37] M Ibrahim Sezan, *Social physics: How good ideas spread-the lessons from a new science*, Research Technology Management 58 (2015), no. 1, 61.

[38] Tamás Vicsek, András Czirók, Eshel Ben-Jacob, Inon Cohen, and Ofer Shochet, *Novel type of phase transition in a system of self-driven particles*, Physical review letters 75 (1995), no. 6, 1226.

[39] Simon Rosenfeld, *Are the somatic mutation and tissue organization field theories of carcinogenesis incompatible?*, Cancer informatics 12 (2013), CIN–S13013.

[40] MT Beig, A Svenkeson, M Bologna, BJ West, and P Grigolini, *Critical slowing down in networks generating temporal complexity*, PHYSICAL REVIEW E , (2015) 91 (2015), no. 1, 012907.

[41] Javad Usefie Mafahim, David Lambert, Marzieh Zare, and Paolo Grigolini, *Complexity matching in neural networks*, New Journal of Physics 17 (2015), no. 1, 015003.

[42] Herbert Gintis, *Game theory evolving: a problem-centered introduction to modeling stategic interaction*, Princeton, NJ: Princeton UP (2000).

[43] Ibn Khaldun, *The muqaddimah: an introduction to history*, 2015.

[44] Akbar S Ahmed, *Islam under siege: Living dangerously in a post-honor world*, John Wiley & Sons, 2013.

[45] Pensri Pramukkul, Adam Svenkeson, Bruce J West, and Paolo Grigolini, *The value of conflict in stable social networks*, EPL (Europhysics Letters) 111 (2015), no. 5, 58003.

[46] Carlos P Roca, José A Cuesta, and Angel Sánchez, *Imperfect imitation can enhance cooperation*, EPL (Europhysics Letters) 87 (2009), no. 4, 48005.

[47] Daniele Vilone, José J Ramasco, Angel Sánchez, and Maxi San Miguel, *Social and strategic imitation: the way to consensus*, Scientific reports 2 (2012), 686.

[48] Jelena Grujić, Constanza Fosco, Lourdes Araujo, José A Cuesta, and Angel Sánchez, *Social experiments in the mesoscale: Humans playing a spatial prisoner's dilemma*, PloS one 5 (2010), no. 11, e13749.

[49] Carlos Gracia-Lázaro, José A Cuesta, Angel Sánchez, and Yamir Moreno, *Human behavior in prisoner's dilemma experiments suppresses network reciprocity*, Scientific reports 2 (2012), 325.

[50] Jelena Grujić, Carlos Gracia-Lázaro, Manfred Milinski, Dirk Semmann, Arne Traulsen, José A Cuesta, Yamir Moreno, and Angel Sánchez, *A comparative analysis of spatial prisoner's dilemma experiments: Conditional cooperation and payoff irrelevance*, Scientific reports 4 (2014), 4615.

[51] Giulio Cimini, Angel Sanchez, et al., *How evolutionary dynamics affects network reciprocity in prisonerâ s dilemma*, Journal of Artificial Societies and Social Simulation 18 (2015), no. 2, 1–22.

[52] Claudio Castellano, Santo Fortunato, and Vittorio Loreto, *Statistical physics of social dynamics*, Reviews of modern physics 81 (2009), no. 2, 591.

[53] Krzysztof Suchecki, Víctor M Eguíluz, and Maxi San Miguel, *Voter model dynamics in complex networks: Role of dimensionality, disorder, and degree distribution*, Physical Review E 72 (2005), no. 3, 036132.

[54] Malgorzata Turalska, Bruce J. West, and Paolo Grigolini, *Temporal complexity of the order parameter at the phase transition*, Phys. Rev. E 83 (2011), 061142.

[55] Malgorzata Turalska, Bruce J West, and Paolo Grigolini, *Role of committed minorities in times of crisis*, Scientific reports 3 (2013), 1371.

[56] Nicholas W Hollingshad, Malgorzata Turalska, Paolo Allegrini, Bruce J West, and Paolo Grigolini, *A new measure of network efficiency*, Physica A: Statistical Mechanics and its Applications 391 (2012), no. 4, 1894–1899.

[57] Nicholas W Hollingshad, Adam Svenkeson, Bruce J West, and Paolo Grigolini, *Time to consensus*, Physica A: Statistical Mechanics and its Applications 392 (2013), no. 9, 2302–2310.

[58] Malgorzata Turalska, Elvis Geneston, Bruce J West, Paolo Allegrini, and Paolo Grigolini, *Cooperation-induced topological complexity: a promising road to fault tolerance and hebbian learning*, Frontiers in physiology 3 (2012), 52.

[59] György Szabó and Gabor Fath, *Evolutionary games on graphs*, Physics reports 446 (2007), no. 4-6, 97–216.

[60] Marco Archetti and István Scheuring, *Evolution of optimal hill coefficients in nonlinear public goods games*, Journal of theoretical biology 406 (2016), 73–82.

[61] Oliver P Hauser, David G Rand, Alexander Peysakhovich, and Martin A Nowak, *Cooperating with the future*, Nature 511 (2014), no. 7508, 220.

[62] Alexander J Stewart and Joshua B Plotkin, *Small groups and long memories promote cooperation*, Scientific reports 6 (2016), 26889.

[63] Korosh Mahmoodi and Paolo Grigolini, *Evolutionary game theory and criticality*, Journal of Physics A: Mathematical and Theoretical 50 (2016), no. 1, 015101.

[64] Janina Hesse and Thilo Gross, *Self-organized criticality as a fundamental property of neural systems*, Frontiers in systems neuroscience 8 (2014), 166.

[65] Rosaria Conte, Nigel Gilbert, Giulia Bonelli, Claudio Cioffi-Revilla, Guillaume Deffuant, Janos Kertesz, Vittorio Loreto, Suzy Moat, J-P Nadal, Anxo Sanchez, et al., *Manifesto of computational social science*, The European Physical Journal Special Topics 214 (2012), no. 1, 325–346.

[66] Nicholas W Watkins, Gunnar Pruessner, Sandra C Chapman, Norma B Crosby, and Henrik J Jensen, *25 years of self-organized criticality: concepts and controversies*, Space Science Reviews 198 (2016), no. 1-4, 3–44.

[67] Per Bak and Kan Chen, *The physics of fractals*, Physica D: Nonlinear Phenomena 38 (1989), no. 1-3, 5–12.

[68] Stefano Zapperi, Kent Bækgaard Lauritsen, and H Eugene Stanley, *Self-organized branching processes: mean-field theory for avalanches*, Physical review letters 75 (1995), no. 22, 4071.

[69] Matteo Martinello, Jorge Hidalgo, Amos Maritan, Serena di Santo, Dietmar Plenz, and Miguel A Muñoz, *Neutral theory and scale-free neural dynamics*, Physical Review X 7 (2017), no. 4, 041071.

[70]

[71] D. Helbing, *The dream of controlling the world-and why it often fails*, Working Paper (2017).

[72] Marzieh Zare and Paolo Grigolini, *Criticality and avalanches in neural networks*, Chaos, Solitons & Fractals 55 (2013), 80–94.

[73] Roberto Failla, Paolo Grigolini, Massimiliano Ignaccolo, and Arne Schwettmann, *Random growth of interfaces as a subordinated process*, Physical Review E 70 (2004), no. 1, 010101.

[74] JM Kim, AJ Bray, and MA Moore, *Domain growth, directed polymers, and self-organized criticality*, Physical Review A 45 (1992), no. 12, 8546.

[75] CH Hauert and Heinz Georg Schuster, *Effects of increasing the number of players and memory size in the iterated prisoner's dilemma: a numerical approach*, Proceedings of the Royal Society of London B: Biological Sciences 264 (1997), no. 1381, 513–519.

[76] Daniele Nosenzo, Simone Quercia, and Martin Sefton, *Cooperation in small groups: The effect of group size*, Experimental Economics 18 (2015), no. 1, 4–14.

[77] Mirko Luković, Fabio Vanni, Adam Svenkeson, and Paolo Grigolini, *Transmission of information at criticality*, Physica A: Statistical Mechanics and its Applications 416 (2014), 430–438.

[78] Korosh Mahmoodi, Bruce J West, and Paolo Grigolini, *Self-organizing complex networks: individual versus global rules*, Frontiers in physiology 8 (2017), 478.

[79] Wendy K Smith, Marianne W Lewis, and Michael L Tushman, *Both/and leadership*, Harvard Business Review 94 (2016), no. 5, 62–70.

[80] H Kirchner, *Critical phenomena in natural sciences: Chaos, fractals, selforganization and disorder-concepts and tools, by d. sornette*, PURE AND APPLIED GEOPHYSICS 160 (2003), no. 7, 1370–1370.

[81] James G March, *Rationality, foolishness, and adaptive intelligence*, Strategic management journal 27 (2006), no. 3, 201–214.

[82] Daniel Kahneman, *Thinking, fast and slow*, Macmillan, 2011.

[83] David G Rand and Martin A Nowak, *Human cooperation*, Trends in cognitive sciences 17 (2013), no. 8, 413–425.

[84] David G Rand, *Cooperation, fast and slow: Meta-analytic evidence for a theory of social heuristics and self-interested deliberation*, Psychological Science 27 (2016), no. 9, 1192–1206.

[85] Grigory Isaakovich Barenblatt, *Scaling, self-similarity, and intermediate asymptotics: dimensional analysis and intermediate asymptotics*, vol. 14, Cambridge University Press, 1996.

[86] Martin Nowak and Karl Sigmund, *A strategy of win-stay, lose-shift that outperforms tit-for-tat in the prisoner's dilemma game*, Nature 364 (1993), no. 6432, 56.

[87] Charles Darwin, *The origin of species by means of natural selection: or, the preservation of favoured races in the struggle for life and the descent of man and selection in relation to sex*, Modern library, 1872.

[88] David Sloan Wilson and Edward O Wilson, *Rethinking the theoretical foundation of sociobiology*, The Quarterly review of biology 82 (2007), no. 4, 327–348.

[89] Miguel Pais-Vieira, Gabriela Chiuffa, Mikhail Lebedev, Amol Yadav, and Miguel AL Nicolelis, *Corrigendum: Building an organic computing device with multiple interconnected brains*, Scientific reports 5 (2015), 14937.

[90] Nicholas W Watkins, *On the continuing relevance of mandelbrots non-ergodic fractional*

renewal models of 1963 to 1967, The European Physical Journal B 90 (2017), no. 12, 241.

[91] Wendy K Smith and Marianne W Lewis, *Toward a theory of paradox: A dynamic equilibrium model of organizing*, Academy of management Review 36 (2011), no. 2, 381–403.

[92] M Archetti, *M. archetti and i. scheuring, j. theor. biol. 299, 9 (2012).*, J. Theor. Biol. 299 (2012), 9.

[93] Jonathan Haidt, *The righteous mind: Why good people are divided by politics and religion*, Vintage, 2012.

[94] Vilfredo Pareto, *The rise and fall of the elites: an application of theoretical sociology*, Transaction Publishers, 1991.

[95] Ernst Ising, *Beitrag zur theorie des ferromagnetismus*, Zeitschrift für Physik 31 (1925), no. 1, 253–258.

[96] Lars Onsager, *Crystal statistics. i. a two-dimensional model with an order-disorder transition*, Physical Review 65 (1944), no. 3-4, 117.

[97] Thierry Mora and William Bialek, *Are biological systems poised at criticality?*, Journal of Statistical Physics 144 (2011), no. 2, 268–302.

[98] Daniel Fraiman, Pablo Balenzuela, Jennifer Foss, and Dante R Chialvo, *Ising-like dynamics in large-scale functional brain networks*, Physical Review E 79 (2009), no. 6, 061922.

[99] Dante R Chialvo, *Emergent complex neural dynamics*, Nature physics 6 (2010), no. 10, 744.

[100] MG Kitzbichler, *Mg kitzbichler, ml smith, sr christensen, and e. bullmore, plos comput. biol. 5, e1000314 (2009).*, PLoS Comput. Biol. 5 (2009), e1000314.

[101] Per Bak and Maya Paczuski, *Complexity, contingency, and criticality*, Proceedings of the National Academy of Sciences 92 (1995), no. 15, 6689–6696.

[102] Wilson Truccolo, Leigh R Hochberg, and John P Donoghue, *Collective dynamics in*

human and monkey sensorimotor cortex: predicting single neuron spikes, Nature neuroscience 13 (2010), no. 1, 105.

[103] E Schneidman, *E. schneidman, mj berry, r. segev, and w. bialek, nature (london) 440, 1007 (2006).*, Nature (London) 440 (2006), 1007.

[104] Paolo Paradisi and Paolo Allegrini, *Scaling law of diffusivity generated by a noisy telegraph signal with fractal intermittency*, Chaos, Solitons & Fractals 81 (2015), 451–462.

[105] Enzo Tagliazucchi, Dante R Chialvo, Michael Siniatchkin, Enrico Amico, Jean-Francois Brichant, Vincent Bonhomme, Quentin Noirhomme, Helmut Laufs, and Steven Laureys, *Large-scale signatures of unconsciousness are consistent with a departure from critical dynamics*, Journal of The Royal Society Interface 13 (2016), no. 114, 20151027.

[106] Paolo Allegrini, Paolo Paradisi, Danilo Menicucci, and Angelo Gemignani, *Fractal complexity in spontaneous eeg metastable-state transitions: new vistas on integrated neural dynamics*, Frontiers in physiology 1 (2010), 128.

[107] Bernard Gert, *Morality: A new justification of the moral rules*, (1988).

[108] Herbert Alexander Simon, *Models of bounded rationality: Empirically grounded economic reason*, vol. 3, MIT press, 1997.

[109] Gerd Gigerenzer, *Risk savvy: How to make good decisions*, Penguin, 2015.

[110] April Pease, Korosh Mahmoodi, and Bruce J West, *Complexity measures of music*, Chaos, Solitons and Fractals 108 (2018), 82–86.

[111] K Mahmoodi, P Grigolini, and BJ West, *On social sensitivity to either zealot or independent minorities*, Chaos, Solitons & Fractals 110 (2018), 185–190.

[112] Paolo Allegrini, Mauro Bologna, Paolo Grigolini, and Bruce J West, *Fluctuation-dissipation theorem for event-dominated processes*, Physical review letters 99 (2007), no. 1, 010603.

[113] Nagi Khalil, Maxi San Miguel, and Raul Toral, *Zealots in the mean-field noisy voter model*, Physical Review E 97 (2018), no. 1, 012310.

[114] William Bialek, *Perspectives on theory at the interface of physics and biology*, Reports on Progress in Physics 81 (2017), no. 1, 012601.

[115] Miguel A Muñoz, *Colloquium: Criticality and dynamical scaling in living systems*, arXiv preprint arXiv:1712.04499 (2017).

[116] Damon Centola and Andrea Baronchelli, *The spontaneous emergence of conventions: An experimental study of cultural evolution*, Proceedings of the National Academy of Sciences 112 (2015), no. 7, 1989–1994.

[117] Dina Mistry, Qian Zhang, Nicola Perra, and Andrea Baronchelli, *Committed activists and the reshaping of status-quo social consensus*, Physical Review E 92 (2015), no. 4, 042805.

[118] Lada Adamic et al., *The diffusion of support in an online social movement: Evidence from the adoption of equal-sign profile pictures*, Proceedings of the 18th ACM Conference on Computer Supported Cooperative Work & Social Computing, ACM, 2015, pp. 1741–1750.

[119] A Svenkeson and A Swami, *Reaching consensus by allowing moments of indecision*, Scientific reports 5 (2015), 14839.

[120] Casey Doyle, Sameet Sreenivasan, Boleslaw K Szymanski, and Gyorgy Korniss, *Social consensus and tipping points with opinion inertia*, Physica A: Statistical Mechanics and its Applications 443 (2016), 316–323.

[121] Hai-Bo Hu, Cang-Hai Li, and Qing-Ying Miao, *Opinion diffusion on multilayer social networks*, Advances in Complex Systems 20 (2017), no. 06n07, 1750015.

[122] Haibo Hu and Jonathan JH Zhu, *Social networks, mass media and public opinions*, Journal of Economic Interaction and Coordination 12 (2017), no. 2, 393–411.

[123] Pramesh Singh, Sameet Sreenivasan, Boleslaw K Szymanski, and Gyorgy Korniss, *Threshold-limited spreading in social networks with multiple initiators*, Scientific reports 3 (2013), 2330.

[124] Enzo Tagliazucchi and Dante R Chialvo, *Brain complexity born out of criticality*, AIP Conference Proceedings, vol. 1510, AIP, 2013, pp. 4–13.

[125] Enzo Tagliazucchi, Pablo Balenzuela, Daniel Fraiman, and Dante R Chialvo, *Criticality in large-scale brain fmri dynamics unveiled by a novel point process analysis*, Frontiers in physiology 3 (2012), 15.

[126] Paolo Paradisi and Paolo Allegrini, *Intermittency-driven complexity in signal processing*, Complexity and Nonlinearity in Cardiovascular Signals, Springer, 2017, pp. 161–195.

[127] TA Amor, R Russo, I Diez, P Bharath, M Zirovich, S Stramaglia, JM Cortes, L De Arcangelis, and Dante Renato Chialvo, *Extreme brain events: Higher-order statistics of brain resting activity and its relation with structural connectivity*, EPL (Europhysics Letters) 111 (2015), no. 6, 68007.

[128] Paolo Allegrini, Paolo Paradisi, Danilo Menicucci, Marco Laurino, Andrea Piarulli, and Angelo Gemignani, *Self-organized dynamical complexity in human wakefulness and sleep: Different critical brain-activity feedback for conscious and unconscious states*, Physical Review E 92 (2015), no. 3, 032808.

[129] YF Contoyiannis, FK Diakonos, and A Malakis, *Intermittent dynamics of critical fluctuations*, Physical review letters 89 (2002), no. 3, 035701.

[130] Jierui Xie, Sameet Sreenivasan, Gyorgy Korniss, Weituo Zhang, Chjan Lim, and Boleslaw K Szymanski, *Social consensus through the influence of committed minorities*, Physical Review E 84 (2011), no. 1, 011130.

[131] Weituo Zhang, Chjan Lim, and Boleslaw K Szymanski, *Analytic treatment of tipping points for social consensus in large random networks*, Physical Review E 86 (2012), no. 6, 061134.

[132] Arda Halu, Kun Zhao, Andrea Baronchelli, and Ginestra Bianconi, *Connect and win: The role of social networks in political elections*, EPL (Europhysics Letters) 102 (2013), no. 1, 16002.

[133] Seth A Marvel, Hyunsuk Hong, Anna Papush, and Steven H Strogatz, *Encouraging moderation: clues from a simple model of ideological conflict*, Physical review letters 109 (2012), no. 11, 118702.

[134] Bruce J West, Elvis L Geneston, and Paolo Grigolini, *Maximizing information exchange between complex networks*, Physics Reports 468 (2008), no. 1-3, 1–99.

[135] Patrick J Deneen, *Why liberalism failed*, Yale University Press, 2018.

[136] Jean François Revel and Branko M Lazić, *How democracies perish*, Harper Perennial, 1985.

[137] Plamen Ch Ivanov, Luis A Nunes Amaral, Ary L Goldberger, Shlomo Havlin, Michael G Rosenblum, Zbigniew R Struzik, and H Eugene Stanley, *Multifractality in human heartbeat dynamics*, Nature 399 (1999), no. 6735, 461.

[138] Plamen Ch Ivanov, Luus A Nunes Amaral, Ary L Goldberger, Shlomo Havlin, Michael G Rosenblum, H Eugene Stanley, and Zbigniew R Struzik, *From 1/f noise to multifractal cascades in heartbeat dynamics*, Chaos: An Interdisciplinary Journal of Nonlinear Science 11 (2001), no. 3, 641–652.

[139] Luís A Nunes Amaral, Plamen Ch Ivanov, Naoko Aoyagi, Ichiro Hidaka, Shinji Tomono, Ary L Goldberger, H Eugene Stanley, and Yoshiharu Yamamoto, *Behavioral-independent features of complex heartbeat dynamics*, Physical Review Letters 86 (2001), no. 26, 6026.

[140] Plamen Ch Ivanov, Qianli DY Ma, Ronny P Bartsch, Jeffrey M Hausdorff, Luís A Nunes Amaral, Verena Schulte-Frohlinde, H Eugene Stanley, and Mitsuru Yoneyama, *Levels of complexity in scale-invariant neural signals*, Physical Review E 79 (2009), no. 4, 041920.

[141] P. Allegrini, P. Grigolini, P. Hamilton, L. Palatella, and G. Raffaelli, *Memory beyond memory in heart beating, a sign of a healthy physiological condition*, Phys. Rev. E 65 (2002), 041926.

[142] Yosef Ashkenazy, Shlomo Havlin, Plamen Ch Ivanov, Chung-K Peng, Verena Schulte-Frohlinde, and H Eugene Stanley, *Magnitude and sign scaling in power-law correlated time series*, Physica A: Statistical Mechanics and its Applications 323 (2003), 19–41.

[143] Manuel Gómez-Extremera, Pedro Carpena, Plamen Ch Ivanov, and Pedro A Bernaola-

Galván, *Magnitude and sign of long-range correlated time series: Decomposition and surrogate signal generation*, Physical Review E 93 (2016), no. 4, 042201.

[144] Gyanendra Bohara, David Lambert, Bruce J West, and Paolo Grigolini, *Crucial events, randomness, and multifractality in heartbeats*, Physical Review E 96 (2017), no. 6, 062216.

[145] P Ch Ivanov, LA Nunes Amaral, Ary L Goldberger, and H Eugene Stanley, *Stochastic feedback and the regulation of biological rhythms*, EPL (Europhysics Letters) 43 (1998), no. 4, 363.

[146] Yosef Ashkenazy, Jeffrey M Hausdorff, Plamen Ch Ivanov, and H Eugene Stanley, *A stochastic model of human gait dynamics*, Physica A: Statistical Mechanics and its Applications 316 (2002), no. 1-4, 662–670.

[147] Didier Delignières and Vivien Marmelat, *Fractal fluctuations and complexity: current debates and future challenges*, Critical Reviews in Biomedical Engineering 40 (2012), no. 6.

[148] Simone Bianco, Elvis Geneston, Paolo Grigolini, and Massimiliano Ignaccolo, *Renewal aging as emerging property of phase synchronization*, Physica A: Statistical Mechanics and its Applications 387 (2008), no. 56, 1387 – 1392.

[149] Gerardo Aquino, Mauro Bologna, Bruce J. West, and Paolo Grigolini, *Transmission of information between complex systems:* $1/f$ *resonance*, Phys. Rev. E 83 (2011), 051130.

[150] Didier Delignières, Zainy MH Almurad, Clément Roume, and Vivien Marmelat, *Multifractal signatures of complexity matching*, Experimental brain research 234 (2016), no. 10, 2773–2785.

[151] Benoit B. Mandelbrot, *The fractal geometry of nature*, 1 ed., W.H. Freeman, 1982.

[152] Nicola Scafetta and Paolo Grigolini, *Scaling detection in time series: diffusion entropy analysis*, Physical Review E 66 (2002), no. 3, 036130.

[153] Rika Soma, Daichi Nozaki, Shin Kwak, and Yoshiharu Yamamoto, *1/f noise outperforms white noise in sensitizing baroreflex function in the human brain*, Physical review letters 91 (2003), no. 7, 078101.

[154] Yuguo Yu, Richard Romero, and Tai Sing Lee, *Preference of sensory neural coding for 1/f signals*, Physical Review Letters 94 (2005), no. 10, 108103.

[155] Pulin Gong, Andrey R Nikolaev, and Cees van Leeuwen, *Intermittent dynamics underlying the intrinsic fluctuations of the collective synchronization patterns in electrocortical activity*, Physical Review E 76 (2007), no. 1, 011904.

[156] Paolo Allegrini, Danilo Menicucci, Remo Bedini, Leone Fronzoni, Angelo Gemignani, Paolo Grigolini, Bruce J. West, and Paolo Paradisi, *Spontaneous brain activity as a source of ideal* $1/f$ *noise*, Phys. Rev. E 80 (2009), 061914.

[157] Marco Buiatti, David Papo, P-M Baudonnière, and Carl van Vreeswijk, *Feedback modulates the temporal scale-free dynamics of brain electrical activity in a hypothesis testing task*, Neuroscience 146 (2007), no. 3, 1400–1412.

[158] Daekeun Kim, Seung Wan Kang, Kyung-Mi Lee, JongWha Kim, and Min-Cheol Whang, *Dynamic correlations between heart and brain rhythm during autogenic meditation*, Frontiers in human neuroscience 7 (2013), 414.

[159] Alex Pentland, *To signal is human: Real-time data mining unmasks the power of imitation, kith and charisma in our face-to-face social networks*, American scientist 98 (2010), no. 3, 204–211.

[160] Arthur S Iberall, *A physical (homeokinetic) foundation for the gibsonian theory of perception and action*, Ecological Psychology 7 (1995), no. 1, 37–68.

[161] Mark C Leake, *The physics of life: one molecule at a time*, 2013.

[162] Stas Burov, Jae-Hyung Jeon, Ralf Metzler, and Eli Barkai, *Single particle tracking in systems showing anomalous diffusion: the role of weak ergodicity breaking*, Physical Chemistry Chemical Physics 13 (2011), no. 5, 1800–1812.

[163] Damian G Stephen and James A Dixon, *Strong anticipation: Multifractal cascade dynamics modulate scaling in synchronization behaviors*, Chaos, Solitons & Fractals 44 (2011), no. 1-3, 160–168.

[164] Petr Jizba and Jan Korbel, *Multifractal diffusion entropy analysis: Optimal bin width*

of probability histograms, Physica A: Statistical Mechanics and its Applications 413 (2014), 438–458.

[165] Jens Feder, *Fractals plenum*, New York 9 (1988).

[166] Kensuke Ikeda and Kenji Matsumoto, *High-dimensional chaotic behavior in systems with time-delayed feedback*, Physica D: Nonlinear Phenomena 29 (1987), no. 1-2, 223–235.

[167] K Ikeda, H Daido, and O Akimoto, *Optical turbulence: chaotic behavior of transmitted light from a ring cavity*, Physical Review Letters 45 (1980), no. 9, 709.

[168] Henning U Voss, *Anticipating chaotic synchronization*, Physical review E 61 (2000), no. 5, 5115.

[169] Marzieh Zare and Paolo Grigolini, *Cooperation in neural systems: bridging complexity and periodicity*, Physical Review E 86 (2012), no. 5, 051918.

[170] J. Kantelhardt, S. Zschiegner, E. Koscielnybunde, S. Havlin, A. Bunde, and H. Stanley, *Multifractal detrended fluctuation analysis of nonstationary time series*, Physica A: Statistical Mechanics and its Applications 316 (2002), no. 1-4, 87–114.

[171] C-K Peng, Sergey V Buldyrev, Shlomo Havlin, Michael Simons, H Eugene Stanley, and Ary L Goldberger, *Mosaic organization of dna nucleotides*, Physical review e 49 (1994), no. 2, 1685.

[172] Paolo Allegrini, Francesco Barbi, Paolo Grigolini, and Paolo Paradisi, *Renewal, modulation, and superstatistics in times series*, Physical Review E 73 (2006), no. 4, 046136.

[173] Jean-François Muzy, Emmanuel Bacry, and Alain Arneodo, *Wavelets and multifractal formalism for singular signals: Application to turbulence data*, Physical review letters 67 (1991), no. 25, 3515.

[174] J F Muzy, E Bacry, and A Arneodo, *The multifractal formalism revisited with wavelets*, International Journal of Bifurcation and Chaos 4 (1994), no. 02, 245–302.

[175] Leon Glass, *Introduction to controversial topics in nonlinear science: Is the normal heart rate chaotic?*, 2009.

[176] Igor M Sokolov, *Solutions of a class of non-markovian fokker-planck equations*, Physical Review E 66 (2002), no. 4, 041101.

[177] Elliott W Montroll and George H Weiss, *Random walks on lattices. ii*, Journal of Mathematical Physics 6 (1965), no. 2, 167–181.

[178] Michael F Shlesinger, *Origins and applications of the montroll-weiss continuous time random walk*, The European Physical Journal B 90 (2017), no. 5, 93.

[179] Gianluca Ascolani, Mauro Bologna, and Paolo Grigolini, *Subordination to periodic processes and synchronization*, Physica A: Statistical Mechanics and its Applications 388 (2009), no. 13, 2727–2740.

[180] Paolo Grigolini, Gerardo Aquino, Mauro Bologna, Mirko Luković, and Bruce J West, *A theory of 1/f noise in human cognition*, Physica A: Statistical Mechanics and its Applications 388 (2009), no. 19, 4192–4204.

[181] Lijia Lin and Ming Li, *Optimizing learning from animation: Examining the impact of biofeedback*, Learning and Instruction 55 (2018), 32–40.

[182] Martin Karplus and John Kuriyan, *Molecular dynamics and protein function*, Proceedings of the National Academy of Sciences of the United States of America 102 (2005), no. 19, 6679–6685.

[183] Mario Compiani, Teresa Fonseca, Paolo Grigolini, and Roberto Serra, *Theory of activated reaction processes: Non-linear coupling between reactive and non-reactive modes*, Chemical physics letters 114 (1985), no. 5-6, 503–506.

[184] Richard F Voss and John Clarke, *Flicker (1/f) noise: Equilibrium temperature and resistance fluctuations*, Physical Review B 13 (1976), no. 2, 556.